UTILIZATION OF MASS SPECTROMETRIC TECHNIQUES TO IDENTIFY NOVEL LIPID BIOMARKERS OF TRAUMATIC BRAIN INJURY AND OTHER PRACTICAL APPLICATIONS.

A Dissertation
Presented to
The Academic Faculty

By

Scott Richard Hogan

In Partial Fulfillment
Of the Requirements for the Degree
Doctor of Philosophy in the
School of Chemistry and Biochemistry

Georgia Institute of Technology
May 2020

Utilization of Mass Spectrometric Techniques to Identify Novel Lipid Biomarkers of Traumatic Brain Injury and Other Practical Applications.

Approved By

Dr. Facundo M. Fernández, Co-advisor
School of Chemistry and Biochemistry
Georgia Institute of Technology

Dr. Michelle LaPlaca, Co-advisor
School of Biomedical Engineering
Georgia Institute of Technology

Dr. Alfred Merrill
School of Biology and Petit Institute for Bioengineering and Bioscience
Georgia Institute of Technology

Dr. Neha Garg
School of Chemistry and Biochemistry
Georgia Institute of Technology

Dr. M.G. Finn
School of Chemistry and Biochemistry
Georgia Institute of Technology

Date Approved: December 4th, 2019

Whatever the struggle, continue the climb. It may be only one step to the summit.

– Diane Westlake.

This is dedicated to all the friends, family and colleagues who helped push me beyond my limits to create and complete this dissertation. Thank you all for the continued support.

ACKNOWLEDGEMENTS

There are many people who deserve to share the credit for my research efforts throughout the years at Georgia Tech, without whom the completion of this dissertation would never have been possible. Most of all, I would like to acknowledge my research advisors, Dr. Michelle LaPlaca and Dr. Facundo Fernández, who let me choose my own direction in designing the research objectives of this dissertation. Each of my advisors played a different but equally important role in the success of this research. Dr. Fernández, you provided me with unwavering support in learning the applied principles of mass spectrometry and how to effectively communicate my results to the scientific community. Dr. LaPlaca, you helped introduce me to the field of traumatic brain injury and provided me with access to a network of like-minded researchers. Also, to the members of my thesis committee: Dr. Alfred Merrill, Dr. Neha Garg, Dr. M.G. Finn, thank you all for providing me with valuable feedback and asking the difficult questions to ensure the quality of my contributions to the scientific community.

Next, to all my friends and family, I thank you for never letting me down or leaving my side. Graduate school will always be a difficult journey, but the support of those close to me inspired me to keep going even in the darkest of times. Specifically, I am thankful for my mother, Joanne Deutchman, who inspired me from a young age to become a scientist, as I vowed to go into research and find a cure for her multiple sclerosis. While I may not have followed the path my 6-year-old self laid out exactly, I was able to learn about the field of traumatic brain injury and provide something meaningful back in the form of this research. I would also like to thank my sister Lesley,

my stepdad Lenny, the Hogan cousins, my friends Zachary Shindell, Stephen Wettstein, Brian Hurowitz, Kailey Fregd, Young Kim, Tetsu Nakasaka and countless others for helping keep my spirit alive, as well as Ashley Lorenzo and the wonderful yoga community in Atlanta that uplifted my body and soul..

I also must thank all of my current and former lab mates for all the advice, technical expertise, and constructive criticism I received along the way. From the Fernández Group: Dr. Manshui Zhou, Dr. David Gaul, Dr. Rachel Bennett-Stryffeler, Dr. Christina Jones, Dr. Martin Paine, Dr. Li Li, Dr. Xiaoling Zhang, Dr. Yafeng Li, Dr. Marcos Bouza Areces, Dr. Clint Alfaro, Stephen Zambrzycki, Kristin McKenna, Danning Huang, Samyukta Sah, and Eric Gier as well as my colleagues from the LaPlaca group: Dr. Brian Rooney, Eric Gaupp, Kyle Milligan, Alexis Pulliam; thank you all for your help in getting my projects off the ground. Each and every one of you were instrumental in helping me learn the complexities of experimental design and understanding the relevant scientific principles which guided the work within this dissertation, as well as their assistance in solving problems as they arose with research equipment. I am tremendously thankful for all the current students who aim to continue to build upon my efforts over the next few years. I would also like to thank the support staff from the Waters Corporation, specifically Nick Ringo and Angelique Dupont, for their dedication to their work and support of my research endeavors. Without you all, I never could have learned and accomplished all that I did during my time at Georgia Tech. Also, thank you to my collaborators from the traumatic brain injury projects: Dr. May Wang and Dr. John Phan (bioinformatics), Dr. Ravi Bellamkonda and Melissa Alvarado-Velez (animal research) as well as those from the plankton project: Dr. Remington Poulin and Dr. Julia

Kubanek, thank you for providing me the means to study and understand such a unique, biologically important model system.

A few other groups played a critical role in the completion of the experiments described within. I would like to acknowledge Georgia Tech's Systems Mass Spectrometry Core (SyMS-C) facility and the dedicated researchers involved (Dr. David Gaul, Dr. David Smalley, and Samuel Moore) for access to their research equipment, expertise, and assistance in running many of the final experiments necessary for the completion of this thesis, as well as the Mass Spectrometry core (David Bostwick). And finally, thank you to the funding agencies who financially supported these research endeavors, including the Georgia Institute of Technology Chemistry and Biochemistry department, the GT Biomaterials training grant, the National Institutes of Health, the Center for Chemical Evolution, and the Vasser Woolley Foundation, as well as the American Society for Mass Spectrometry for access to travel funding for the Fall Lipidomics workshop.

Table of Contents

LIST OF TABLES

LIST OF FIGURES

Page

LIST OF ABBREVIATIONS

4-HNE	**4-hydroxynonenal**
AA	**Arachidonic acid**
ACN	**Acetonitrile**
ACP	**Acyl carrier protein**
AD	**Alzheimer's disease**
AGC	**Automatic gain control**
ANAM	**Automated neuropsychological assessment metrics**
ANOVA	**Analysis of variance**
ApoE	**Apolipoprotein E**
ATP	**Adenosine triphosphate**
AUC	**Area under the curve**
Aβ	**Amyloid-beta**
BBB	**Blood-brain barrier**
BESS	**Balance error scoring system**
BOLD	**Blood-oxygen-level-dependent**
BPI	**Base peak intensity chromatogram**
C	**Closed-cell foam**
C-tau	**Cleaved tau**
CBF	**Cerebral blood flow**
CCI	**Controlled cortical impact**
CE	**Cholesteryl ester**
Cer	**Ceramide**
CI	**Chemical ionization**
CID	**Collision-induced dissociation**
CL	**Cardiolipin**
CNS	**Central nervous system**
CoA	**Coenzyme A**
COSY	**Correlation spectroscopy**
COX	**Cyclooxygenase**
CS	**Cholesterol sulfate**
CSF	**Cerebrospinal fluid**
CT	**Computerized tomography**
CTE	**Chronic traumatic encephalopathy**
CV	**Cross-validation**
CV_b	**Biological coefficient of variation**
CVE	**Cross-validation error**
CV_m	**Coefficient of variation measured**

D	**Cohen's effect size**
Da	**Dalton**
DAI	**Diffuse axonal injury**
DDA	**Data-dependent acquisition**
DESI	**Desorption electrospray ionization**
DETECT	**Display enhanced testing for cognitive impairment and traumatic brain injury**
DG	**Diacylglycerol**
DGCC	**Diacylglyceryl carboxyhydroxymethylcholine**
DGDG	**Digalactosyldiacylglycerol**
DGTA	**Diacylglyceryl hydroxymethyl trimethyl-β-alanine**
DGTS	**Diacylglyceryl trimethyl homoserine**
DHA	**Docosahexaenoic acid**
DNA	**Deoxyribonucleic acid**
DPA	**Docosapentaenoic acid**
DSM-5	**Diagnostic and statistical manual–5th edition**
DTI	**Diffusion tensor imaging**
EAA	**Excitatory amino acid**
ECFA	**Even chain fatty acid**
EI	**Electron impact**
ELISA	**Enzyme-linked immunosorbent assay**
EPA	**Eicosapentaenoic acid**
ESI	**Electrospray ionization**
FA	**Fractional anisotropy**
FAB	**Fast-atom bombardment**
FAD	**Flavin adenine dinucleotide**
FDA	**Food and Drug Administration**
FFA	**Free fatty acid**
fMRI	**Functional magnetic resonance imaging**
FPI	**Fluid percussion injury**
FT-ICR	**Fourier transform ion cyclotron resonance**
g	**Relative centrifugal force**
GC	**Gas chromatography**
GC-MS	**Gas chromatography-mass spectrometry**
GCS	**Glasgow coma scale**
GFAP	**Glial fibrillary acidic protein**
GM1	**Ganglioside monosialic 1**
h	**Hour(s)**
HABs	**Harmful algal blooms**
HCD	**Higher-energy collisional dissociation**

Hex	**Hexose**
HMBC	**Heteronuclear multiple bond correlation spectroscopy**
HMDB	**Human metabolome database**
HRMS	**High-resolution mass spectrometry**
HSQC	**Heteronuclear single quantum coherence**
ICP	**Intracranial pressure**
IL	**Interleukin**
ImPACT	**Immediate post-concussion assessment and cognitive testing**
IPA	**Isopropyl alcohol**
iPLS-DA	**Interval partial least squares discriminant analysis**
IS	**Internal standard**
ISF	**Interstitial fluid**
IT	**Ion trap**
KEGG	**Kyoto encyclopedia of genes and genomes**
KNN	**K-nearest neighbors**
L	**Liter(s)**
LC	**Liquid chromatography**
LC-MS	**Liquid chromatography mass spectrometry**
LC-MS/MS	**Liquid chromatography tandem mass spectrometry**
LIPID MAPS	**Lipid Metabolites and Pathways Strategy**
LOBSTAHS	**Lipid and oxylipin biomarker screening through adduct hierarchy sequences**
LOX	**Lipoxygenase**
LP	**Lipid peroxidation**
LV	**Latent variable**
LysoPC	**Lysophosphatidylcholine**
LysoPE	**Lysophosphatidylethanolamine**
M	**Molar concentration**
M	**Marmarou foam**
m/z	**Mass to charge ratio**
M1	**Macrophage 1**
MALDI	**Matrix-assisted laser desorption ionization**
MDA	**Malondialdehyde**
MGDG	**Monogalactosyldiacylglycerol**
min	**Minute(s)**
MPC	**Matched-pair control**
MRI	**Magnetic resonance imaging**
MRM	**Multiple reaction monitoring**
mRMR	**Minimum redundancy, maximum relevance**
MS	**Mass spectrometry**

MSI	**Mass spectrometry imaging**
MS/MS	**Tandem mass spectrometry**
MTBE	**Methyl tert-butyl ether**
mTBI	**Mild traumatic brain injury**
NAD+	**Nicotinamide adenine dinucleotide**
NADPH	**Nicotinamide adenine dinucleotide phosphate**
NCE	**Normalized collision energy**
NF	**Neurofilament**
NFH	**Neurofilament heavy chain**
NFL	**Neurofilament light chain**
NFM	**Neurofilament medium chain**
NMDA	**N-methyl-D-aspartate**
NMR	**Nuclear magnetic resonance**
NP	**Neuropsychological**
NSE	**Neuron specific enolase**
OCFA	**Odd chain fatty acid**
oPLS-DA	**Orthogonal partial least squares discriminant analysis**
OT	**Orbitrap**
P	**Polyurethane foam**
p-tau	**Phosphorylated tau**
PA	**Phosphatidic acid**
PC	**Phosphatidylcholine**
PCA	**Principal component analysis**
PCS	**Post-concussive syndrome**
PE	**Phosphatidylethanolamine**
PFAA	**Primary fatty acid amide**
PG	**Phosphatidylglycerol**
$PGF_{2\alpha}$	**Prostaglin-$F2_{\alpha}$**
PI	**Phosphatidylinositol**
PL	**Phospholipid**
PLA_2	**Phospholipase A_2**
PLC	**Phospholipase C**
PLS-DA	**Partial least squares discriminant analysis**
pNFH	**Phosphorylated neurofilament heavy**
ppm	**Parts per million**
PS	**Phosphatidylserine**
PUA	**Polyunsaturated aldehyde**
PUFA	**Polyunsaturated fatty acid**
QC	**Quality control**
QE	**Quadrupole Exactive**

QTOF	**Quadrupole time-of-flight**
RNS	**Reactive nitrogen species**
ROS	**Reactive oxygen species**
RT	**Retention time**
S1P	**Sphingosine-1-phosphate**
$S1P_1$	**Sphingosine-1-phosphate receptor subtype 1**
SBDP	**Spectrin breakdown product**
SCAT5	**Sport concussion assessment tool 5_{th} edition**
SDMT	**Symbol digit modalities test**
SIMS	**Secondary ion mass spectrometry**
SM	**Sphingomyelin**
SQDG	**Sulfoquinovosyldiacylglycerol**
SULF	**Sulfonated lipid**
SVMs	**Support vector machines**
TBA	**Thiobarbituric acid**
TBARS	**Thiobarbituric reactive substances**
TBI	**Traumatic brain injury**
TCA	**Tricarboxylic acid**
TG	**Triacylglycerol**
TOF	**Time-of-flight**
UCH-L1	**Ubiquitin C-terminal hydrolase**
UPLC-MS	**Ultra-performance liquid chromatography-mass spectrometry**
USD	**United States dollars**
V	**Volt(s)**
v	**Volume**
Y	**Yellow generic foam**

SUMMARY

This dissertation is intended to highlight the recent advancements in the field of lipidomics, particularly in reference to the discovery of novel biomarkers of traumatic brain injury (TBI). Lipidomics falls under the umbrella of the related 'omics technique known as metabolomics and refers specifically to the study of the lipidome, or collection of all lipophilic metabolites in a biological system. Lipids play critical roles in cellular structure and function, including acting as signaling molecules, regulating energy storage, and maintaining membrane integrity. The use of omics' techniques has led to the proposal of a number of biomarkers for the study of TBI, though most have stemmed from targeted proteomic approaches, with researchers focusing on a few proteins in the brain and central nervous system that are upregulated as a consequence of TBI. The response of the lipidome to TBI is less understood, so a non-targeted approach is suggested here for the purpose of generating hypotheses regarding lipidomic responses to TBI using data-driven, discovery-oriented techniques.

Research interest into TBI has been accelerated due to heightened awareness of the growing concussion epidemic in the military, sports, and general population. With diagnosis of subtle cognitive dysfunction typically based on the presence of subjective self-reported symptoms, the number mild traumatic brain injuries (mTBIs) is vastly underestimated, as many injuries may go unreported or misdiagnosed due to lack of perceived symptoms. Chapter 1 introduces the commonly utilized techniques for clinical diagnosis of TBI and outlines the known pathophysiology associated with the onset of injury. Ranging from simple grading schemes that measure a patient's verbal, motor and

eye-opening responses to more advanced radiologic imaging and neuropsychological testing modalities, the field of mTBI diagnostics is growing rapidly. However, a substantial gap remains between the literature and clinical translation, indicating a need for further scientific collaboration.

Biomarker discovery studies have been enabled by the advent of sophisticated instrumentation, fueling the growth of the fields of metabolomics and lipidomics. Such studies often involve careful measurement of a large number of molecular targets, so advanced techniques are required beyond simple single-target assays. Mass spectrometry (MS) and nuclear magnetic resonance (NMR) are the two most commonly utilized platforms for metabolomics analysis, and each offers complementary advantages to research efforts. MS-based techniques are used throughout this dissertation in order to study the lipidomic response within the serum of rodents incurring TBI induced by controlled cortical impact.

Two distinct severities of injury are investigated and modeled in chapters 2 and 3. Chapter 2 first focuses on an injury of moderate severity in an effort to measure the response of lipids to injury. A standard metabolomics workflow was utilized, and a number of novel biomarker candidates for TBI were identified in the serum lipidome of adult male Sprague-Dawley rats in the first week following injury. Serum samples were analyzed in positive and negative modes by Ultra Performance Liquid Chromatography Mass Spectrometry (UPLC-MS). A predictive panel for the classification of injured and uninjured sera samples, consisting of 26 dysregulated species belonging to a variety of lipid classes, was developed with a cross-validated accuracy of 85.3% using omniClassifier software to optimize feature selection. Polyunsaturated fatty acids

(PUFAs) and PUFA-containing diacylglycerols were found to be upregulated in sera from injured rats, while changes in sphingolipids and other membrane phospholipids were also observed, many of which map to known secondary injury pathways. Cholesterol sulfate, a sterol sulfate that plays a stabilizing role in cellular membranes and serves as a precursor in the synthesis of other sulfonated adrenal steroids, was found to be significantly decreased in the TBI cohort. Overall, the identified biomarker panel presents a number of viable molecular candidates representing lipids affected by of TBI pathophysiology.

In chapter 3, we proposed to study mild injury at an early acute time point (t=24 h). Using a matched pair study design to improve statistical power, a panel of 16 lipid metabolites was developed with a classification accuracy of 88.5%, a small improvement from the previous study despite the use of a less complex metabolite panel (reduction by 50% of the number species studied) and the occurrence of a milder form of injury in which the average effect size of lipid alterations was reduced. These promising results demonstrate the feasibility of utilizing non-targeted lipidomics to detect mild, concussive events in serum.

The broad applicability of non-targeted lipidomics experiments is then demonstrated in chapter 4 through the study of phytoplankton competitor responses to exposure to *Karenia brevis*, the dinoflagellate responsible for forming harmful algal blooms commonly referred to as red tides. MS-based analysis of phytoplankton lipidomes led to the identification of 80 distinct lipid metabolites whose concentrations differed significantly in *T. pseudonana* following exposure to *K. brevis* allelopathy. These 80 metabolites represent nine major lipid classes, of which members of five

(phosphatidylcholines [PCs], sulfoquinovosyldiacylglycerols [SQDGs], monogalactosyldiacylglycerols [MGDGs], digalactosyldiacylglycerols [DGDGs], and phosphatidylglycerols [PGs]) were generally less abundant when *T. pseudonana* was subjected to *K. brevis* allelopathy, whereas members of four classes (non-SQDG sulfonated lipids [SULFs], free fatty acids [FFAs], primary fatty acid amides [PFAAs], and phosphatidylethanolamines [PEs]) were generally more abundant. In contrast, for the other competitor, *A. glacialis*, concentrations of only six metabolites were significantly affected by allelopathy, reinforcing the hypothesis that *A. glacialis* maintains a more robust metabolism in response to *K. brevis* allelopathy due to an evolved resistance stemming from periods of prior co-habitation.

A majority of the lipids formed (PFAAs, FFAs, and SULFs) by allelopathic exposure were either metabolic breakdown products or metabolic precursors of PCs and SQDGs, whose pools shrunk in *T. pseudonana* upon exposure to allelopathy. Globally, concentrations of membrane-associated lipids (MGDG, DGDG, SQDG, PC) were significantly suppressed for *T. pseudonana* exposed to allelopathy, leading membranes of living cells to become more permeable. Increased membrane permeability as well as decreased photosynthetic capability both likely occurred due to decreases in the concentrations of membrane- and thylakoid-associated lipids. *K. brevis* allelopathy appears to target lipid anabolism, affecting multiple physiological pathways. This suggests that exuded compounds have the ability to significantly alter competitor physiology through effects on metabolism, giving *K. brevis* an edge over sensitive species.

Finally, chapter 5 explores the potential future work associated with the projects contained within this dissertation. Critical points of exploration include validation of proposed biomarkers in another cohort of rats and examination of altered response patterns based on sex, strain, and age of the animals. Use of human samples for the purposes of clinical translation is also proposed. Limitations of the current work are examined, and suggestions are made for future experiments to better understand efflux pathways for biomarker clearance and answer questions regarding specificity of the proposed biomarkers to the brain and brain injury.

CHAPTER 1: INTRODUCTION TO TRAUMATIC BRAIN INJURY AND LIPIDOMICS

1.1 Abstract

A substantial portion of the population will sustain a traumatic brain injury (TBI) at some point in their lifetime, and heightened awareness of the potentially devastating effects of even mild injuries, often referred to as concussions, in the setting of military and sports has led to increased research efforts towards the development of objective diagnostic modalities. This chapter outlines the different mechanisms of injury and subsequent pathophysiological changes that may result. Additionally, the strengths and limitations of existing diagnostic modalities for TBI are examined. Non-targeted lipidomics is suggested as a tool to objectively determine the presence of injury through the measurement of all lipids in a biological system and can be used to guide research efforts towards the development of novel biomarkers of injury. Lipidomics can also be broadly applied to understand the role of lipid metabolism involved in other biological systems, such as the allelopathic effects exerted by *Karenia brevis* on phytoplankton competitors.

1.2 Traumatic Brain Injury Epidemiology

Traumatic brain injury (TBI) is a complex, heterogeneous disease that affects millions of people, with an average of 1.4 million TBIs occurring annually in the United States alone. In the US, injury was the leading cause of death for the 1-44 age group in 2009, and TBI was diagnosed in at least 1/3 of these cases.[2] Incidence rates of TBI are

similar in other countries, though it is difficult to make direct comparisons due to differences in health care and admission criteria.[3,4] The direct costs associated with TBI, including medical treatment and deaths, have been estimated at over $9 billion annually. On top of that, loss of productivity and wages due to TBI-related work absences accounts for over $51 billion, bringing the economic burden of TBI to over $60 billion annually in the US alone.[5] The majority of all reported cases are classified as mild TBI (mTBI), though cognitive deficits are still present a year post-injury in about 10% of cases.[6]

About 80% of TBI cases are diagnosed in emergency departments, with head injuries accounting for 1.4% of emergency department visits, and 4.8% of injury related visits.[3] As many patients sustaining TBIs, especially mild, may not report to hospitals for diagnosis or treatment, it is expected that the total number of TBI cases actually exceeds these totals, with estimates ranging from 11%[7] to 75%[8] of TBIs going undiagnosed. Approximately 52,000 people die of TBI related injury annually in the US, accounting for about 30% of injury related deaths, though death rates have been steadily declining since 1989.[3, 9, 10] The leading causes of TBI include falls, struck-by or struck-against events, and motor vehicle crashes. People in the early and late stages of life are most vulnerable to fall related TBI. Males (548 per 100,000) have a higher incidence of TBI than do females (386 per 100,000).[3] Heterogeneity within mechanism of injury and amongst persons experiencing TBI is a primary impediment in the design of effective treatments and is thought to be a major reason for the failure of clinical trials.[11] Factors such as age, sex, and previous TBI exposure may all affect the extent of damage and clinical manifestation of symptoms of TBI.

1.3 Primary Injury Mechanisms

In addition to the variability in the affected clinical population, the type of injury mechanism (fall, penetrating, blast, etc.) contributes to the heterogeneity of injury pathology. Mechanisms for primary injury, damage which evolves acutely as a direct result of injury to the brain, include blast, focal injury, contusions, and rotational acceleration/ deceleration forces.[12] Primary damage typically stems from contact and/or inertial forces occurring at the moment of injury.

1.3.1 Focal Injury

The term focal is used to describe injuries that are caused by direct focused contact to the head. The blunt force of the injury results in deformation of the brain tissue and leads to localized damage at or near the injury site. Focal injuries are believed to be responsible for the majority of injury related deaths and are often characterized by contusions, skull fractures, lacerations and hemorrhage.[13] Animal models of focal injury are designed to produce consistent injury by directly injuring the brain while carefully controlling the injury parameters. *In vivo* studies serve as foundational research for guiding clinical studies. The controlled cortical impact (CCI) and fluid percussion injury (FPI) models are the most commonly used models to induce focal injury.

1.3.1.1 Controlled Cortical Impact

CCI injuries are induced using an air-driven pneumatic piston to impact the exposed cortex with intact dura mater following a craniectomy, rapidly compressing brain tissue. CCI can be used to model injuries of different severities by varying mechanical parameters such as impact velocity, dwell time and depth of impact. The ease with which these mechanical parameters can be changed makes CCI a useful pre-clinical model.[14] For

example, by varying these parameters, CCI can be used to model mTBI, where there is little damage, as well as more severe injuries, where large cortical areas are destroyed.[15]

1.3.1.2 Fluid Percussion Injury

The FPI model rapidly applies a pressurized column of liquid to the intact dura matter following craniectomy, causing the brain to move within the skull. The resulting lesion is less localized compared to CCI, and hemorrhage, brain swelling and progressive grey matter damage are seen.[16] By controlling the pressure of the liquid, FPI can also be used to model different severities of TBI.

1.3.2 Diffuse Injury

Diffuse injuries are caused by inertial forces or acceleration/ deceleration of the brain within the skull, leading to widespread microscopic damage across large areas of the brain. These forces are often seen in clinical TBI following car accidents or falls, in addition to the focal injury at the contact site.[17] Acceleration/ deceleration forces are difficult to model in rodents, though the weight drop and blast injury models may substitute as examples of diffuse injury, even if they are not caused by the same mechanism of action, e.g. rotation of the head.

1.3.2.1 Weight Drop

The weight drop model involves the release of a weight dropped from a known height onto the closed skull. Injury severity can be altered by varying the mass of the dropped weight and the height from which it is dropped. A stainless-steel disc is mounted to the skull midline to prevent skull fracture. This model produces general brain movement and has been shown to result in diffuse axonal injury (DAI).[18]

1.3.2.2 Blast Injury

While blast injuries also fall within the diffuse subcategory, there are a variety of different mechanisms of damage resulting from injuries of this type. Rather than high levels of brain deformation, blast is characterized by small deformations delivered at relatively much higher rates than the other modalities described. Blast TBI can be modeled pre-clinically using shock tubes driven by compressed air or helium.[19,20]

1.4 Secondary Injury Mechanisms

In addition to the primary injury imparted by the TBI, a complex secondary injury cascade follows, which can lead to necrotic and apoptotic neuronal and glial death. Necrosis occurs when the acute trauma causes cell death directly in the injured area of the brain and is associated with the generation of free radicals and excitotoxins. It is often characterized by mitochondrial and nuclear swelling, rupture of the nuclear and cytoplasmic membranes, and enzymatic degradation of deoxyribonucleic acid (DNA). The process is very rapid, and because neuronal tissue has little regenerative ability, necrotic cell death is very difficult to prevent.[21] Necrosis and apoptosis of neurons has also been observed in the days and weeks following injury, and it is generally thought to occur continuously after injury.[22,23] Secondary injury cascade mechanisms also include oxidative stress, glutamate excitotoxicity, inflammation, and cytotoxicity of metabolites formed in the central nervous system (CNS), amongst others.[24]

1.4.1 Glutamate Excitotoxicity and the Neurometabolic Cascade

A significant increase in the release of neurotransmitters and other excitatory amino acids (EAAs), specifically glutamate, is a significant part of the secondary injury cascade. The neurometabolic cascade is a series of events resulting from TBI, disrupting homeostatic brain function to different degrees depending on injury severity. Release of neurotransmitters and ionic fluxes occur immediately following TBI.[25] Disruption of neuronal membranes, axonal stretching and voltage dependent potassium channel openings following the primary injury lead to membrane depolarization and efflux of potassium ions (K^+).[26] The resultant non-specific release of excitatory neurotransmitters such as glutamate overwhelms the surrounding glial cells' ability to regulate excess K^+, leading to the release of additional EAAs, activation of the respective receptor channels and further ion imbalance.[27] The binding of excitatory neurotransmitters to glutamatergic receptors leads to further membrane depolarization, calcium ion influx, and excitotoxicity. Efflux of potassium causes the sodium-potassium pump to work harder to restore equilibrium intracellular concentrations, requiring energy in the form of adenosine triphosphate (ATP) and vastly increasing glucose metabolism.[28]

1.4.2 Energy Crisis in the Brain

This increase in glucose utilization occurs almost immediately in the injured cortex and neighboring hippocampus, though it may persist for hours in distant brain areas following severe injury. To combat this increased energy demand, the brain responds by increasing glycolysis, the breakdown of glucose into pyruvate, which leads to increased lactate production.[29] The resulting lactate accumulation leads to neuronal dysfunction by inducing acidosis, membrane damage, cerebral edema, and altering blood-brain barrier

(BBB) permeability.[30] The hyperglycolysis demands a concomitant increase in cerebral blood flow (CBF), but instead CBF may be reduced by up to 50%, furthering the brain's energy crisis by reducing the energy substrates and oxygen supplied to the brain.[31] Following this period of hypermetabolism, in an effort to combat the energy crisis, the brain goes into a period of decreased metabolism, reducing cerebral glycolysis and CBF while calcium ion influx continues to disrupt mitochondrial oxidative metabolism.[32]

1.4.3 Mitochondrial Dysfunction

Calcium can flow through the open N-methyl-D-aspartate (NMDA) receptor channels, and an increase in intracellular calcium is observed within minutes after injury and sustained for days.[33] This increase in calcium leads to overactivation of degradative enzymes including phospholipases, causing destruction of cellular membranes. Lactic acid, free radicals and inflammatory mediators are also generated upon initiation of the neurometabolic cascade.

Mitochondria are small organelles found within most cells and are responsible for cellular respiration and energy production. Within mitochondria, carbohydrates and fatty acids are converted into ATP. Neurons rely heavily on mitochondrial oxidative metabolism and ATP production, which is known to be disrupted following TBI.[34] Damage to mitochondria reduces ATP production, again signaling the activation of glycolysis despite a decrease in lactate metabolism. Ischemic necrosis primarily results from anaerobic inactivation of the oxidative phosphorylation process. Mitochondrial cytochrome c release has also been demonstrated in TBI, resulting in increased neuronal apoptosis.[35] Persistent accumulation of intracellular calcium, especially in the mitochondria, is associated with

more severe injuries and may also activate cell death pathways and disrupt neurofilaments (NFs) and microtubules.[36]

1.4.4 Oxidative Stress

While reactive oxygen species (ROS) and reactive nitrogen species (RNS) are generated during normal physiological processes, their production is vastly increased following TBI, overwhelming antioxidant defenses and mediating damage to vital cell structures such as cell membranes and mitochondria.[37] Overproduction of ROS can lead to damage to both DNA and proteins as well as lipid peroxidation (LP) due to oxidative stress in mitochondria.

Much research has focused on the oxidative stress mechanism in TBI involving the peroxidation of lipids by free radicals. The brain has a number of characteristics that make it especially susceptible to free radical-mediated oxidative stress, including a high oxygen consumptions rate, elevated levels of polyunsaturated fatty acids (PUFAs), and high iron concentrations in the substantia nigra and striatum, which can catalyze LP.[38] High metabolic rates in brain cells also stimulate a high baseline ROS production.[39] Low energy stores and a reliance on aerobic glucose metabolism leaves the brain highly vulnerable to ischemic injury. Neurons are susceptible to ischemia, hypoxia, or hypoglycemia, and a major consequence of oxidative stress is damage to cellular macromolecules.[40]

1.4.5 Edema

Edema, or swelling of the brain, is one of numerous secondary injury events associated with TBI. Edema can be caused by BBB disruptions leading to accumulation of extracellular fluid (vasogenic) or by sustained collection of intracellular fluid (cytotoxic/cellular).[41] A third category, interstitial, may occur when outflow of

cerebrospinal fluid (CSF) is obstructed, though there is considerable overlap between the types of edemas.[42] This can result in increased intracranial pressure (ICP), requiring a craniotomy to relieve built up pressure in the skull in severe cases.

1.4.6 Inflammation

Progressive and prolonged neuroinflammation is amongst the major secondary injury pathways hypothesized to play a significant role in TBI. Although the brain was once believed to be an immune privileged organ (unable to elicit and not susceptible to inflammatory responses), it is now clear that that inflammation represents a key pathology in TBI.[43] This process includes glial activation and leukocyte recruitment as well as upregulation and secretion of molecules such as cytokines and chemokines. Involving both pro- and anti-inflammatory mediators, inflammation following TBI can be either beneficial or detrimental, depending if the process is controlled and regulated.[44] Cytokines are polypeptides normally present in healthy tissue at non-detectable levels but are rapidly upregulated in response to TBI and other pathologies.[45]

Interleukins (ILs) are a family of cytokines produced by leukocytes that are necessary for regulating immune responses. The IL-1 family of cytokines plays a key role in initiating the immune response, and IL-1β has been shown to be elevated in the CSF and brain parenchyma in both rodents and humans following brain injury.[46,47] Belonging to the neuropoitin family of cytokines, IL-6 has also been reported to be elevated in CSF and serum in the setting of severe BBB dysfunction.[48] In addition, IL-10 possesses neuroprotective effects including activation of microglia and suppression of pro-inflammatory cytokines.[49,50] Administration of IL-10 in rats promoted neurological recovery, though an increase in its concentration in the CSF of children with brain injury

was associated with negative outcomes, highlighting the conflicting roles of inflammation in brain injury.[51,52] More recent studies of ILs have confirmed their role as potential biomarkers of BBB dysfunction and severe TBI.[53,54] IL-1 can also alter lipid metabolism and stimulate the production of eicosanoids, ceramides (Cers) and further accumulation of ROS.[55]

1.5 Clinical Diagnostic Modalities

1.5.1 Glasgow Coma Scale

Clinical diagnosis of TBI is typically based on self-reported symptoms, observer report, imaging, and/or the Glasgow Coma Scale (GCS), a simple grading scheme which serves to separate injury into subtypes (mild, moderate, and severe).[56] The GCS combines measures of motor, verbal and eye movement ability, yielding a final score of 3-15. Motor skills are scored from 1-6, verbal 1-5 and eye opening 1-4 to account for a total of 15 points. Mild injuries (score 13-15) account for nearly 80% of injuries, while moderate (9-12) and severe (< 9) each account for approximately half of the remaining cases. As substance use, e.g. alcohol, is commonly present upon admission, initial GCS scores may not be an accurate representation of cognitive deficits.[57]

1.5.2 Self-reported Symptoms

Self-reported symptoms are a primary method for evaluating mTBI. Symptoms may include headache, nausea, dizziness, loss of consciousness, balance impairment, blurred vision, light or noise sensitivity, memory deficits, drowsiness, inability to sleep, irritability and confusion, amongst others. Sideline assessments such as the Sport Concussion Assessment Tool 5th Edition (SCAT5) for sports-related concussion

diagnostics include reporting of these symptoms.[58] However, because athletes may have a tendency to underreport symptoms in an effort to stay on the field, more objective diagnostic criteria are likely required for accurate assessment.[59]

1.5.3 Imaging Modalities

Advanced imaging techniques such as computerized tomography (CT) and magnetic resonance imaging (MRI) are capable of detecting intracranial lesions, acute hemorrhage and skull fracture; however, scans are often negative for mTBI due to a lack of macrostructural damage.[60,61] Diffusion Tensor Imaging (DTI) is an advanced MRI modality that measures the diffusional patterns of water in tissue.[62] The uniform collinear structure of normal white matter allows DTI to detect microscopic abnormalities, enabling the assessment of traumatic axonal injury in the absence of macroscopic tissue damage.[63] Measurements such as fractional anisotropy (FA), mean diffusivity, axial diffusivity, and radial diffusivity describe the magnitude and direction of water diffusion in tissue. Most commonly FA values are reported, and abnormally low values for FA have been associated with TBI.[64, 65, 66] Functional magnetic resonance imaging (fMRI), which measures cortical responses to controlled stimuli through changes in blood flow, also offers promise for detection of TBI in clinical populations.[67,68] Blood-oxygen-level-dependent (BOLD) imaging signals measure activity in the brain, and an increase in brain activity or blood flow in one region leads to a reduction in deoxyhemoglobin and reduction in signal in another. A study of concussed patients showed increased activation in the dorsal-lateral prefrontal cortex and cerebellum when performing spatial memory tasks, consistent with the majority of previous reports.[66]

1.5.4 Balance Assessments

The ability to maintain both static and dynamic balance has been shown to be disrupted following TBI.[69,70] In fact, balance deficits present in close to 30% of sports-related concussion cases, trailing only headache, dizziness, confusion, disorientation and blurred vision in terms of frequency of occurrence.[71] Romberg's test of balance and postural stability was long considered the hallmark for balance assessment.[72] Created in 1846, Romberg's test measures postural equilibrium in the absence of vision, leaving only somatosensory or proprioceptive cues and the vestibular system to maintain balance. However, the test lacks objectivity and sensitivity for mild balance deficits exhibited as a consequence of concussion, especially in elite athletes. A variety of balance tests integrating technology have been designed to measure balance deficits more sensitively, though these require sophisticated measurement of force and sensory information integration. The balance error scoring system (BESS) was thus developed to provide a more cost-effective approach to quantifying balance deficits. Here balance is measured on two differing stability surfaces across multiple stances (single leg, double leg, tandem) for 20 seconds each with eyes closed and hands on hips. Errors are counted to a maximum of 10 per trial. Concussed college football players experienced an average increase in total errors of 5.7 from their pre-injury baselines (average 12 errors) immediately following the game/practice in which injury occurred, though this had dropped to only 2.7 points by 1-day post-injury. Overall, most players returned to baseline balance performance after 3-7 days.[73] Test scores may be affected by type of sport played, history of ankle injuries, and fatigue, but incorporation of the BESS in concussion evaluation can increase sensitivity and specificity of evaluation.[74]

1.5.5 Neuropsychological Testing

Neuropsychological (NP) testing can also be used for diagnosis and clinical management of concussion and more severe TBI. The Diagnostic and Statistical Manual–5th Edition (DSM–5) diagnostic criteria for post-concussive syndrome (PCS) requires evidence of sustained cognitive impairment, which can be detected in concussed athletes by NP assessment.[73,75] Attention, information processing speed, working memory, recall and other related skills are measured through a variety of tests designed to yield diagnostic feedback within 20-30 minutes. NP assessments have been shown to be sensitive enough to measure cognitive performance decreases in the days following injury, providing an additional diagnostic tool beyond self-reported symptoms.[76] Computerized tests such as Immediate Post-Concussion Assessment and Cognitive Testing (ImPACT)[77,78], Automated Neuropsychological Assessment Metrics (ANAM), Symbol Digit Modalities Test (SDMT),[79] and Display Enhanced Testing for Cognitive Impairment and Traumatic Brain Injury (DETECT)[80] allow for the detection of transient cognitive deficits that result from mTBI by comparing performance post-injury with pre-injury baseline assessments. To better track and understand TBI, The US Naval Academy utilized the ANAM test to collect over 4800 baseline scores for comparison of post-concussive effects.[81] In addition to symptoms reporting, NP testing has been utilized for return to play decisions in college athletics, as well as in professional football, baseball and hockey.[82-85] However, these tests are typically limited by practice effects, test-retest reliability, test duration, and sensitivity/specificity issues. Additionally, no direct comparison between tests exists to document interpretation of results, and none have yet met all the criteria necessary for routine clinical application.[86-88]

1.6 Biomarkers

Biomarkers are defined as indicators of a medical state that can be measured accurately and reproducibly.[89] Biomarkers of TBI offer the ability to supplement or supplant prohibitively expensive and sometimes ineffective diagnostic modalities, and there is a wealth of scientific literature showing their potential utility in the diagnosis and prognosis of TBI. The ideal biomarker can be measured non-invasively, such as through the use of easily collected biological fluids like urine and blood.[90] To create more objective measures of brain injury diagnosis, research efforts have been focused on the identification of blood-based biomarkers, with a heavy emphasis on targeted studies focusing on a small number of neuronal, axonal or astroglial specific proteins as well as a variety of inflammatory mediators which are up-regulated as a consequence of TBI.[91]

1.6.1 Protein Biomarkers of TBI

1.6.1.1 Axonal Proteins and Neuronal Proteins

Although found in the cytoplasm of neurons, NFs are particularly abundant in axons, forming their cytoskeletal components. NFs are heteropolymers found in the CNS, including neurofilament light (NFL), medium (NFM), and heavy (NFH), as well as α-internexin polypeptides.[92] Detection of markers of axonal injury and degeneration such as NFL in the blood or CSF offers an alternative means to diagnosis of injury. NFL is most abundant in large myelinated axons that project deep into the brain and spinal cord. NFL has been suggested to be the most sensitive and specific marker of axonal injury, and its concentration has been shown to be elevated in the CSF of boxers as well as the serum of college football players over the course of a full season.[93,94] After injury, calcium activates calcineurin, altering the phosphorylation states of NFs.[95] Quantified by an

enzyme-linked immunosorbent assay (ELISA), higher levels of phosphorylated neurofilament heavy (pNFH) were seen in cases of DAI and were also associated with poorer outcomes on the Glasgow Outcome Scale in children sustaining TBI.[96] Because pNFHs are resistant to calpain and other proteases, they should remain undegraded in peripheral biofluids and may be useful biomarkers of TBI at clinically relevant timepoints.[97]

Neuronal proteins such as Ubiquitin C-terminal hydrolase (UCH-L1) and neuron specific enolase (NSE) have also been proposed as potential biomarkers of TBI, with UCHL-L1 having been identified in both rat and human models.[98,99] UCH-L1 is a 25 kDa cysteine protease typically expressed in neurons. Present in almost all neurons, UCH-L1 makes up about 2% of total soluble brain protein.[100] As the name suggests, it hydrolyzes the C-terminal of ubiquitin or unfolded polypeptides, and data suggest that it plays an important role in the removal of misfolded proteins during normal conditions and following injury. Mean CSF levels of the protein were found to be highly elevated in patients with severe TBI as measured by ELISA.[101] UCH-L1 was also found to be elevated in serum of severe TBI patients in the acute phase, typically defined as <24 h post-injury, and elevation of UCH-L1 persisted for over a week post-injury.[102]

NSE, an iso-enzyme of enolase, is a glycolytic pathway enzyme that is highly expressed in the neuronal cytoplasm.[103] It is also highly specific to neuronal cell death. A two-fold increase in NSE was observed across 85 patients sustaining severe TBI compared to normal reference values, and NSE serum levels were also correlated with injury severity and CT findings.[104] However, NSE concentrations were unable to differentiate mTBI patients (GCS 13-15) presenting with symptoms from an

asymptomatic head contusion group (GCS = 15).[105] These results indicate that the utility of NSE as a biomarker may be limited to severe TBI.

Alpha-II spectrin is a 240 kDa structural protein abundant in axons, and spectrin breakdown products (SBDPs) have also been implicated as biomarkers of TBI.[106] The cytoskeletal protein α-II spectrin is involved in both apoptotic (caspase-3-mediated) and necrotic (calpain-mediated) cell death. Calpain cleaves the protein to breakdown products SBDP150 and SBDP145, whereas capsase-3-mediated cleavage results in the formation of SBDP120.[107] Increased CSF concentrations of SBDPs have been found in both rat and human severe TBI samples.[108,109]

Tau, a natively unfolded protein, binds to and stabilizes microtubules in brain cells.[110] Tau is subject to a number of post-translational modifications, including phosphorylation.[111] Buildup of phosphorylated-tau (p-tau) protein is a hallmark of Alzheimer's disease (AD).[112] Following injury, tau is cleaved by calpain-1 and capsase-3, forming cleaved tau (c-tau), which can diffuse through a disrupted BBB into serum and CSF.[113] Concentrations in CSF are 10 times higher than in plasma due to clearance rates, making CSF a better sample source than blood.[114] In a study of severe DAI, levels of c-tau were shown to rise nearly 1000-fold by 1 h and 40,000-fold at 24 h post-injury.[115,116] A recent study showed a measurable increase total tau in the plasma of concussed hockey players compared to preseason baselines.[117] Tau, and other proteins localized to the neurons offer attractive targets for proteomic biomarker studies of TBI.

1.6.1.2 Astroglial Proteins

Because glial fibrillary acidic protein (GFAP) is not found outside the nervous system but only in the astroglial cytoskeleton, it is considered a very promising candidate for selective TBI diagnosis. During brain injury, astroglial cells enter a reactive state and increase production of GFAP, while levels of the protein do not spike without brain injury even when other injuries are present.[118] Patients with mTBI were also found to have elevated concentrations of GFAP breakdown products.[119] Additionally, GFAP histological staining is commonly used as a technique to quantify reactive astrocytes and identify pathologies associated with TBI.[120] A panel combining UCH-L1 and GFAP was recently developed to determine the need for CT scan in the setting of TBI, but again this is limited to detection of injury that results in visible hemorrhage, intracranial lesions and other macrostructural damage, which does not typically result from mTBI.[121]

S100β is a calcium binding protein involved in signal transduction and is a structural damage marker of CNS injury.[122] S100β is found predominantly in astroglia and Schwann cells, but it is not brain specific as it is also found in adipocytes, epidermal, chondrocytes, and Langerhans cells.[123,124] Its concentration has been found to increase after injury, but it has a biological half-life of only 2 h and thus must be measured quickly after injury in order to be detectable.[125] It is also upregulated in the setting of infection, bone fractures and other non-TBI related disease states, indicating that general trauma without brain injury can increase S100β concentration levels, limiting its clinical utility.[126]

1.6.2 Lipophilic Molecules

Lipids are generally defined as organic molecules that are soluble in organic solvents such as methanol, isopropyl alcohol (IPA), or hexane.[127,128] Lipids can be subdivided into 8 distinct classes based on their structure: 1) fatty acyls, 2) glycerolipids, 3) glycerophospholipids, 4) sphingolipids, 5) sterol lipids, 6) prenol lipids, 7) saccharolipids, and 8) polyketides.[129] The primary component of all lipids, or the smallest basic subunit, is a fatty acid, an amphiphilic organic molecule with a neutral hydrocarbon tail at one end and a terminal, polar carboxyl head at the other. Lipids' primary functions include energy storage (primarily as triglycerides), acting as first and second messengers in signal transduction, and playing a critical role in cellular membrane composition, metabolism.[130] Outside of the cell, a primary messenger, or chemical signaling molecule, binds to the surface of the cell membrane receptors. Sensing this ligand binding, the cells respond by activating enzymes in the lipid bilayer, causing the cleavage of lipids in the membrane. Referred to as secondary messengers, these molecules can then bind to intracellular enzymes and cause the activation of a desired intracellular process. Fatty acid amides, such an anandamide and oleamide, commonly serve as signaling molecules *in vivo*. Concentrations of these signaling molecules, belonging to a class of lipids known as N-acylethanolamines, are tightly regulated by enzymatic synthesis and degradation, though their biological role is mediated through receptor binding.[131] For instance, the binding of vitamin D3 to the lipid membrane induces sphingomyelinase activity, initiating a sphingomyelin (SM) signaling pathway through the generation of ceramides by hydrolysis, which serve as second messengers in many biological processes.[132, 133] The hydrocarbon chain of each fatty acyl typically varies between 12 and 26 carbon units in

length, with even numbered chains composing the vast majority of endogenous molecules in mammalian species, although odd chain fatty acids (OCFAs) may be found more commonly in plant-based organisms. The difference in fatty acid composition in animals arises from their synthetic pathway, in which the coupling of 2-acetyl-CoenzymeA (CoA) molecules leads to the generation of exclusively even chain fatty acids (ECFAs). The synthetic process is initiated by the transfer of acetyl-CoA from the mitochondria to the cytosol.[134]

Fatty acid synthesis starts with the irreversible conversion (carboxylation) of acetyl-CoA to malonyl-CoA through the hydrolysis of ATP. The intermediates are then linked to an acyl carrier protein (ACP), forming acetyl-ACP and CoA. Malonyl transferase ($C_3H_4O_4$) is highly specific, ensuring that the fatty acid chain will be lengthened by exactly 2 carbon units per elongation cycle, while acetyl transferase can transfer a non-acetyl ($C_2H_4O_2$) group at a reduced rate. The acetyl-ACP and malonyl-ACP complexes condense to form acetoacetyl-ACP, releasing energy through a decarboxylation. The keto group at C3 is then reduced to a methylene group, with nicotinamide adenine dinucleotide phosphate (NADPH) acting as the reducing agent. The resultant D-3-hydroxybutyrl-ACP is dehydrated to form crotonyl-ACP, which is ultimately reduced to butyryl-ACP again using NADPH as the reducing agent, completing the first elongation cycle. The condensation reaction with malonyl-ACP, reduction, dehydration, and reduction processes can then be repeated to further elongate the fatty acid hydrocarbon chain. The enzymes that initiate fatty acid synthesis collectively form a single polypeptide chain called fatty acid synthase. This process stops

at palmitate (16:0), and double bonds as well as further elongation occurs *via* other enzymes.

Two separate systems exist for the synthesis of fatty acids: 1) the non-mitochondrial system which produces only palmitic acid (16:0) and is a true *de novo* synthesis, and 2) the mitochondrial system which produces stearic (18:0), palmitic, arachidic (20:0), myristic (14:0) and lauric (12:0) from the elongation of shorter chain fatty acids.[135]

While it was initially hypothesized as such, the β-oxidation degradation pathway is not in fact simply a reversal of the synthetic pathway. Degradation instead takes place in the mitochondria, and intermediates are covalently linked to the sulfhydryl group of CoA rather than that of the ACP as in synthesis. Nicotinamide adenine dinucleotide (NAD^+) and flavin adenine dinucleotide (FAD) act as the oxidants. The steps of the synthetic pathway are reversed, and the enzymes that catalyze the reaction are thus appropriately named ketoacyl reductase, hydroxyacyl dehydratase, and enoyl reductase.[136]

1.6.3 Lipid Biomarkers of TBI

1.6.3.1 Markers of Lipid Peroxidation

While brain specificity is a key characteristic for a number protein biomarker candidates of TBI, the inability to detect changes in their concentrations within biofluids in the setting of mTBI has led to questions over their utility.[137] Lipids constitute more than half of the dry weight of the brain, and a lipophilic barrier (the BBB) composed of endothelial cells acts to prevent the flux of molecules between the blood and brain. While CNS-specific proteins have proven to be outstanding markers of severe TBI, lipophilic

molecules can more easily permeate an intact BBB, and therefore serve as attractive targets for biomarker research into mTBI. Thus, changes in lipid profiles should be more readily detectable in biological matrices such as serum and plasma in mTBI where little or no disruption of the BBB is believed to occur.

Early lipidomic studies focused on markers of inflammation and oxidative stress, such as malondialdehyde (MDA), 4-hydroxynonenal (4-HNE) and thiobarbituric reactive substances (TBARS), produced by the autooxidation of PUFAs.[138,139] This research investigated the role of the oxidative stress mechanism in TBI, involving the peroxidation of lipids by ROS. The brain is especially susceptible to free radical-mediated oxidative stress due to its elevated PUFA content.[38,39]

Following TBI, ROS react with proteins and lipids in the brain, inducing oxidative damage. Autooxidation proceeds *via* a process consisting of initiation, propagation and termination, beginning with the abstraction of a hydrogen atom from the carbon adjacent to a double bond where a new hydroxyl bond can form.[140] Oxygen is then added to the carbon radical *via* a number of free radical sources, after which cyclization, rearrangement of atoms or termination of the process is likely to occur. Lipids are essential components of cell membranes and also represent the primary targets of free radical mediated oxidative damage. In addition to its role in TBI pathophysiology. LP has been implicated in a host of other diseases such as cancer[141], diabetes,[142] and AD.[143]

The LP process leads to fragmentation of PUFAs, with MDA and 4-HNE being the most abundant products and acrolein (2-propenal) as the most reactive product.[24] These cytotoxic aldehyde end products can bind to amino acids such as lysine, histidine,

and cysteine to form "protein carbonyls," disrupting cellular protein function.[144] A wide range of aldehydes are formed in biological systems from the oxidation of both linoleic acid and arachidonic acid (AA).[145] These cytotoxic aldehydes were discovered in the early 1960s and can be used as an index of LP.[146] A study of mTBI in rats showed that MDA rose immediately from non-detectable levels in controls, reaching maximum values within 2 h.[138] Intense immunostaining for 4-HNE was apparent in rat brain tissues within 1 h of TBI, increasing up to 24 h and persisting until 96 h post-injury.[139]

MDA and like compounds can react with thiobarbituric acid (TBA) to form adducts with a measurable colorimetric change.[24] TBI has been shown to significantly increase TBARS levels in rat brain tissue homogenate.[147] Significant changes in concentration were found in human plasma at 30 h and 72 h post-injury, and increased TBARS compared to healthy controls were observed as early as 12 h post-injury.[38] Significant differences in TBARS levels have also been observed in TBI survivors vs. non-survivors, and a correlation between graded head injury and erythrocyte TBARS levels has been established.[148,149] However, other studies indicated that TBARS were not specific markers of LP, and levels of both MDA and TBARS remained unchanged in patients after isolated head injury.[150] Additionally, when MDA and 4-HNE bind to proteins, the LP products will not react with TBA and will not be detected. Therefore a major criticism is that the assay only measures the unbound portion, which is relatively minor.[38] It has become increasingly evident that oxidation of membrane lipids is a primary consequence in certain sub-populations incurring a TBI, and further study into products detectable in readily accessible biological fluids such as serum and CSF could form the basis of future biomarker studies.

Oxidation of PUFAs also leads to the formation of a biologically active series of lipid mediators, a subclass of eicosanoids known as prostaglandins.[151] Based on the 20-carbon prostanoic fatty acid, prostaglandins are formed by enzymatic oxidation of PUFAs, specifically AA. This process is catalyzed in the brain by the highly expressed cyclooxygenase (COX)-2 enzyme.[152] This enzyme does not attack arachidonoyl residues of phospholipids, rather only free fatty acids (FFAs). The non-enzymatic, free radical-catalyzed peroxidation of AA esterified to phospholipids leads to the formation of F_2-isoprostanes, prostaglin-F2$_\alpha$-like compounds ($PGF_{2\alpha}$).[153] Interestingly, F_2-isoprostanes were discovered as bi-products of improper storage of arachidonoyl-containing lipids in plasma and are stable products of the oxidation of AA. They are produced *in vivo* independent of COX activity. An F_2-isoprostane with inverted stereochemistry at the side chain hydroxyl group, 8-iso-$PGF_{2\alpha}$ or 8-epi-$PGF_{2\alpha}$ is considered the most reliable marker of LP, and most studies of lipid biomarkers of TBI have focused on measurements of this molecule.[122,154,155] While isoprostanes can be markers of improper sample storage conditions, their formation by autoxidation of lipids is completely inhibited at -70°C.[156]

F_2-isoprostanes are relatively stable molecules that can be used to measure oxidative stress. Though similar in structure to prostaglandins, isoprostanes are typically found in blood at concentrations one to two orders of magnitude higher.[155] Autoxidation can involve the non-enzymatic oxidation of either free or esterified PUFAs with free radicals and is catalyzed by transition metals. However, *in vivo* the majority of isoprostanes are formed *via* the oxidation of AA in the SN2 position of phospholipids, because these fatty acids at these ester sites are much more readily oxidized than unbound fatty acids.[157] 8-*iso*-$PGF_{2\alpha}$ is also found in plasma as a FFA, but it is not formed directly

from the oxidation of free AA. Rather it is still formed in situ and subsequently cleaved from the ester site, though the esterified species are always more prevalent.[153] Numerous studies have demonstrated the utility of these lipid mediators as potential biomarkers of TBI. F2-isoprostanes were increased in CSF after severe TBI in young children.[158] 8-*iso* $PGF_{2\alpha}$ was increased in brain extracts at 6 h and 24 h post injury, as were fluorescent end products of LP.[159] 8-*iso* $PGF_{2\alpha}$ was increased in both the CSF and serum of a clinical cohort after severe TBI.[160]

Containing a tetrahydrofuran ring but formed under similar conditions, isofurans were increased in the CSF of patients after severe TBI, as were F4-neuroprostanes, the oxidized products of docosahexaenoic acid (DHA).[161] The 8,12-iso-iPF2a-VI isomer has also been shown to be increased at acute timepoints following moderate TBI using the FPI model to induce injury in rats.[162]

1.6.3.2 Fatty Acids

FFAs have been shown to exhibit measurable increases as a consequence of TBI, likely stemming from the activation of phospholipase A_2 (PLA_2), resulting in their cleavage from membrane phospholipids.[163] In one study, free AA and DHA were increased within 30 min, and this was followed by hydrolysis of DHA containing phospholipids. Increases in FFAs were still observed at 24 h, with increases in DHA and stearic acid being most significant.[164] Similarly AA, DHA, and myristic acid were all shown to be increased in CSF of humans after TBI of varying severity, and higher levels of these FFAs were associated with poorer outcome.[165] Other studies have demonstrated increases in a variety of other fatty acids in serum following TBI, including decanoic and octanoic acid, and these increases were strongly associated with injury severity.[166,167]

Additionally, depletion of PUFAs such as DHA appears to have detrimental effects on recovery, as depletion of DHA in the brain resulting from diet led to slower recovery and worse outcomes in mice.[168] DHA supplementation also appears to attenuate increases in the protein biomarker NFL following injury in a population of American football players, and similar results were demonstrated for DHA administered pre-injury in a pre-clinical population.[169,170] These studies indicate that DHA in the brain may provide resilience against propagation of injury.

1.6.3.3 Phospholipids

Phospholipids are the building blocks of both plasma and intercellular membranes, and they also compose about 25% of the dry weight of the brain.[171] Glycerophospholipids such as phosphatidylcholines (PCs) and phosphatidylethanolamines (PEs) comprise the majority of phospholipids in mammalian cell membranes.[172] These two types of lipids are also the most abundant in mitochondria, with PE species being highly enriched in the inner leaflet. PCs and PEs also play a critical role in the formation and stability of lipoproteins. Several studies have investigated the role of membrane phospholipids in TBI. Using CCI injury in a mouse model, lower levels of cortical and cerebellar PCs, SMs and PEs have been discovered, while hippocampal PCs, PEs, and SMs were elevated. Levels of ether PCs were found to be lower in the cortices and plasma of injured animals, while PUFA containing PCs, especially those containing esterified DHA, were lower in cortices, hippocampi, and plasma of injured animals.[173] Increased levels of PCs and PEs in CSF have been associated with worse outcome in severe TBI patients.[174]Another group discovered that ether containing PE species were elevated at 24 h, while AA and DHA containing

phospholipids significantly decreased at chronic stages, including lower levels of PCs, PEs, phosphatidylinositols (PIs), and SMs at 24 months post-injury, indicating that TBI results in long term, significant decreases in circulating phospholipids.[175]

Overall, many of the studies describing alterations in lipid profiles have been conducted in brain tissue using 2-dimensional sections to study changes at the injury site. One study using mass spectrometry imaging (MSI) demonstrated that the potassiated adduct of the most abundant PC species PC(16:1/16:0) was significantly decreased in the brain of a rat injured by CCI, with a corresponding increase in the sodiated adduct, likely influenced by the loss of Na^+/K^+-ATPase activity and ionic fluxes caused by injury.[176] Recently, the first 3-dimensional study of brain lipid alterations stemming from TBI demonstrated that one species, PC(42:9), was uniquely expressed in injured tissue while a different PC species (*m/z* 797.59) showed increased distribution in the ventricular system.[177] The data collected were limited to positive mode, where PCs are highly abundant and dominate the spectra, indicating that more can be learned by mapping the complete spatial distribution of lipid alterations in the brain following TBI.

Phosphatidic acids (PAs) are lipid messengers involved in protein synthesis *via* the mTOR signaling pathway.[178] PAs have been shown to be elevated in the CSF within 24 h post-injury.[179] Through direct analysis of brain tissue, dramatic increases in lysoPA and lysoPA precursors in the brain were discovered within 1 h post-injury.[180] Levels of lysoPA have also been shown to increase in CSF and blood within 24 h post-injury, making these molecules interesting biomarker candidates.

Like many other lipids, diacylglycerols (DGs) play a variety of roles within the cell, including serving as intermediates in lipid metabolism, functioning as components

of cell membranes, and acting as second messengers in signal transduction, stimulating protein phosphorylation.[181,182] DGs have been shown to be increased in the cerebellum and the injured frontal right motor cortex 1 day post-injury, with DHA containing DGs showing the largest increase.[164] DGs were also increased following CCI in the brain extracts of rats at 4 days post-injury in all frontal and occipital cortical areas, while they were even further increased in all cortical areas over one month post-injury. The highest measured increases were associated with DHA, stearic acid and AA containing DGs.[183]

Increases in DGs at injury site have also been demonstrated in tissue, likely resulting from increases in phospholipase C (PLC) activity. Subsequent degradation of phospholipids including decreases in two DHA-containing PEs (16:0_22:6, 18:0_22:6), PC(34:1), and an AA containing PI species, PI(16:0_20:4), were observed at 3 days post-injury.[184] Another group showed that DHA containing membrane lipids PE(18:0_22:6), PE(p18:0_22:6) and PS(18:0_22:6) were decreased in the acute phase, while they were gradually increased in the chronic repair phase.[185] Accordingly, LysoPE(22:6) was increased initially but decreased at later time points.

Changes in lipid concentrations have be used to objectively classify TBI samples from controls through the combination of multiple related biomarkers into a single diagnostic panel. In one such study, a panel of 6 lipids was able to discriminate between athletes with mTBI and non-injured teammates at each of the time points measured (<6 h, 2d, 3d, and 7d post-mTBI). This panel consisted of 2 PUFA-containing PE species, lysoPC(20:4) and a number of fatty acids- FFA(18:0), FA 2-OH C16:0, and tauroursodeoxycholic acid- with the direction of change being species specific.[186] The ability of these 6 lipids to classify injury in both the initial college athlete cohort as well

as a separate independent cohort indicates the utility of lipid biomarkers to detect changes associated with TBI and make predictive assessments of TBI using objective methods.

Cardiolipins (CLs) are a class of diphosphatidylglycerol lipids that have been implicated as biomarkers of oxidative damage stemming from TBI.[187,188] CLs consist of two phosphate head groups, three glycerol molecules and four total fatty acyl chains. CLs are exclusively present in the mitochondria of eukaryotic cells and are highly enriched in the mitochondrial inner membrane.[189] The diversity of CLs in the brain compared to other tissues allows for the selection of these molecules as target biomarkers of TBI. Brain CLs typically possess high PUFA content, resulting in LP induced by hydrogen peroxide or other sources of free radicals. The exclusive presence of these PUFA containing CLs in brain mitochondria reveals the potential susceptibility of brain CL to oxidative stress. Detection of these specific molecules at elevated levels in locations outside of the brain, e.g. in blood, may be indicative of a BBB breach. Highly unsaturated CLs, each containing at least one AA residue, were particularly susceptible to this trend. Applying oxidative lipidomics to study lipids in the brain after TBI, it was shown that CLs were selective targets for oxidative, while PCs and PEs were unaffected acutely, despite their high abundance. While all major phospholipid classes contain readily oxidizable PUFA residues, only the formation of oxidized CLs was observed at early acute timepoints while only minor oxidation of other species, mainly minor anionic phospholipids, was observed at 24 h post-injury.[190] Preventing CL oxidation in the brain has also been shown to reduce neuronal death, behavioral deficits and cortical lesion volume.[191] Similarly, other anionic phospholipids such as phosphatidylserines (PSs), sulfatides and PIs, have proven to be selective targets for oxidative damage in a number of studies.[188,192]

1.6.3.4 Sphingolipids

Representing one of 8 major classes of lipids, sphingolipids such as SMs and ceramides were named for the tissues in which they were first discovered but are not necessarily unique to neuronal tissues.[193] They play key roles in signaling pathways such as cellular senescence, proliferation, differentiation and cell cycle arrest as well as programmed cell death.[194] SM is a phospholipid enriched in the brain that plays a large role in structural organization, tightly packing with saturated fatty acids and cholesterol in the intracellular membrane to form membrane rafts.[195] While sphingolipids compose 22% of the dry weight in white matter, their abundance is much lower in plasma (5%), though they are major components of plasma membranes.[196,197] Therefore, changes in circulating levels of sphingolipids are hypothesized to relate to changes originating in the brain. Many sphingolipids also modulate cellular calcium homeostasis, which is a critical outcome of TBI pathophysiology.[198] Playing a role in signaling pathways, sphingosine receptors modulate both pro- and anti-inflammatory cascades. Sphingosine-1-phosphate (S1P) receptors have been related to microglial activation and vascular dysfunction using a mouse model of cerebral ischemia.[199] Sphingosine-1-phosphate receptor subtype 1 ($S1P_1$), the most abundant S1P receptor, can trigger microglial activation, leading to ischemic brain damage.[200] It has been shown to act *via* regulation of macrophage 1 (M1)/M2 polarization, which modulates both pro- and anti-inflammatory cascades.[201] Other S1P receptors exert pathogenic roles in cerebral ischemia through microglial activation and vascular dysfunction. Another study of CCI injury in rats demonstrated increases in circulating sphingolipids, specifically the molecules SM(37:1) and SM(38:3).[202]

Much of the endogenous SM in a cell exists in lipid rafts, which are the sites of ceramide generation and signal transduction. Ceramides serve as precursors for the synthesis of complex sphingolipids and also promote non-lamellar phase formation. Ceramides undergo transmembrane movements much faster than do SMs, moving across the lipid bilayer and facilitating the movement of other lipids.[203] The release of ceramides as secondary messengers can be indicative of cell growth suppression or the onset of apoptotic or necrotic cell death.[204] Numerous studies have demonstrated increases in ceramides in the brain associated with TBI pathophysiology. For instance, Hankin *et. al.* showed an increase in Cer(d18:1/18:0) in the hippocampal region following ischemia/ reperfusion injury in rats.[176] Roux *et. al*. also demonstrated an increase of the same molecule as early as 1-day post-injury, while low mass SMs were increased near the injury site and decreased in the rest of the brain. Intermediate mass ceramides and SMs showed opposite trends (SM decrease, Cer increase), as was seen throughout the whole brain.[184] Interestingly, other studies of TBI resulted in increases in a variety of ceramides including Cer(34:1), Cer(36:2), Cer(36:1), and Cer(38:1), specifically in the dorsal half of the section containing the injury site following CCI, and their concentrations were shown to decrease with treatment with a peptide agonist, indicating that prevention of ceramide dysregulation after injury may result in better outcomes.[205] However another study demonstrated a uniform decrease in all measured ceramides in the mouse brain after blast injury.[206] Decreases in brain ceramides are likely related to the utilization of ceramides for SM synthesis.[207] These mixed results demonstrate the difficulty in studying the chemical response to heterogenous injury subtypes and severities, given the complex interplay of beneficial and detrimental inflammatory pathways.

Gangliosides are glycosphingolipids located in the outer leaflet of neuronal membranes. They are composed of a ceramide and an oligosaccharide with sialic acid(s) linked to the sugar chain and represent approximately 6% of the total brain lipid. A number of studies have looked at changes in gangliosides in addition to the previously discussed ceramides and SMs since these lipids are much more highly concentrated in the CNS.[184,206] Ganglioside monosialic 1 (GM1) is highly abundant, composing 21% of total gangliosides, while GM2 represents just a fraction of this at < 0.5%. An increase in the ganglioside GM2(d18:1/C18:0) was discovered after blast injury in mouse brain tissue. These changes were localized to the hippocampus, thalamus, and hypothalamus, and increases were observed at early acute timepoints (<24 h) but had normalized by 72 h.[206] Overall, the dysregulation of sphingolipids stemming from onset of TBI requires further investigation, but offers promise due to their heightened association with the CNS.

1.6.3.5 Sterols

The sterol class of lipids, including cholesterol, steroids and bile acids, may be vitally important to the regulation of neurological disorders. Disproportionate to the relative mass of the brain, greater than 25% of total cholesterol is found within the brain, where it plays a critical role in membrane function and serves as the precursor for the synthesis of neurosteroid hormones such as progesterone and pregnanolone.[208] Lecithin: cholesterol acyltransferase forms the majority of cholesteryl esters (CEs) in circulation, transferring long chain fatty acids from PC species to esterify the free cholesterol.[209] Cholesterol may also be metabolized to a variety of other end products, such as cholesterol sulfate (CS), which regulates membrane packing efficiency and is found in higher abundance in DHA rich membranes.[210] Altered cholesterol metabolism in the

brain may be linked to genotype. Apolipoprotein E (ApoE) is critical to maintenance, growth and repair of neurons, and is responsible for sterol transport. A specific allele, ApoE4, was also associated with large changes in both sterol and sphingolipid content in the brains of AD patients.[211] The ApoE4 allele has long been associated with early onset and faster progression of AD, and may also play a role in determining outcome in TBI.[212]

1.7 Tools for Measuring Biomarkers

Metabolomics is the comprehensive study of all small molecules in a biological system related to the organism's metabolism.[213] Lipidomics, a subset of the metabolomics field, involves the study of all lipids within such systems.[214] Both methods of research are commonly used to generate data for the purpose of biomarker discovery. Biomarker studies can be classified as either targeted or non-targeted, each involving slightly different approaches.[215] Typical non-targeted studies are data-driven and focus on the study of the full complement of molecules in a given biological system, attempting to discover which analytes are influenced most by the presence or absence a given disease state or condition. Workflows involve a number of steps, including sample collection, preparation, analysis and subsequent chemical identification of target molecules. Once identified, biomarkers can be mapped to their metabolic pathways to relate these products to their role in a specific disease state such as TBI.[216]

Targeted studies follow a slightly different approach, as a smaller number of molecules known to be involved in the onset of disease are selected prior to sample analysis. For instance, class-specific changes in lipids are investigated using mass spectrometry (MS) through the development of product ion scans, multiple reaction

monitoring (MRM), or neutral loss scans in order to identify and quantify one or more target molecules within a specific lipid class. Based on the method of data acquisition, unknown targets cannot be identified using these studies as the approach is limited to the preselected molecules of interest.[217] Targeted studies are advantageous when a defined pathophysiological outcome can be used to generate a hypothesis about how specific analytes will be affected by the occurrence of a disease. Based on the limited research guiding lipid biomarkers of TBI, the work contained within this thesis was generated using non-targeted approaches, which are described in more detail below.

1.7.1 Sample Collection and Storage

While preliminary experiments must investigate direct changes in the affected brain tissue to discover injury specific changes in biomarker composition, collection must be done post-mortem, which presents an obvious challenge for the diagnosis of concussion in living patients. Because of this, collection of peripheral biofluids is necessary for clinically useful biomarker studies and the potential development of future diagnostic tools. Biofluids such as blood (including whole blood, serum, or plasma), urine, CSF and saliva have all been implemented successfully for use in discovery-based, data-driven lipidomics approaches.[218,219,220,221] To ensure reproducibility of results it is imperative that all samples be collected using identical methods and stored under the same conditions to ensure the only variable being investigated relates to the biological question of interest. Typically, samples are stored at low temperatures (e.g. -80° C) to prevent degradation from storage for long periods of time.[222,223]

1.7.2 Sample Preparation

Many sample preparation techniques have been developed and compared for use in lipidomic biomarker studies.[224] Biological fluids such as blood samples contain large amounts of both lipid and protein, which must be separated in order to conduct MS analysis. Typical separation techniques can be classified as either protein precipitations or liquid/liquid extractions. Protein precipitation methods are simpler, allowing for higher throughput studies. Typically, an excess (≥3:1 v/v) of organic solvent such as methanol or IPA is added to a small amount of aqueous sample.[224] Upon centrifugation, the proteins that were soluble in the aqueous biofluid are precipitated out of solution, and the lipophilic portion of the samples is collected within the supernatant. Based on chemical interactions, methanol is a useful solvent for extracting cell-membrane lipids (e.g. phospholipids, and cholesterol) and is commonly used in metabolomics experiments.[225] However, these simple methods often lead to incomplete extraction of lipids, specifically neutral lipids, and truly quantitative experiments should use liquid/liquid extraction approaches such as the Folch[226] or Bligh-Dyer[227] methods, which combine chloroform, methanol, and water to form distinct aqueous and organic phases into which the proteins and lipids can be partitioned. These extractions are advantages for the study of a more diverse range of lipids. Alternative extractions utilizing methyl tert-butyl ether (MTBE) have been proposed, which offer similar extraction efficiencies but place the organic phase on top of the aqueous phase due to solvent density, allowing for easier collection of the lipid layer of interest.[228]

1.7.3 Instrumental analysis

The increasing popularity of metabolomics and lipidomics biomarker studies has been aided by advancements in technology and instrumentation.[229] Since the mixtures being analyzed in non-targeted metabolomics studies are highly complex, MS and nuclear magnetic resonance (NMR) are the two most widely utilized techniques in the field.[230]

1.7.3.1 Mass Spectrometry

Biomarker discovery studies have been enabled by the advent of sophisticated MS instrumentation, fueling the growth of the fields of metabolomics and lipidomics.[229] Metabolomics studies often involve careful measurement of a large number of molecular targets, so advanced techniques are required beyond simple single-target assays. MS and NMR are the most commonly utilized platforms for metabolomics analysis, and each offers complementary advantages to research efforts.[231] MS studies are very fast, depending on the front-end separation, and offer unparalleled sensitivity.[232] MS techniques, principally liquid chromatography-mass spectrometry (LC-MS) and tandem mass spectrometry (MS/MS), are used throughout this thesis to study the serum and brain tissue of rodents incurring TBI induced by CCI as well as the cell extracts of phytoplankton competitors.

Different ionization modes and techniques can be used to analyze a wide range of target molecules, and a primary advantage of MS studies relates to sensitivity, which can reach into the pico- to femtomolar concentrations.[232] MS is also the preferred technology for targeted experiments due to the ease of separations coupling and the existence of a wide variety of analytical methods suited to single target analysis.[233] MS instrumentation

consists of three main components: an ionization source, a mass analyzer and a detector.[234] Ion sources produce gaseous ions from the sample, and commonly utilized sources include electrospray ionization (ESI) and matrix assisted laser desorption ionization (MALDI). Many other sources exist, including electron impact (EI), chemical ionization (CI), desorption electrospray ionization (DESI), fast-atom bombardment (FAB), secondary ion mass spectrometry (SIMS), etc. Different ionization modalities as well as the use of multiple polarities, allows for the ionization of a wider variety of molecules. Once in the gaseous state, the mass analyzer then separates ions on the basis of their mass to charge ratio (*m/z*). Common mass analyzers include quadrupole, time-of-flight (TOF), ion trap, or Fourier transform ion cyclotron resonance (FT-ICR) analyzers.[231] These ions are then detected based on *m/z* and their relative abundance is recorded. Common mass detectors include electron multipliers, photomultipliers, Faraday cups, and Orbitraps, which function as both a mass analyzer and detector.[235,236]

The front end of the mass spectrometer can be coupled to a separation technique, such as gas chromatography (GC) or liquid chromatography (LC) in order to separate the components of complex mixtures by time of elution, or retention time (RT). This ensures that all the ions are not detected simultaneously, which may lead to inaccuracy in relative quantification based on ion suppression. Additionally, separation prior to detection minimizes overlapping structural isomers as well as difficulty in accounting for isotopes from precursors of consecutive nominal masses.[237] A variety of front-end separation techniques take advantage of chemical interactions between the stationary phase and eluting analytes, including normal phase and reversed phased LC separations, which can separate a variety of lipid classes based on time of elution. Normal phase LC separates

mixtures based on head group polarity, but the presence of water in the solvent can alter analyte affinity to silica.[238] Reverse phase LC instead separates complex mixtures based on lipophilicity, such that fatty acyl chains determine the elution order while many classes of lipids may overlap in RTs, such as PEs and PCs.

1.7.3.2 Nuclear Magnetic Resonance

NMR offers distinct advantages over MS, as it is directly quantitative and does not require separation or derivatization steps. Additionally, NMR offers enhanced reproducibility and is non-destructive to samples. However, NMR instruments require highly skilled technicians to operate, are often more expensive to acquire and maintain, and require large amounts of space.[231] Though less than the capabilities of MS, approximately 100-200 metabolites can be measured in a single NMR experiment, depending on spectral resolution.

No single technique can quantify and identify all types of molecules within a sample, so a combination of techniques can be advantageous when studying complex biological systems. As complementary techniques, MS and NMR make a powerful impact, as is demonstrated in the fourth chapter of this thesis, relating to the study of the effects induced by *Karenia brevis* exposure.[239]

1.7.4 Chemometric Analysis

Advanced chemometric methods, such as Principal Component Analysis (PCA) and Partial Least Squares Discriminant Analysis (PLS-DA) can be used to identify important changes in individual components of complex mixtures, referred to as features and defined by their RT and *m/z* until chemically identified in data-driven experiments.[240] By projecting complex datasets into lower dimensional space (e.g. 2D or 3D), changes in

composition can be identified and readily visualized. PCA can be used to visualize inherent differences in the data and is classified as an unsupervised method. Variance captured will be based on inherent differences in the data, as class information is not considered in PCA analysis.[241] PLS-DA instead is a supervised approach, in that the class information is contained within the dataset being investigated and used to construct the multivariate models. The maximum variance between classes (or sample types) will be captured and defined by a hypothetical decision boundary. A sample's score will be a sum of each feature's relative abundance multiplied by its weighted contribution to the model, defining a sample as a point in Euclidean space.[242] Only features that contribute to accurate classification of different sample types will be selected by feature selection methods, ensuring that maximum variance is captured using the simplest possible multivariate model. Samples with similar scores on the statistical model can be classified collectively as a group will be separated by less Euclidian distance, allowing for clustering of similar and separation of different samples. Features can be combined linearly to calculate a score for a multi-feature model, which is then used to create a classification panel for distinction of sample types. Other common classifiers used for feature selection operate under similar principles but may offer inherent advantages based on the specific dataset being analyzed. Examples include Bayesian, K-nearest neighbors (KNN), logistic regression, support vector machines (SVMs), and random forest algorithms.[243]

1.7.5 Chemical Identification and Pathway Mapping

NMR offers the advantage of providing clear structural information for analytes, this technique is inherently limited by moderate sensitivity and overlapping signals in ^{1}H

NMR spectra of lipids. Liquid chromatography tandem mass spectrometry (LC-MS/MS) is the most powerful tool for structural identification of lipid mediators due to high sensitivity and specificity provided by the combined separation of complex mixtures and unique fragmentation patterns.[244] Lipids can be categorized into 8 distinct classes, and these classes such as phospholipids, a main focus of study in the field of TBI biomarkers, can be similarly subdivided using MS/MS fragmentations patterns to identify distinct polar headgroups.[129,245] Negative mode data are more useful for chemical identification of lipids, as esterified fatty acid chains can be determined, reducing the number of possible structural isomers to a single molecule.[246] The feature selection methods described above coupled to chemical identifications leads to the discovery of a host of potential biomarker candidates. Chemical identification of these unknown features in non-targeted experiments is critical in relating experimental observations to known metabolic pathways.[247,248]

1.8 References

1. Langlois, J. A.; Rutland-Brown, W.; Wald, M. M., The epidemiology and impact of traumatic brain injury: a brief overview. *The Journal of head trauma rehabilitation* **2006,** 21, (5), 375-378.

2. Faul, M.; Xu, L.; Wald, M. M.; Coronado, V., Traumatic Brain Injury in the United States. *Atlanta, GA: Centers for Disease Control and Prevention, National Center for Injury Prevention and Control* **2010**.

3. Berg, J.; Tagliaferri, F.; Servadei, F., Cost of trauma in Europe. *European Journal of Neurology* **2005,** 12, (s1), 85-90.

4. Bruns, J.; Hauser, W. A., The Epidemiology of Traumatic Brain Injury: A Review. *Epilepsia* **2003,** 44, 2-10.

5. Finkelstein, E.; Corso, P. S.; Miller, T. R., *The incidence and economic burden of injuries in the United States*. Oxford University Press, USA: 2006.

6. Kraus, J. F.; Fife, D.; Conroy, C., Pediatric brain injuries: the nature, clinical course, and early outcomes in a defined United States' population. *Pediatrics* **1987,** 79, (4), 501-507.

7. Kay, T.; Harrington, D. E.; Adams, R.; Anderson, T.; Berrol, S.; Cicerone, K.; Dahlberg, C.; Gerber, D.; Goka, R.; Harley, P.; Hilt, J.; Horn, L.; Lehmkuhl, D.; Malec, J., Definition of mild traumatic brain injury. *Journal of Head Trauma Rehabilitation* **1993,** 8, (3), 86-87.

8. Adekoya, N.; Thurman, D. J.; White, D. D.; Webb, K. W., Surveillance for traumatic brain injury deaths--United States, 1989-1998. *MMWR. Surveillance summaries : Morbidity and mortality weekly report. Surveillance summaries / CDC* **2002,** 51, (10), 1-14.

9. Langlois, J. A.; Kegler, S. R.; Butler, J. A.; Gotsch, K. E.; Johnson, R. L.; Reichard, A. A.; Webb, K. W.; Coronado, V. G.; Selassie, A. W.; Thurman, D. J., Traumatic brain injury-related hospital discharges. *MMWR Surveill Summ* **2003,** 52, (4), 1-20.

10. Stein, D. G., Embracing failure: what the phase III progesterone studies can teach about TBI clinical trials. *Brain injury* **2015,** 29, (11), 1259-1272.

11. Davis, A. E., Mechanisms of traumatic brain injury: biomechanical, structural and cellular considerations. *Critical care nursing quarterly* **2000,** 23, (3), 1-13.

12. Adams, J.; Graham, D.; Scott, G.; Parker, L.; Doyle, D., Brain damage in fatal non-missile head injury. *Journal of clinical pathology* **1980,** 33, (12), 1132.

13. Dixon, C. E.; Clifton, G. L.; Lighthall, J. W.; Yaghmai, A. A.; Hayes, R. L., A controlled cortical impact model of traumatic brain injury in the rat. *Journal of neuroscience methods* **1991,** 39, (3), 253-262.

14. Marklund, N.; Hillered, L., Animal modelling of traumatic brain injury in preclinical drug development: where do we go from here? *British journal of pharmacology* **2011,** 164, (4), 1207-1229.

15. Thompson, H. J.; Lifshitz, J.; Marklund, N.; Grady, M. S.; Graham, D. I.; Hovda, D. A.; McIntosh, T. K., Lateral fluid percussion brain injury: a 15-year review and evaluation. *Journal of neurotrauma* **2005,** 22, (1), 42-75.

16. Prins, M.; Greco, T.; Alexander, D.; Giza, C. C., The pathophysiology of traumatic brain injury at a glance. *Disease models & mechanisms* **2013,** 6, (6), 1307-1315.

17. Marmarou, A.; Foda, M. A. A.-E.; Van Den Brink, W.; Campbell, J.; Kita, H.; Demetriadou, K., A new model of diffuse brain injury in rats: Part I: Pathophysiology and biomechanics. *Journal of neurosurgery* **1994,** 80, (2), 291-300.

18. Wang, Y.; Wei, Y.; Oguntayo, S.; Wilkins, W.; Arun, P.; Valiyaveettil, M.; Song, J.; Long, J. B.; Nambiar, M. P., Tightly coupled repetitive blast-induced traumatic brain injury: development and characterization in mice. *Journal of neurotrauma* **2011,** 28, (10), 2171-2183.

19. Cernak, I.; Savic, J.; Malicevic, Z.; Zunic, G.; Radosevic, P.; Ivanovic, I.; Davidovic, L., Involvement of the central nervous system in the general response to pulmonary blast injury. *Journal of Trauma and Acute Care Surgery* **1996,** 40, (3S), 100S-104S.

20. Friedlander, R. M., Apoptosis and Caspases in Neurodegenerative Diseases. *New England Journal of Medicine* **2003,** 348, (14), 1365-1375.

21. Zhou, H.; Chen, L.; Gao, X.; Luo, B.; Chen, J., Moderate traumatic brain injury triggers rapid necrotic death of immature neurons in the hippocampus. *Journal of neuropathology and experimental neurology* **2012,** 71, (4), 348-359.

22. Raghupathi, R.; Graham, D. I.; McIntosh, T. K., Apoptosis after traumatic brain injury. *J Neurotrauma* **2000,** 17, (10), 927-38.

23. Mendes Arent, A.; Souza, L. F. d.; Walz, R.; Dafre, A. L., Perspectives on Molecular Biomarkers of Oxidative Stress and Antioxidant Strategies in Traumatic Brain Injury. *BioMed Research International* **2014,** 2014, 18.

24. Giza, C. C.; Hovda, D. A., The new neurometabolic cascade of concussion. *Neurosurgery* **2014,** 75, (0 4), S24.

25. Takahashi, H.; Manaka, S.; Sano, K., Changes in extracellular potassium concentration in cortex and brain stem during the acute phase of experimental closed head injury. *Journal of neurosurgery* **1981,** 55, (5), 708-717.

26. Ballanyi, K.; Grafe, P.; Ten Bruggencate, G., Ion activities and potassium uptake mechanisms of glial cells in guinea-pig olfactory cortex slices. *The Journal of Physiology* **1987,** 382, (1), 159-174.

27. Giza, C. C.; Hovda, D. A., The neurometabolic cascade of concussion. *Journal of athletic training* **2001,** 36, (3), 228.

28. Yoshino, A.; Hovda, D. A.; Kawamata, T.; Katayama, Y.; Becker, D. P., Dynamic changes in local cerebral glucose utilization following cerebral concussion in rats: evidence of a hyper-and subsequent hypometabolic state. *Brain research* **1991,** 561, (1), 106-119.

29. Gardiner, M.; Smith, M.-L.; Kågström, E.; Shohami, E.; Siesjö, B. K., Influence of blood glucose concentration on brain lactate accumulation during severe hypoxia and subsequent recovery of brain energy metabolism. *Journal of Cerebral Blood Flow & Metabolism* **1982,** 2, (4), 429-438.

30. Kochanek, P. M.; Hendrich, K. S.; Dixon, C. E.; Schiding, J. K.; Williams, D. S.; Ho, C., Cerebral blood flow at one year after controlled cortical impact in rats: assessment by magnetic resonance imaging. *Journal of neurotrauma* **2002,** 19, (9), 1029-1037.

31. Leão, A. A., Further observations on the spreading depression of activity in the cerebral cortex. *Journal of neurophysiology* **1947,** 10, (6), 409-414.

32. Osteen, C.; Giza, C.; Hovda, D., Injury-induced changes in NMDA receptor subunit composition contribute to prolonged calcium-45 accumulation in intact cortex. *J Neurotrauma* **2002,** 19, (10), 1384.

33. Robertson, C. L., Mitochondrial Dysfunction Contributes to Cell Death Following Traumatic Brain Injury in Adult and Immature Animals. *Journal of Bioenergetics and Biomembranes* **2004,** 36, (4), 363-368.

34. Lewén, A.; Fujimura, M.; Sugawara, T.; Matz, P.; Copin, J.-C.; Chan, P. H., Oxidative stress–dependent release of mitochondrial cytochrome c after traumatic brain injury. *Journal of Cerebral Blood Flow & Metabolism* **2001,** 21, (8), 914-920.

35. Büki, A.; Povlishock, J., All roads lead to disconnection?–Traumatic axonal injury revisited. *Acta neurochirurgica* **2006,** 148, (2), 181-194.

36. McAllister, T. W., Neurobiological consequences of traumatic brain injury. *Dialogues in clinical neuroscience* **2011,** 13, (3), 287.

37. Hohl, A.; Gullo, J. d. S.; Silva, C. C. P.; Bertotti, M. M.; Felisberto, F.; Nunes, J. C.; de Souza, B.; Petronilho, F.; Soares, F. M. S.; Prediger, R. D. S.; Dal-Pizzol, F.; Linhares, M. N.; Walz, R., Plasma levels of oxidative stress biomarkers and hospital mortality in severe head injury: A multivariate analysis. *Journal of Critical Care* **2012,** 27, (5), 523.e11-523.e19.

38. Collin, C.; Minami, M.; Parvez, H.; Saito, H.; Parvez, S.; Reiss, C., *Advances in Neuroregulation and Neuroprotection*. Taylor & Francis: 2005.

39. Siegel, G. J.; Agranoff, B. W.; Albers, R. W.; Fisher, S. K.; Uhler, M. D., Basic neurochemistry. **1999**.

40. Unterberg, A.; Stover, J.; Kress, B.; Kiening, K., Edema and brain trauma. *Neuroscience* **2004,** 129, (4), 1019-1027.

41. Jha, S., Cerebral edema and its management. *Medical Journal, Armed Forces India* **2003,** 59, (4), 326.

42. Quan, N.; Banks, W. A., Brain-immune communication pathways. *Brain, behavior, and immunity* **2007,** 21, (6), 727-735.

43. Ziebell, J. M.; Morganti-Kossmann, M. C., Involvement of pro-and anti-inflammatory cytokines and chemokines in the pathophysiology of traumatic brain injury. *Neurotherapeutics* **2010,** 7, (1), 22-30.

44. Lucas, S. M.; Rothwell, N. J.; Gibson, R. M., The role of inflammation in CNS injury and disease. *British journal of pharmacology* **2006,** 147, (S1), S232-S240.

45. Woodroofe, M.; Sarna, G.; Wadhwa, M.; Hayes, G.; Loughlin, A.; Tinker, A.; Cuzner, M., Detection of interleukin-1 and interleukin-6 in adult rat brain, following mechanical injury, by in vivo microdialysis: evidence of a role for microglia in cytokine production. *Journal of neuroimmunology* **1991,** 33, (3), 227-236.

46. Winter, C. D.; Iannotti, F.; Pringle, A. K.; Trikkas, C.; Clough, G. F.; Church, M. K., A microdialysis method for the recovery of IL-1β, IL-6 and nerve growth factor from human brain in vivo. *Journal of neuroscience methods* **2002,** 119, (1), 45-50.

47. Kossmann, T.; Hans, V.; Imhof, H.-G.; Stocker, R.; Grob, P.; Trentz, O.; Morganti-Kossmann, C., Intrathecal and serum interleukin-6 and the acute-phase response in patients with severe traumatic brain injuries. *Shock (Augusta, Ga.)* **1995,** 4, (5), 311-317.

48. Csuka, E.; Morganti-Kossmann, M. C.; Lenzlinger, P. M.; Joller, H.; Trentz, O.; Kossmann, T., IL-10 levels in cerebrospinal fluid and serum of patients with severe traumatic brain injury: relationship to IL-6, TNF-α, TGF-β1 and blood–brain barrier function. *Journal of neuroimmunology* **1999,** 101, (2), 211-221.

49. Kremlev, S. G.; Palmer, C., Interleukin-10 inhibits endotoxin-induced pro-inflammatory cytokines in microglial cell cultures. *Journal of neuroimmunology* **2005,** 162, (1-2), 71-80.

50. Bell, M.J.; Kochanek, P. M.; Doughty, L.A.; Carcillo, J.A.; Adelson, P.D.; Clark, R.S.; Wisniewski, S.R.; Whalen, M.J.; Dekosky, D.T., Interleukin-6 and interleukin-10 in cerebrospinal fluid after severe traumatic brain injury in children. *Journal of neurotrauma* **1997,** 14, (7), 451-457.

51. Knoblach, S. M.; Faden, A. I., Interleukin-10 improves outcome and alters proinflammatory cytokine expression after experimental traumatic brain injury. *Experimental neurology* **1998,** 153, (1), 143-151.

52. Soares, F. M. S.; de Souza, N. M.; Schwarzbold, M. L.; Diaz, A. P.; Nunes, J. C.; Hohl, A.; da Silva, P. N. A.; Vieira, J.; de Souza, R. L.; Bertotti, M. M., Interleukin-10 is an independent biomarker of severe traumatic brain injury prognosis. *Neuroimmunomodulation* **2012,** 19, (6), 377-385.

53. Ferreira, L. C. B.; Regner, A.; Miotto, K. D. L.; Moura, S. d.; Ikuta, N.; Vargas, A. E.; Chies, J. A. B.; Simon, D., Increased levels of interleukin-6,-8 and-10 are associated with fatal outcome following severe traumatic brain injury. *Brain injury* **2014,** 28, (10), 1311-1316.

54. Adibhatla, R. M.; Hatcher, J., Altered lipid metabolism in brain injury and disorders. In *Lipids in health and disease*, Springer: 2008; pp 241-268.

55. Teasdale, G.; Jennett, B., Assessment of coma and impaired consciousness: a practical scale. *The Lancet* **1974,** 304, (7872), 81-84.

56. Andelic, N.; Jerstad, T.; Sigurdardottir, S.; Schanke, A.-K.; Sandvik, L.; Roe, C., Effects of acute substance use and pre-injury substance abuse on traumatic brain injury severity in adults admitted to a trauma centre. *Journal of trauma management & outcomes* **2010,** 4, (1), 6.

57. McCrory, P.; Meeuwisse, W.; Dvorak, J.; Aubry, M.; Bailes, J.; Broglio, S.; Cantu, R. C.; Cassidy, D.; Echemendia, R. J.; Castellani, R. J., Consensus statement on concussion in sport—the 5th international conference on concussion in sport held in Berlin, October 2016. *Br J Sports Med* **2017,** 51, (11), 838-847.

58. McCrea, M.; Hammeke, T.; Olsen, G.; Leo, P.; Guskiewicz, K., Unreported concussion in high school football players: implications for prevention. *Clinical Journal of Sport Medicine* **2004,** 14, (1), 13-17.

59. Bruns Jr, J. J.; Jagoda, A. S., Mild traumatic brain injury. *Mount Sinai Journal of Medicine: A Journal of Translational and Personalized Medicine: A Journal of Translational and Personalized Medicine* **2009,** 76, (2), 129-137.

60. Hofman, P. A.; Stapert, S. Z.; van Kroonenburgh, M. J.; Jolles, J.; de Kruijk, J.; Wilmink, J. T., MR imaging, single-photon emission CT, and neurocognitive performance after mild traumatic brain injury. *American Journal of Neuroradiology* **2001,** 22, (3), 441-449.

61. Hulkower, M.; Poliak, D.; Rosenbaum, S.; Zimmerman, M.; Lipton, M. L., A decade of DTI in traumatic brain injury: 10 years and 100 articles later. *American Journal of Neuroradiology* **2013,** 34, (11), 2064-2074.

62. Niogi, S. N.; Mukherjee, P., Diffusion tensor imaging of mild traumatic brain injury. *The Journal of head trauma rehabilitation* **2010,** 25, (4), 241-255.

63. Bazarian, J. J.; Zhong, J.; Blyth, B.; Zhu, T.; Kavcic, V.; Peterson, D., Diffusion tensor imaging detects clinically important axonal damage after mild traumatic brain injury: a pilot study. *Journal of neurotrauma* **2007,** 24, (9), 1447-1459.

64. Wilde, E.; McCauley, S.; Hunter, J.; Bigler, E.; Chu, Z.; Wang, Z.; Hanten, G.; Troyanskaya, M.; Yallampalli, R.; Li, X., Diffusion tensor imaging of acute mild traumatic brain injury in adolescents. *Neurology* **2008,** 70, (12), 948-955.

65. Zhang, K.; Johnson, B.; Pennell, D.; Ray, W.; Sebastianelli, W.; Slobounov, S., Are functional deficits in concussed individuals consistent with white matter structural alterations: combined FMRI & DTI study. *Experimental Brain Research* **2010,** 204, (1), 57-70.

66. Scheibel, R.; Pearson, D.; Faria, L.; Kotrla, K.; Aylward, E.; Bachevalier, J.; Levin, H., An fMRI study of executive functioning after severe diffuse TBI. *Brain Injury* **2003,** 17, (11), 919-930.

67. McAllister, T. W.; Flashman, L. A.; McDonald, B. C.; Saykin, A. J., Mechanisms of working memory dysfunction after mild and moderate TBI: evidence from functional MRI and neurogenetics. *Journal of neurotrauma* **2006,** 23, (10), 1450-1467.

68. Ingersoll, C. D.; Armstrong, C. W., The effects of closed-head injury on postural sway. *Medicine and science in sports and exercise* **1992,** 24, (7), 739-743.

69. Kaufman, K. R.; Brey, R. H.; Chou, L.-S.; Rabatin, A.; Brown, A. W.; Basford, J. R., Comparison of subjective and objective measurements of balance disorders following traumatic brain injury. *Medical engineering & physics* **2006,** 28, (3), 234-239.

70. Guskiewicz, K. M.; Weaver, N. L.; Padua, D. A.; Garrett, W. E., Epidemiology of concussion in collegiate and high school football players. *The American journal of sports medicine* **2000,** 28, (5), 643-650.

71. Khasnis, A.; Gokula, R., Romberg's test. *Journal of Postgraduate Medicine* **2003,** 49, (2), 169-72.

72. McCrea, M.; Guskiewicz, K. M.; Marshall, S. W.; Barr, W.; Randolph, C.; Cantu, R. C.; Onate, J. A.; Yang, J.; Kelly, J. P., Acute effects and recovery time following concussion in collegiate football players: the NCAA Concussion Study. *Jama* **2003,** 290, (19), 2556-2563.

73. McCREA, M.; Barr, W. B.; Guskiewicz, K.; Randolph, C.; Marshall, S. W.; Cantu, R.; Onate, J. A.; Kelly, J. P., Standard regression-based methods for measuring recovery after sport-related concussion. *Journal of the International Neuropsychological Society* **2005,** 11, (1), 58-69.

74. Association, A. P., *Diagnostic and statistical manual of mental disorders (DSM-5®)*. American Psychiatric Pub: 2013.

75. Levin, H. S., A guide to clinical neuropsychological testing. *Archives of neurology* **1994,** 51, (9), 854-859.

76. Iverson, G. L.; Lovell, M. R.; Collins, M. W., Validity of ImPACT for measuring processing speed following sports-related concussion. *Journal of Clinical and Experimental Neuropsychology* **2005,** 27, (6), 683-689.

77. Maroon, J. C.; Lovell, M. R.; Norwig, J.; Podell, K.; Powell, J. W.; Hartl, R., Cerebral concussion in athletes: evaluation and neuropsychological testing. *Neurosurgery* **2000,** 47, (3), 659-672.

78. Smith, A., Symbol digit modalities test (SDMT) manual (revised) Western Psychological Services. *Los Angeles* **1982**.

79. LaPlaca, M. C.; Wright, D. W., Display enhanced testing for concussions and mild traumatic brain injury. In Google Patents: 2013.

80. Helmick, K. M.; Spells, C. A.; Malik, S. Z.; Davies, C. A.; Marion, D. W.; Hinds, S. R., Traumatic brain injury in the US military: epidemiology and key clinical and research programs. *Brain imaging and behavior* **2015,** 9, (3), 358-366.

81. Lovell, M., Evaluation of the professional athlete. *Sports-related concussion* **1999**, 200-214.

82. Lovell, M.; Burke, C., Neuropsychological testing in ice hockey. *Neurological Disorders of the Head and Spine. Philadelphia, WB Saunders Co* **2000**, 109-116.

83. Lovell, M. R.; Collins, M. W., Neuropsychological assessment of the college football player. *The Journal of head trauma rehabilitation* **1998,** 13, (2), 9-26.

84. Collins, M. In *Neuropsychological testing in sports*, A paper presented at the Annual Winter Meeting of Major League Baseball, Boston, MA, 2001; 2001.

85. Randolph, C.; McCrea, M.; Barr, W. B., Is neuropsychological testing useful in the management of sport-related concussion? *Journal of athletic training* **2005,** 40, (3), 139.

86. Echemendia, R. J.; Putukian, M.; Mackin, R. S.; Julian, L.; Shoss, N., Neuropsychological test performance prior to and following sports-related mild traumatic brain injury. *Clinical Journal of Sport Medicine* **2001,** 11, (1), 23-31.

87. Echemendia, R. J.; Iverson, G. L.; McCrea, M.; Macciocchi, S. N.; Gioia, G. A.; Putukian, M.; Comper, P., Advances in neuropsychological assessment of sport-related concussion. *Br J Sports Med* **2013,** 47, (5), 294-298.

88. Strimbu, K.; Tavel, J. A., What are biomarkers? *Current Opinion in HIV and AIDS* **2010,** 5, (6), 463.

89. Sahu, P.; Pinkalwar, N.; Dubey, R. D.; Paroha, S.; Chatterjee, S.; Chatterjee, T., Biomarkers: an emerging tool for diagnosis of a disease and drug development. *Asian Journal of Research in Pharmaceutical Sciences* **2011,** 1, (1), 09-16.

90. Papa, L.; Edwards, D.; Ramia, M., Exploring serum biomarkers for mild traumatic brain injury. In *Brain neurotrauma: molecular, neuropsychological, and rehabilitation aspects*, CRC Press/Taylor & Francis: 2015.

91. Yuan, A.; Rao, M. V.; Nixon, R. A., Neurofilaments at a glance. In The Company of Biologists Ltd: 2012.

92. Zetterberg, H.; Hietala, M. A.; Jonsson, M.; Andreasen, N.; Styrud, E.; Karlsson, I.; Edman, Å.; Popa, C.; Rasulzada, A.; Wahlund, L.-O., Neurochemical aftermath of amateur boxing. *Archives of neurology* **2006,** 63, (9), 1277-1280.

93. Oliver, J. M.; Jones, M. T.; Kirk, K. M.; Gable, D. A.; Repshas, J. T.; Johnson, T. A.; Andreasson, U.; Norgren, N.; Blennow, K.; Zetterberg, H., Serum neurofilament light in American football athletes over the course of a season. *Journal of neurotrauma* **2016,** 33, (19), 1784-1789.

94. Petzold, A., Neurofilament phosphoforms: surrogate markers for axonal injury, degeneration and loss. *Journal of the neurological sciences* **2005,** 233, (1-2), 183-198.

95. Žurek, J.; Bartlová, L.; Fedora, M., Hyperphosphorylated neurofilament NF-H as a predictor of mortality after brain injury in children. *Brain injury* **2011,** 25, (2), 221-226.

96. Shaw, G.; Yang, C.; Zhang, L.; Cook, P.; Pike, B.; Hill, W. D., Characterization of the bovine neurofilament NF-M protein and cDNA sequence, and identification of in vitro and in vivo calpain cleavage sites. *Biochemical and biophysical research communications* **2004,** 325, (2), 619-625.

97. Papa, L.; Akinyi, L.; Liu, M. C.; Pineda, J. A.; Tepas III, J. J.; Oli, M. W.; Zheng, W.; Robinson, G.; Robicsek, S. A.; Gabrielli, A., Ubiquitin C-terminal hydrolase is a novel biomarker in humans for severe traumatic brain injury. *Critical care medicine* **2010,** 38, (1), 138.

98. Liu, M. C.; Akinyi, L.; Scharf, D.; Mo, J.; Larner, S. F.; Muller, U.; Oli, M. W.; Zheng, W.; Kobeissy, F.; Papa, L., Ubiquitin C-terminal hydrolase-L1 as a biomarker for

ischemic and traumatic brain injury in rats. *European Journal of Neuroscience* **2010,** 31, (4), 722-732.

99. Setsuie, R.; Wada, K., The functions of UCH-L1 and its relation to neurodegenerative diseases. *Neurochemistry international* **2007,** 51, (2-4), 105-111.

100. Brophy, G. M.; Mondello, S.; Papa, L.; Robicsek, S. A.; Gabrielli, A.; Tepas III, J.; Buki, A.; Robertson, C.; Tortella, F. C.; Hayes, R. L., Biokinetic analysis of ubiquitin C-terminal hydrolase-L1 (UCH-L1) in severe traumatic brain injury patient biofluids. *Journal of neurotrauma* **2011,** 28, (6), 861-870.

101. Mondello, S.; Akinyi, L.; Buki, A.; Robicsek, S.; Gabrielli, A.; Tepas, J.; Papa, L.; Brophy, G. M.; Tortella, F.; Hayes, R. L., Clinical utility of serum levels of ubiquitin C-terminal hydrolase as a biomarker for severe traumatic brain injury. *Neurosurgery* **2012,** 70, (3), 666.

102. De Kruijk, J.; Leffers, P.; Menheere, P.; Meerhoff, S.; Twijnstra, A., S-100B and neuron-specific enolase in serum of mild traumatic brain injury patients A comparison with healthy controls. *Acta neurologica scandinavica* **2001,** 103, (3), 175-179.

103. Vos, P. E.; Lamers, K.; Hendriks, J.; Van Haaren, M.; Beems, T.; Zimmerman, C.; Van Geel, W.; De Reus, H.; Biert, J.; Verbeek, M., Glial and neuronal proteins in serum predict outcome after severe traumatic brain injury. *Neurology* **2004,** 62, (8), 1303-1310.

104. Geyer, C.; Ulrich, A.; Gräfe, G.; Stach, B.; Till, H., Diagnostic value of S100B and neuron-specific enolase in mild pediatric traumatic brain injury. *Journal of Neurosurgery: Pediatrics* **2009,** 4, (4), 339-344.

105. Kobeissy, F., Exploring Serum Biomarkers for Mild Traumatic Brain Injury--Brain Neurotrauma: Molecular, Neuropsychological, and Rehabilitation Aspects. **2015**.

106. Wang, K. K.; Posmantur, R.; Nath, R.; McGinnis, K.; Whitton, M.; Talanian, R. V.; Glantz, S. B.; Morrow, J. S., Simultaneous degradation of αII-and βII-spectrin by caspase 3 (CPP32) in apoptotic cells. *Journal of Biological Chemistry* **1998,** 273, (35), 22490-22497.

107. Ringger, N. C.; O'steen, B.; Brabham, J.; Silver, X.; Pineda, J.; Wang, K.; Hayes, R.; Papa, L., A novel marker for traumatic brain injury: CSF αII-spectrin breakdown product levels. *Journal of neurotrauma* **2004,** 21, (10), 1443-1456.

108. Pineda, J. A.; Lewis, S. B.; Valadka, A. B.; Papa, L.; Hannay, H. J.; Heaton, S. C.; Demery, J. A.; Liu, M. C.; Aikman, J. M.; Akle, V., Clinical significance of α II-spectrin breakdown products in cerebrospinal fluid after severe traumatic brain injury. *Journal of neurotrauma* **2007,** 24, (2), 354-366.

109. Guo, T.; Noble, W.; Hanger, D. P., Roles of tau protein in health and disease. *Acta neuropathologica* **2017,** 133, (5), 665-704.

110. Hanger, D. P.; Anderton, B. H.; Noble, W., Tau phosphorylation: the therapeutic challenge for neurodegenerative disease. *Trends in molecular medicine* **2009,** 15, (3), 112-119.

111. McKhann, G. M.; Knopman, D. S.; Chertkow, H.; Hyman, B. T.; Jack Jr, C. R.; Kawas, C. H.; Klunk, W. E.; Koroshetz, W. J.; Manly, J. J.; Mayeux, R., The diagnosis of dementia due to Alzheimer's disease: Recommendations from the National Institute on Aging-Alzheimer's Association workgroups on diagnostic guidelines for Alzheimer's disease. *Alzheimer's & dementia* **2011,** 7, (3), 263-269.

112. Zemlan, F.; Rosenberg, W. S.; Luebbe, P. A.; Campbell, T. A.; Dean, G. E.; Weiner, N. E.; Cohen, J. A.; Rudick, R. A.; Woo, D., Quantification of axonal damage in traumatic brain injury: affinity purification and characterization of cerebrospinal fluid tau proteins. *Journal of neurochemistry* **1999,** 72, (2), 741-750.

113. Teunissen, C. E.; Dijkstra, C.; Polman, C., Biological markers in CSF and blood for axonal degeneration in multiple sclerosis. *The Lancet Neurology* **2005,** 4, (1), 32-41.

114. Zemlan, F. P.; Jauch, E. C.; Mulchahey, J. J.; Gabbita, S. P.; Rosenberg, W. S.; Speciale, S. G.; Zuccarello, M., C-tau biomarker of neuronal damage in severe brain injured patients: association with elevated intracranial pressure and clinical outcome. *Brain research* **2002,** 947, (1), 131-139.

115. Cengiz, P.; Zemlan, F.; Ellenbogen, R.; Hawkins, D.; Zimmerman, J. J., Cerebrospinal fluid cleaved-tau protein and 9-hydroxyoctadecadienoic acid concentrations in pediatric patients with hydrocephalus. *Pediatric Critical Care Medicine* **2008,** 9, (5), 524-529.

116. Shahim, P.; Tegner, Y.; Wilson, D. H.; Randall, J.; Skillbäck, T.; Pazooki, D.; Kallberg, B.; Blennow, K.; Zetterberg, H., Blood biomarkers for brain injury in concussed professional ice hockey players. *JAMA neurology* **2014,** 71, (6), 684-692.

117. Pelinka, L. E.; Kroepfl, A.; Schmidhammer, R.; Krenn, M.; Buchinger, W.; Redl, H.; Raabe, A., Glial fibrillary acidic protein in serum after traumatic brain injury and multiple trauma. *Journal of Trauma and Acute Care Surgery* **2004,** 57, (5), 1006-1012.

118. McMahon, P. J.; Panczykowski, D. M.; Yue, J. K.; Puccio, A. M.; Inoue, T.; Sorani, M. D.; Lingsma, H. F.; Maas, A. I.; Valadka, A. B.; Yuh, E. L., Measurement of the glial fibrillary acidic protein and its breakdown products GFAP-BDP biomarker for the detection of traumatic brain injury compared to computed tomography and magnetic resonance imaging. *Journal of neurotrauma* **2015,** 32, (8), 527-533.

119. Bramlett, H. M.; Dietrich, W. D.; Green, E. J.; Busto, R., Chronic histopathological consequences of fluid-percussion brain injury in rats: effects of post-traumatic hypothermia. *Acta neuropathologica* **1997,** 93, (2), 190-199.

120. Bazarian, J. J.; Biberthaler, P.; Welch, R. D.; Lewis, L. M.; Barzo, P.; Bogner-Flatz, V.; Gunnar Brolinson, P.; Büki, A.; Chen, J. Y.; Christenson, R. H.; Hack, D.; Huff, J. S.; Johar, S.; Jordan, J. D.; Leidel, B. A.; Lindner, T.; Ludington, E.; Okonkwo, D. O.; Ornato, J.; Peacock, W. F.; Schmidt, K.; Tyndall, J. A.; Vossough, A.; Jagoda, A. S., Serum GFAP and UCH-L1 for prediction of absence of intracranial injuries on head CT (ALERT-TBI): a multicentre observational study. *The Lancet Neurology* **2018,** 17, (9), 782-789.

121. Kochanek, P. M.; Berger, R. P.; Bayr, H.; Wagner, A. K.; Jenkins, L. W.; Clark, R. S., Biomarkers of primary and evolving damage in traumatic and ischemic brain injury: diagnosis, prognosis, probing mechanisms, and therapeutic decision making. *Current opinion in critical care* **2008,** 14, (2), 135-141.

122. Haimoto, H.; Hosoda, S.; Kato, K., Differential distribution of immunoreactive S100-alpha and S100-beta proteins in normal nonnervous human tissues. *Laboratory investigation; a journal of technical methods and pathology* **1987,** 57, (5), 489-498.

123. Halawi, A.; Abbas, O.; Mahalingam, M., S100 proteins and the skin: a review. *Journal of the European Academy of Dermatology and Venereology* **2014,** 28, (4), 405-414.

124. Woertgen, C.; Rothoerl, R. D., Serum S-100B protein in severe head injury. *Neurosurgery* **2000,** 46, (4), 1026-1027.

125. Undén, J.; Bellner, J.; Eneroth, M.; Alling, C.; Ingebrigtsen, T.; Romner, B., Raised serum S100B levels after acute bone fractures without cerebral injury. *Journal of Trauma and Acute Care Surgery* **2005,** 58, (1), 59-61.

126. Fasman, G. D.; Sober, H. A., *Handbook of biochemistry and molecular biology*. CRC press Cleveland: 1977; Vol. 1.

127. Perkins, E., Nomenclature and classification of lipids. *Analyses of Fats, Oils and Derivatives. AOCS Press, Champaign, IL* **1993**, 1-19.

128. Fahy, E.; Subramaniam, S.; Murphy, R. C.; Nishijima, M.; Raetz, C. R.; Shimizu, T.; Spener, F.; van Meer, G.; Wakelam, M. J.; Dennis, E. A., Update of the LIPID MAPS comprehensive classification system for lipids. *Journal of lipid research* **2009,** 50, (Supplement), S9-S14.

129. German, J. B.; Gillies, L. A.; Smilowitz, J. T.; Zivkovic, A. M.; Watkins, S. M., Lipidomics and lipid profiling in metabolomics. *Current opinion in lipidology* **2007,** 18, (1), 66-71.

130. Lucanic, M.; Held, J. M.; Vantipalli, M. C.; Klang, I. M.; Graham, J. B.; Gibson, B. W.; Lithgow, G. J.; Gill, M. S., N-acylethanolamine signaling mediates the effect of diet on lifespan in C. elegans. *Nature* **2011,** 473, (7346), 226.

131. Hannun, Y. A.; Luberto, C.; Argraves, K. M., Enzymes of sphingolipid metabolism: from modular to integrative signaling. *Biochemistry* **2001,** 40, (16), 4893-4903.

132. Mathias, S.; KOLESNICK, R. N., Signal transduction of stress via ceramide. *Biochemical Journal* **1998,** 335, (3), 465-480.

133. Berg, J.; Tymoczko, J.; Stryer, L., Fatty acids are synthesized and degraded by different pathways. *Biochemistry* **2002**.

134. Porter, J. W.; Wakil, S. J.; Tietz, A.; Jacob, M. I.; Gibson, D. M., Studies on the mechanism of fatty acid synthesis II. Cofactor requirements of the soluble pigeon liver system. *Biochimica et biophysica acta* **1957,** 25, 35-41.

135. Wakil, S. J., Mechanism of fatty acid synthesis. *Journal of Lipid Research* **1961,** 2, (1), 1-24.

136. Dash, P. K.; Zhao, J.; Hergenroeder, G.; Moore, A. N., Biomarkers for the diagnosis, prognosis, and evaluation of treatment efficacy for traumatic brain injury. *Neurotherapeutics* **2010,** 7, (1), 100-114.

137. Vagnozzi, R.; Marmarou, A.; Tavazzi, B.; Signoretti, S.; Di Pierro, D.; Del Bolgia, F.; Amorini, A. M.; Fazzina, G.; Sherkat, S.; Lazzarino, G., Changes of cerebral energy metabolism and lipid peroxidation in rats leading to mitochondrial dysfunction after diffuse brain injury. *Journal of neurotrauma* **1999,** 16, (10), 903-913.

138. Hall, E. D.; Detloff, M. R.; Johnson, K.; Kupina, N. C., Peroxynitrite-mediated protein nitration and lipid peroxidation in a mouse model of traumatic brain injury. *Journal of neurotrauma* **2004,** 21, (1), 9-20.

139. Yin, H.; Xu, L.; Porter, N. A., Free radical lipid peroxidation: mechanisms and analysis. *Chemical reviews* **2011,** 111, (10), 5944-5972.

140. Hammad, L. A.; Wu, G.; Saleh, M. M.; Klouckova, I.; Dobrolecki, L. E.; Hickey, R. J.; Schnaper, L.; Novotny, M. V.; Mechref, Y., Elevated levels of hydroxylated phosphocholine lipids in the blood serum of breast cancer patients. *Rapid Communications in Mass Spectrometry: An International Journal Devoted to the Rapid Dissemination of Up-to-the-Minute Research in Mass Spectrometry* **2009,** 23, (6), 863-876.

141. Silverstein, R. L.; Febbraio, M., CD36, a scavenger receptor involved in immunity, metabolism, angiogenesis, and behavior. *Sci. Signal.* **2009,** 2, (72).

142. Montine, T. J.; Montine, K. S.; McMahan, W.; Markesbery, W. R.; Quinn, J. F.; Morrow, J. D., F2-isoprostanes in Alzheimer and other neurodegenerative diseases. *Antioxidants & redox signaling* **2005,** 7, (1-2), 269-275.

143. Hall, E.; Vaishnav, R.; Mustafa, A., Antioxidant therapies for traumatic brain injury. *Neurotherapeutics* **2010,** 7, (1), 51-61.

144. Esterbauer, H.; Schaur, R. J.; Zollner, H., Chemistry and biochemistry of 4-hydroxynonenal, malonaldehyde and related aldehydes. *Free radical Biology and medicine* **1991,** 11, (1), 81-128.

145. Schauenstein, E., Autoxidation of polyunsaturated esters in water: chemical structure and biological activity of the products. *Journal of lipid research* **1967,** 8, (5), 417-428.

146. Ozdemir, D.; Uysal, N.; Gonenc, S.; Acikgoz, O.; Sonmez, A.; Topcu, A.; Ozdemir, N.; Duman, M.; Semin, I.; Ozkan, H., Effect of melatonin on brain oxidative damage induced by traumatic brain injury in immature rats. *Physiological research* **2005,** 54, (6), 631.

147. Nayak, C.; Nayak, D.; Bhat, S.; Raja, A.; Rao, A., Relationship between neurological outcome and early oxidative changes in erythrocytes in head injury patients. *Clinical Chemical Laboratory Medicine* **2007,** 45, (5), 629-633.

148. Nayak, C. D.; Nayak, D. M.; Raja, A.; Rao, A., Erythrocyte indicators of oxidative changes in patients with graded traumatic head injury. *Neurology India* **2008,** 56, (1).

149. Scholpp, J.; Schubert, J. K.; Miekisch, W.; Noeldge-Schomburg, G. F., Lipid peroxidation early after brain injury. *Journal of neurotrauma* **2004,** 21, (6), 667-677.

150. Farias, S. E.; Heidenreich, K. A.; Wohlauer, M. V.; Murphy, R. C.; Moore, E. E., Lipid mediators in cerebral spinal fluid of traumatic brain injured patients. *Journal of Trauma and Acute Care Surgery* **2011,** 71, (5), 1211-1218.

151. Tyurin, V. A.; Tyurina, Y. Y.; Borisenko, G. G.; Sokolova, T. V.; Ritov, V. B.; Quinn, P. J.; Rose, M.; Kochanek, P.; Graham, S. H.; Kagan, V. E., Oxidative stress following traumatic brain injury in rats. *Journal of neurochemistry* **2000,** 75, (5), 2178-2189.

152. Morrow, J. D.; Hill, K. E.; Burk, R. F.; Nammour, T. M.; Badr, K. F.; Roberts, L. n., A series of prostaglandin F2-like compounds are produced in vivo in humans by a

non-cyclooxygenase, free radical-catalyzed mechanism. *Proceedings of the National Academy of Sciences* **1990,** 87, (23), 9383-9387.

153. Bayir, H.; Marion, D. W.; Puccio, A. M.; Wisniewski, S. R.; Janesko, K. L.; Clark, R. S.; Kochanek, P. M., Marked gender effect on lipid peroxidation after severe traumatic brain injury in adult patients. *Journal of neurotrauma* **2004,** 21, (1), 1-8.

154. Morrow, J. D.; Awad, J. A.; Boss, H. J.; Blair, I. A.; Roberts, L. J., Non-cyclooxygenase-derived prostanoids (F2-isoprostanes) are formed in situ on phospholipids. *Proceedings of the National Academy of Sciences* **1992,** 89, (22), 10721-10725.

155. Morrow, J. D.; Harris, T. M.; Jackson Roberts II, L., Noncyclooxygenase oxidative formation of a series of novel prostaglandins: analytical ramifications for measurement of eicosanoids. *Analytical biochemistry* **1990,** 184, (1), 1-10.

156. Frei, B.; Stocker, R.; Ames, B. N., Antioxidant defenses and lipid peroxidation in human blood plasma. *Proceedings of the National Academy of Sciences* **1988,** 85, (24), 9748-9752.

157. Bayir, H.; Kagan, V. E.; Tyurina, Y. Y.; Tyurin, V.; Ruppel, R. A.; Adelson, P. D.; Graham, S. H.; Janesko, K.; Clark, R. S.; Kochanek, P. M., Assessment of antioxidant reserves and oxidative stress in cerebrospinal fluid after severe traumatic brain injury in infants and children. *Pediatric research* **2002,** 51, (5), 571.

158. Tyurin, V. A.; Tyurina, Y. Y.; Borisenko, G. G.; Sokolova, T. V.; Ritov, V. B.; Quinn, P. J.; Rose, M.; Kochanek, P.; Graham, S. H.; Kagan, V. E., Oxidative stress following traumatic brain injury in rats: quantitation of biomarkers and detection of free radical intermediates. *Journal of neurochemistry* **2000,** 75, (5), 2178-2189.

159. Seifman, M. A.; Adamides, A. A.; Nguyen, P. N.; Vallance, S. A.; Cooper, D. J.; Kossmann, T.; Rosenfeld, J. V.; Morganti-Kossmann, M. C., Endogenous melatonin increases in cerebrospinal fluid of patients after severe traumatic brain injury and correlates with oxidative stress and metabolic disarray. *Journal of Cerebral Blood Flow & Metabolism* **2008,** 28, (4), 684-696.

160. Corcoran, T. B.; Mas, E.; Barden, A. E.; Durand, T.; Galano, J.-M.; Roberts, L. J.; Phillips, M.; Ho, K. M.; Mori, T. A., Are isofurans and neuroprostanes increased after subarachnoid hemorrhage and traumatic brain injury? In Mary Ann Liebert, Inc. 140 Huguenot Street, 3rd Floor New Rochelle, NY 10801 USA: 2011.

161. Praticò, D.; Reiss, P.; Tang, L. X.; Sung, S.; Rokach, J.; McIntosh, T. K., Local and systemic increase in lipid peroxidation after moderate experimental traumatic brain injury. *Journal of neurochemistry* **2002,** 80, (5), 894-898.

162. Wieloch, T.; Siesjö, B., Ischemic brain injury: the importance of calcium, lipolytic activities, and free fatty acids. *Pathologie-biologie* **1982,** 30, (5), 269-277.

163. Homayoun, P.; Parkins, N.; Soblosky, J.; Carey, M.; De Turco, E. R.; Bazan, N., Cortical impact injury in rats promotes a rapid and sustained increase in polyunsaturated free fatty acids and diacylglycerols. *Neurochemical research* **2000,** 25, (2), 269-276.

164. Pilitsis, J. G.; Coplin, W. M.; O'Regan, M. H.; Wellwood, J. M.; Diaz, F. G.; Fairfax, M. R.; Michael, D. B.; Phillis, J. W., Free fatty acids in cerebrospinal fluids from patients with traumatic brain injury. *Neuroscience letters* **2003,** 349, (2), 136-138.

165. Posti, J. P.; Dickens, A. M.; Orešič, M.; Hyötyläinen, T.; Tenovuo, O., Metabolomics profiling as a diagnostic tool in severe traumatic brain injury. *Frontiers in neurology* **2017,** 8, 398.

166. Orešič, M.; Posti, J. P.; Kamstrup-Nielsen, M. H.; Takala, R. S.; Lingsma, H. F.; Mattila, I.; Jäntti, S.; Katila, A. J.; Carpenter, K. L.; Ala-Seppälä, H., Human serum metabolites associate with severity and patient outcomes in traumatic brain injury. *EBioMedicine* **2016,** 12, 118-126.

167. Desai, A.; Kevala, K.; Kim, H.-Y., Depletion of brain docosahexaenoic acid impairs recovery from traumatic brain injury. *PloS one* **2014,** 9, (1), e86472.

168. Oliver, J. M.; Jones, M. T.; Kirk, K. M.; Gable, D. A.; Repshas, J. T.; Johnson, T. A.; Andreasson, U.; Norgren, N.; Blennow, K.; Zetterberg, H., Effect of docosahexaenoic acid on a biomarker of head trauma in American football. *Medicine & Science in Sports & Exercise* **2016,** 48, (6), 974-982.

169. Mills, J. D.; Hadley, K.; Bailes, J. E., Dietary supplementation with the omega-3 fatty acid docosahexaenoic acid in traumatic brain injury. *Neurosurgery* **2011,** 68, (2), 474-481.

170. Yusuf, H. K., *Understanding the brain and its development: A chemical approach*. World Scientific: 1992.

171. van der Veen, J. N.; Kennelly, J. P.; Wan, S.; Vance, J. E.; Vance, D. E.; Jacobs, R. L., The critical role of phosphatidylcholine and phosphatidylethanolamine metabolism in health and disease. In Elsevier: 2017.

172. Abdullah, L.; Evans, J. E.; Ferguson, S.; Mouzon, B.; Montague, H.; Reed, J.; Crynen, G.; Emmerich, T.; Crocker, M.; Pelot, R., Lipidomic analyses identify injury-specific phospholipid changes 3 mo after traumatic brain injury. *The FASEB Journal* **2014,** 28, (12), 5311-5321.

173. Pasvogel, A. E.; Miketova, P.; Moore, I. M., Differences in CSF phospholipid concentration by traumatic brain injury outcome. *Biological research for nursing* **2010,** 11, (4), 325-331.

174. Emmerich, T.; Abdullah, L.; Ojo, J.; Mouzon, B.; Nguyen, T.; Laco, G. S.; Crynen, G.; Evans, J. E.; Reed, J.; Mullan, M., Mild TBI results in a long-term decrease in circulating phospholipids in a mouse model of injury. *Neuromolecular medicine* **2017,** 19, (1), 122-135.

175. Hankin, J. A.; Farias, S. E.; Barkley, R. M.; Heidenreich, K.; Frey, L. C.; Hamazaki, K.; Kim, H.-Y.; Murphy, R. C., MALDI Mass Spectrometric Imaging of Lipids in Rat Brain Injury Models. *Journal of The American Society for Mass Spectrometry* **2011,** 22, (6), 1014.

176. Mallah, K.; Quanico, J.; Trede, D.; Kobeissy, F.; Zibara, K.; Salzet, M.; Fournier, I., Lipid Changes Associated with Traumatic Brain Injury Revealed by 3D MALDI-MSI. *Analytical Chemistry* **2018,** 90, (17), 10568-10576.

177. Fang, Y.; Vilella-Bach, M.; Bachmann, R.; Flanigan, A.; Chen, J., Phosphatidic acid-mediated mitogenic activation of mTOR signaling. *Science* **2001,** 294, (5548), 1942-1945.

178. Crack, P. J.; Zhang, M.; Morganti-Kossmann, M. C.; Morris, A. J.; Wojciak, J. M.; Fleming, J. K.; Karve, I.; Wright, D.; Sashindranath, M.; Goldshmit, Y., Anti-lysophosphatidic acid antibodies improve traumatic brain injury outcomes. *Journal of neuroinflammation* **2014,** 11, (1), 37.

179. McDonald, W. S.; Jones, E. E.; Wojciak, J. M.; Drake, R. R.; Sabbadini, R. A.; Harris, N. G., Matrix-Assisted Laser Desorption Ionization Mapping of Lysophosphatidic Acid Changes after Traumatic Brain Injury and the Relationship to Cellular Pathology. *The American journal of pathology* **2018,** 188, (8), 1779-1793.

180. Carrasco, S.; Mérida, I., Diacylglycerol, when simplicity becomes complex. *Trends in biochemical sciences* **2007,** 32, (1), 27-36.

181. Berridge, M. J., Inositol trisphosphate and diacylglycerol as second messengers. *Biochemical Journal* **1984,** 220, (2), 345.

182. Homayoun, P.; Rodriguez de Turco, E.; Parkins, N.; Lane, D.; Soblosky, J.; Carey, M.; Bazan, N., Delayed phospholipid degradation in rat brain after traumatic brain injury. *Journal of neurochemistry* **1997,** 69, (1), 199-205.

183. Roux, A.; Muller, L.; Jackson, S. N.; Post, J.; Baldwin, K.; Hoffer, B.; Balaban, C. D.; Barbacci, D.; Schultz, J. A.; Gouty, S., Mass spectrometry imaging of rat brain lipid profile changes over time following traumatic brain injury. *Journal of neuroscience methods* **2016,** 272, 19-32.

184. Guo, S.; Zhou, D.; Zhang, M.; Li, T.; Liu, Y.; Xu, Y.; Chen, T.; Li, Z., Monitoring changes of docosahexaenoic acid-containing lipids during the recovery process of traumatic brain injury in rat using mass spectrometry imaging. *Scientific reports* **2017,** 7, (1), 5054.

185. Fiandaca, M. S.; Mapstone, M.; Mahmoodi, A.; Gross, T.; Macciardi, F.; Cheema, A. K.; Merchant-Borna, K.; Bazarian, J.; Federoff, H. J., Plasma metabolomic biomarkers accurately classify acute mild traumatic brain injury from controls. *PloS one* **2018,** 13, (4), e0195318.

186. Ji, J.; Kline, A. E.; Amoscato, A.; Samhan-Arias, A. K.; Sparvero, L. J.; Tyurin, V. A.; Tyurina, Y. Y.; Fink, B.; Manole, M. D.; Puccio, A. M., Lipidomics identifies cardiolipin oxidation as a mitochondrial target for redox therapy of brain injury. *Nature neuroscience* **2012,** 15, (10), 1407.

187. Sparvero, L. J.; Amoscato, A. A.; Kochanek, P. M.; Pitt, B. R.; Kagan, V. E.; Bayır, H., Mass-spectrometry based oxidative lipidomics and lipid imaging: applications in traumatic brain injury. *Journal of neurochemistry* **2010,** 115, (6), 1322-1336.

188. Schlame, M.; Brody, S.; Hostetler, K. Y., Mitochondrial cardiolipin in diverse eukaryotes. *European Journal of Biochemistry* **1993,** 212, (3), 727-733.

189. Bayir, H.; Tyurin, V. A.; Tyurina, Y. Y.; Viner, R.; Ritov, V.; Amoscato, A. A.; Zhao, Q.; Zhang, X. J.; Janesko-Feldman, K. L.; Alexander, H., Selective early cardiolipin peroxidation after traumatic brain injury: an oxidative lipidomics analysis. *Annals of neurology* **2007,** 62, (2), 154-169.

190. Ji, J.; Tyurina, Y. Y.; Tang, M.; Feng, W.; Stolz, D. B.; Clark, R. S.; Meaney, D. F.; Kochanek, P. M.; Kagan, V. E.; Bayır, H., Mitochondrial injury after mechanical stretch of cortical neurons in vitro: biomarkers of apoptosis and selective peroxidation of anionic phospholipids. *Journal of neurotrauma* **2012,** 29, (5), 776-788.

191. Sparvero, L. J.; Amoscato, A. A.; Fink, A. B.; Anthonymuthu, T.; New, L. A.; Kochanek, P. M.; Watkins, S.; Kagan, V. E.; Bayır, H., Imaging mass spectrometry reveals loss of polyunsaturated cardiolipins in the cortical contusion, hippocampus, and thalamus after traumatic brain injury. *Journal of neurochemistry* **2016,** 139, (4), 659-675.

192. van Echten-Deckert, G.; Herget, T., Sphingolipid metabolism in neural cells. *Biochimica et Biophysica Acta (BBA)-Biomembranes* **2006,** 1758, (12), 1978-1994.

193. Obeid, L. M.; Hannun, Y. A., Ceramide: a stress signal and mediator of growth suppression and apoptosis. *Journal of cellular biochemistry* **1995,** 58, (2), 191-198.

194. Barenholz, Y., Sphingomyelin and cholesterol: from membrane biophysics and rafts to potential medical applications. In *Membrane Dynamics and Domains*, Springer: 2004; pp 167-215.

195. O'Brien, J. S.; Sampson, E. L., Lipid composition of the normal human brain: gray matter, white matter, and myelin. *Journal of lipid research* **1965,** 6, (4), 537-544.

196. Quehenberger, O.; Armando, A. M.; Brown, A. H.; Milne, S. B.; Myers, D. S.; Merrill, A. H.; Bandyopadhyay, S.; Jones, K. N.; Kelly, S.; Shaner, R. L., Lipidomics reveals a remarkable diversity of lipids in human plasma. *Journal of lipid research* **2010,** 51, (11), 3299-3305.

197. Merrill Jr, A. H., Sphingolipids. In *Biochemistry of lipids, lipoproteins and membranes*, Elsevier: 2008; pp 363-397.

198. Gaire, B. P.; Lee, C.-H.; Sapkota, A.; Lee, S. Y.; Chun, J.; Cho, H. J.; Nam, T.-g.; Choi, J. W., Identification of Sphingosine 1-Phosphate Receptor Subtype 1 (S1P 1) as a Pathogenic Factor in Transient Focal Cerebral Ischemia. *Molecular neurobiology* **2018,** 55, (3), 2320-2332.

199. Moon, E.; Han, J. E.; Jeon, S.; Ryu, J. H.; Choi, J. W.; Chun, J., Exogenous S1P exposure potentiates ischemic stroke damage that is reduced possibly by inhibiting S1P receptor signaling. *Mediators of inflammation* **2015,** 2015.

200. Gaire, B.; Bae, Y.; Choi, J., S1P1 Regulates M1/M2 Polarization toward Brain Injury after Transient Focal Cerebral Ischemia. *Biomolecules & therapeutics* **2019**.

201. Sheth, S. A.; Iavarone, A. T.; Liebeskind, D. S.; Won, S. J.; Swanson, R. A., Targeted lipid profiling discovers plasma biomarkers of acute brain injury. *PLoS One* **2015,** 10, (6), e0129735.

202. Contreras, F.-X.; Villar, A.-V.; Alonso, A.; Kolesnick, R. N.; Goñi, F. M., Sphingomyelinase activity causes transbilayer lipid translocation in model and cell membranes. *Journal of Biological Chemistry* **2003,** 278, (39), 37169-37174.

203. Hannun, Y. A., Functions of ceramide in coordinating cellular responses to stress. *Science* **1996,** 274, (5294), 1855-1859.

204. Barbacci, D. C.; Roux, A.; Muller, L.; Jackson, S. N.; Post, J.; Baldwin, K.; Hoffer, B.; Balaban, C. D.; Schultz, J. A.; Gouty, S., Mass spectrometric imaging of ceramide biomarkers tracks therapeutic response in traumatic brain injury. *ACS chemical neuroscience* **2017,** 8, (10), 2266-2274.

205. Woods, A. S.; Colsch, B.; Jackson, S. N.; Post, J.; Baldwin, K.; Roux, A.; Hoffer, B.; Cox, B. M.; Hoffer, M.; Rubovitch, V., Gangliosides and ceramides change in a

mouse model of blast induced traumatic brain injury. *ACS chemical neuroscience* **2013,** 4, (4), 594-600.

206. Novgorodov, S. A.; Riley, C. L.; Yu, J.; Borg, K. T.; Hannun, Y. A.; Proia, R. L.; Kindy, M. S.; Gudz, T. I., Essential roles of neutral ceramidase and sphingosine in mitochondrial dysfunction due to traumatic brain injury. *Journal of Biological Chemistry* **2014,** 289, (19), 13142-13154.

207. Baulieu, E., Neurosteroids: a novel function of the brain. *Psychoneuroendocrinology* **1998,** 23, (8), 963-987.

208. Fielding, P. E.; Fielding, C. J., A cholesteryl ester transfer complex in human plasma. *Proceedings of the National Academy of Sciences* **1980,** 77, (6), 3327-3330.

209. Schofield, M.; Jenski, L. J.; Dumaual, A. C.; Stillwell, W., Cholesterol versus cholesterol sulfate: effects on properties of phospholipid bilayers containing docosahexaenoic acid. *Chemistry and physics of lipids* **1998,** 95, (1), 23-36.

210. Bandaru, V. V. R.; Troncoso, J.; Wheeler, D.; Pletnikova, O.; Wang, J.; Conant, K.; Haughey, N. J., ApoE4 disrupts sterol and sphingolipid metabolism in Alzheimer's but not normal brain. *Neurobiology of aging* **2009,** 30, (4), 591-599.

211. Smith, C.; Graham, D. I.; Murray, L. S.; Stewart, J.; Nicoll, J. A. R., Association of APOE e4 and cerebrovascular pathology in traumatic brain injury. *J Neurol Neurosurg Psychiatry* **2006,** 77, (3), 363-366.

212. Fiehn, O., Metabolomics—the link between genotypes and phenotypes. In *Functional genomics*, Springer: 2002; pp 155-171.

213. Wenk, M. R., The emerging field of lipidomics. *Nature reviews. Drug discovery* **2005,** 4, (7), 594.

214. Cajka, T.; Fiehn, O., Toward merging untargeted and targeted methods in mass spectrometry-based metabolomics and lipidomics. *Analytical chemistry* **2015,** 88, (1), 524-545.

215. Patti, G. J.; Yanes, O.; Siuzdak, G., Innovation: Metabolomics: the apogee of the omics trilogy. *Nature reviews Molecular cell biology* **2012,** 13, (4), 263.

216. Griffiths, W. J.; Koal, T.; Wang, Y.; Kohl, M.; Enot, D. P.; Deigner, H. P., Targeted metabolomics for biomarker discovery. *Angewandte Chemie International Edition* **2010,** 49, (32), 5426-5445.

217. Zhou, X.; Mao, J.; Ai, J.; Deng, Y.; Roth, M. R.; Pound, C.; Henegar, J.; Welti, R.; Bigler, S. A., Identification of plasma lipid biomarkers for prostate cancer by lipidomics and bioinformatics. *PloS one* **2012,** 7, (11), e48889.

218. Ishikawa, M.; Maekawa, K.; Saito, K.; Senoo, Y.; Urata, M.; Murayama, M.; Tajima, Y.; Kumagai, Y.; Saito, Y., Plasma and serum lipidomics of healthy white adults shows characteristic profiles by subjects' gender and age. *PloS one* **2014,** 9, (3), e91806.

219. Min, H. K.; Lim, S.; Chung, B. C.; Moon, M. H., Shotgun lipidomics for candidate biomarkers of urinary phospholipids in prostate cancer. *Analytical and bioanalytical chemistry* **2011,** 399, (2), 823-830.

220. Pieragostino, D.; Cicalini, I.; Lanuti, P.; Ercolino, E.; di Ioia, M.; Zucchelli, M.; Zappacosta, R.; Miscia, S.; Marchisio, M.; Sacchetta, P., Enhanced release of acid sphingomyelinase-enriched exosomes generates a lipidomics signature in CSF of Multiple Sclerosis patients. *Scientific reports* **2018,** 8, (1), 3071.

221. Elliott, P.; Peakman, T. C., The UK Biobank sample handling and storage protocol for the collection, processing and archiving of human blood and urine. *International journal of epidemiology* **2008,** 37, (2), 234-244.

222. Matthan, N. R.; Ip, B.; Resteghini, N.; Ausman, L. M.; Lichtenstein, A. H., Long-term fatty acid stability in human serum cholesteryl ester, triglyceride, and phospholipid fractions. *Journal of lipid research* **2010,** 51, (9), 2826-2832.

223. Sarafian, M. H.; Gaudin, M.; Lewis, M. R.; Martin, F.-P.; Holmes, E.; Nicholson, J. K.; Dumas, M.-E., Objective set of criteria for optimization of sample preparation procedures for ultra-high throughput untargeted blood plasma lipid profiling by ultra performance liquid Chromatography–Mass spectrometry. *Analytical chemistry* **2014,** 86, (12), 5766-5774.

224. Gaul, D. A.; Mezencev, R.; Long, T. Q.; Jones, C. M.; Benigno, B. B.; Gray, A.; Fernández, F. M.; McDonald, J. F., Highly-accurate metabolomic detection of early-stage ovarian cancer. *Scientific reports* **2015,** 5, 16351.

225. Folch, J.; Lees, M.; Stanley, G. S., A simple method for the isolation and purification of total lipides from animal tissues. *Journal of biological chemistry* **1957,** 226, (1), 497-509.

226. Bligh, E.; Dyer, W., A rapid method of total lipid extraction and purification. *Can. J. Biochem. Physiol* **1959,** 37, 911-917.

227. Yang, Y.; Cruickshank, C.; Armstrong, M.; Mahaffey, S.; Reisdorph, R.; Reisdorph, N., New sample preparation approach for mass spectrometry-based profiling of plasma results in improved coverage of metabolome. *Journal of chromatography A* **2013,** 1300, 217-226.

228. Zhang, A.; Sun, H.; Wang, P.; Han, Y.; Wang, X., Modern analytical techniques in metabolomics analysis. *Analyst* **2012,** 137, (2), 293-300.

229. Pan, Z.; Raftery, D., Comparing and combining NMR spectroscopy and mass spectrometry in metabolomics. *Analytical and bioanalytical chemistry* **2007,** 387, (2), 525-527.

230. Emwas, A.-H. M., The strengths and weaknesses of NMR spectroscopy and mass spectrometry with particular focus on metabolomics research. In *Metabonomics*, Springer: 2015; pp 161-193.

231. Bedair, M.; Sumner, L. W., Current and emerging mass-spectrometry technologies for metabolomics. *TrAC Trends in Analytical Chemistry* **2008,** 27, (3), 238-250.

232. Lu, W.; Bennett, B. D.; Rabinowitz, J. D., Analytical strategies for LC-MS-based targeted metabolomics. *J Chromatogr B Analyt Technol Biomed Life Sci* **2008,** 871, (2), 236-242.

233. De Hoffmann, E., Mass spectrometry. *Kirk-Othmer Encyclopedia of Chemical Technology* **2000**.

234. Medhe, S., *Mass Spectrometry: Detectors Review*. 2018; Vol. 3, p 51-58.

235. Zubarev, R. A.; Makarov, A., Orbitrap mass spectrometry. In ACS Publications: 2013.

236. Holčapek, M.; Jirásko, R.; Lísa, M., Recent developments in liquid chromatography–mass spectrometry and related techniques. *Journal of Chromatography A* **2012,** 1259, 3-15.

237. Abreu, S.; Solgadi, A.; Chaminade, P., Optimization of normal phase chromatographic conditions for lipid analysis and comparison of associated detection techniques. *Journal of Chromatography A* **2017,** 1514, 54-71.

238. Connor, S. C.; Wu, W.; Sweatman, B. C.; Manini, J.; Haselden, J. N.; Crowther, D. J.; Waterfield, C. J., Effects of feeding and body weight loss on the 1H-NMR-based urine metabolic profiles of male Wistar Han rats: implications for biomarker discovery. *Biomarkers* **2004,** 9, (2), 156-179.

239. Poulin, R. X.; Hogan, S.; Poulson-Ellestad, K. L.; Brown, E.; Fernández, F. M.; Kubanek, J., Karenia brevis allelopathy compromises the lipidome, membrane integrity, and photosynthesis of competitors. *Scientific reports* **2018,** 8, (1), 9572.

240. Ramadan, Z.; Jacobs, D.; Grigorov, M.; Kochhar, S., Metabolic profiling using principal component analysis, discriminant partial least squares, and genetic algorithms. *Talanta* **2006,** 68, (5), 1683-1691.

241. Valpola, H., From neural PCA to deep unsupervised learning. In *Advances in Independent Component Analysis and Learning Machines*, Elsevier: 2015; pp 143-171.

242. Wold, S.; Sjöström, M.; Eriksson, L., PLS-regression: a basic tool of chemometrics. *Chemometrics and intelligent laboratory systems* **2001,** 58, (2), 109-130.

243. Singh, A.; Thakur, N.; Sharma, A. In *A review of supervised machine learning algorithms*, 2016 3rd International Conference on Computing for Sustainable Global Development (INDIACom), 2016; IEEE: 2016; pp 1310-1315.

244. Hancock, S. E.; Poad, B. L.; Batarseh, A.; Abbott, S. K.; Mitchell, T. W., Advances and unresolved challenges in the structural characterization of isomeric lipids. *Analytical biochemistry* **2017,** 524, 45-55.

245. Ivanova, P. T.; Milne, S. B.; Byrne, M. O.; Xiang, Y.; Brown, H. A., Glycerophospholipid identification and quantitation by electrospray ionization mass spectrometry. *Methods in enzymology* **2007,** 432, 21-57.

246. Kind, T.; Liu, K.-H.; Lee, D. Y.; DeFelice, B.; Meissen, J. K.; Fiehn, O., LipidBlast in silico tandem mass spectrometry database for lipid identification. *Nature methods* **2013,** 10, (8), 755.

247. Kanehisa, M.; Goto, S., KEGG: kyoto encyclopedia of genes and genomes. *Nucleic acids research* **2000,** 28, (1), 27-30.

248. Draghici, S.; Khatri, P.; Tarca, A. L.; Amin, K.; Done, A.; Voichita, C.; Georgescu, C.; Romero, R., A systems biology approach for pathway level analysis. *Genome research* **2007,** 17, (10), 1537-1545.

CHAPTER 2: DISCOVERY OF LIPIDOME ALTERATIONS FOLLOWING TRAUMATIC BRAIN INJURY *VIA* HIGH-RESOLUTION METABOLOMICS

Reprinted with permission from:
Hogan, S. R., Phan, J. H., Alvarado-Velez, M., Wang, M. D., Bellamkonda, R. V., Fernández, F. M., & LaPlaca, M. C. Discovery of Lipidome Alterations Following Traumatic Brain Injury *via* High-Resolution Metabolomics. *Journal of Proteome Research*, **2018**, *17*(6), 2131-2143.

2.1 Abstract

Traumatic brain injury can occur across wide segments of the population, presenting in a heterogeneous manner that makes diagnosis inconsistent and management challenging. Biomarkers offer the potential to objectively identify injury status, severity, and phenotype by measuring the relative concentrations of endogenous molecules in readily accessible biofluids. Through a data-driven, discovery approach, novel biomarker candidates for TBI were identified in the serum lipidome of adult male Sprague-Dawley rats in the first week following moderate injury induced by controlled cortical impact. Serum samples were analyzed in positive and negative modes by Ultra Performance Liquid Chromatography Mass Spectrometry (UPLC-MS). A predictive panel for the classification of injured and uninjured sera samples, consisting of 26 dysregulated species belonging to a variety of lipid classes, was developed with a cross-validated accuracy of 85.3% using omniClassifier software to optimize feature selection. Polyunsaturated fatty acids (PUFAs) and PUFA-containing diacylglycerols were found to be upregulated in sera from injured rats, while changes in sphingolipids and other membrane phospholipids were also observed, many of which map to known secondary injury pathways. Overall, the identified

biomarker panel offers viable molecular candidates representing lipids that may readily cross the blood-brain barrier and aid in the understanding of TBI pathophysiology.

2.2 Detection of Traumatic Brain Injury

2.2.1 Background

The Centers for Disease Control estimate that TBI is the primary cause of over 50,000 deaths and 300,000 hospitalizations in the United States annually.[1] Many more injuries remain misdiagnosed, undetected, or unreported.[2,3] Heightened awareness of TBI in the military, athletics, and the general public has led to increased efforts towards the development of objective diagnostic measures and clinically relevant treatment options. Assessment tools such as the GCS, radiologic imaging, and symptoms reporting are commonly used and provide valuable information about potential injury status. However, they do not capture the heterogeneous physiologic and neurochemical response, making TBI diagnosis and treatment a challenge.[4] The GCS combines measures of motor, verbal and eye opening responses to stratify injuries into three severities. Mild injuries (score 13-15) account for nearly 80% of injuries, while moderate (9-12) and severe (< 9) each account for approximately half of the remaining cases.[5] Injury severity affects the time-course and extent of BBB breakdown, and while the BBB is disrupted in severe TBI, damage is minimal or non-existent in milder injuries.[6] Injury severity also has a major effect on the extent of impairment resulting from primary and secondary injury cascades, leading to worse prognostic outcomes and increased mortality in more severe injuries, which were the focus of the vast majority of early research.[7,8,9] However the ultimate goal of current innovative diagnostic modalities should focus on the detection of less severe injuries,

specifically mTBI, as diagnosis of these injuries remains elusive even today. Therefore, preliminary studies aimed at understanding moderate TBI pathophysiology may provide valuable insights into the molecular mechanisms and metabolic responses more closely associated with mTBI.

2.2.2 Biomarkers for the Diagnosis of TBI

Biomarkers offer the potential to both sensitively and specifically identify the severity and phenotype of TBI, track pathology and metabolic state, and aid in mechanistically-based treatment decisions. The vast majority of proposed TBI biomarkers are astroglial and neuronal proteins, such as GFAP, S100β, UCH-L1 and tau/p-tau[10,11] that may not readily cross the BBB, although the recently discovered glymphatic system may partially explain their brain-to-blood transport.[12,13] While some of these proteins have proven useful in the diagnosis of severe TBI, they have not yet been shown to be sensitive enough to consistently detect TBI across the full range of severities.[14] Furthermore, while the BBB is disrupted in severe TBI, it remains predominantly impermeable in milder injuries, partially explaining why many biomarkers of severe brain injury do not translate well to mTBI diagnostics.[15,16] Small molecule metabolites may, however, permeate the BBB, though acute changes in tissue metabolite content are significantly more detectable than are alterations in plasma.[17] Blood lipid levels are expected to reflect brain pathophysiology, given the close proximity of the CSF and the brain, the lipophilic nature of the endothelial cells comprising the BBB, the ease of transport of small lipids, and the similarity of lipid content in the CSF and extracellular fluids.[18,19] Lipids are therefore more likely to translate to clinically successful TBI biomarkers than are proteins, especially in readily accessible biofluids such as blood or urine. Exploration of lipid metabolites as

potential biomarkers of TBI is still in its infancy compared to protein-based markers, yet it holds promise given the high lipid content of the brain and its vulnerability to oxidative lipid damage.[20-22]

The dysregulation of lipids after TBI is well documented,[23-27] and identification of altered lipids in the serum may reveal novel biomarker candidates.[20,28] Elevated levels of PUFAs and redox transition metals as well as the high rate of oxygen consumption in the brain make it highly vulnerable to free radical attack.[29] Free radical mediated damage from ROS and RNS is initiated acutely following the primary insult but can persist in the hours and days following injury, overwhelming antioxidant defenses and mediating damage to vital cell structures such as membranes and mitochondria.[30,31] The study of volatile urinary metabolites also offers promise for the detection of inflammatory processes resulting from neurological disorders such as TBI.[32]

Many existing studies into lipid biomarkers have utilized targeted profiling of a handful of specific molecules, which has the disadvantage of being biased toward known pathways and not necessarily revealing the optimum biomarker candidates that can be found with discovery-based approaches.[33] A high-coverage survey of the lipid profile changes associated with TBI can thus help to guide biomarker discovery while providing additional mechanistic understanding of the role of specific lipid-related molecular effectors in TBI pathophysiology. Therefore, the objective of this study was to determine which lipids, or classes of lipids, were dysregulated following moderate TBI in rats using a high-coverage, non-targeted lipidomics approach, ultimately selecting an optimized panel of lipid biomarkers that has the potential to objectively differentiate injured from uninjured Sprague-Dawley rats, which often serve as a suitable pre-clinical model for

human disease.[34] Currently there are no Food and Drug Administration (FDA) approved biomarkers for the diagnosis of TBI, but consideration for the inclusion of lipids in the development of biomarker panels may aid in translation to clinical success.[35]

2.3 Experimental Details

2.3.1 Injury Protocol

All procedures involving animals were performed according to the guidelines set forth in the Guide for the Care and Use of Laboratory Animals (U.S. Department of Health and Human Services, Pub no. 85-23, 1985) and were approved by the Georgia Institute of Technology Institutional Animal Care and Use Committee (protocol #A15013). The study was not pre-registered. Male Sprague-Dawley rats (8 weeks old; Charles River) were kept on a 12-h light–dark cycle, and food and water were available *ad libitum*. Thirty-four animals weighing 300-400 g were randomly assigned to the following groups using a computer based randomization algorithm: (1) naïve (n=10), (2) sham-operated (n= 8; n=4, 3 days post-surgery; n=4, 7 days post-surgery), and (3) TBI (n=16; n=7, 3 days post-injury; n=9, 7 days post-injury). Sham-operated animals were employed to ensure that the stress of surgery did not play a role in sample classification based on lipid profiles, while naïve samples were taken from a subset of animals prior to sham or TBI procedures.

Unilateral contusions of the lateral frontoparietal cortex were created using a CCI device (Pittsburgh Precision Instruments, Pittsburgh, PA) following published procedures.[36,37] Rats were anesthetized (induction, 5% isoflurane; maintenance 2-3% isoflurane), mounted in a stereotaxic frame, and a 6 mm craniectomy was made over the left frontoparietal cortex (center: -3.0 mm AP, +2.0 mm ML from bregma). A pneumatic

piston (tip diameter=5 mm; positioned 15 degrees from vertical in the coronal plane) impacted the cortical tissue to a depth of 2 mm (velocity=4 m/s, duration=200 ms), values consistent with a moderate TBI insult.[38] Following the injury, the wound cavity was thoroughly cleaned and all bleeding stopped before a layer of 2% SeaKem agarose (Lonza, MD) was applied to the injury site and the scalp sutured.[39,40] The bone flap was not replaced as per standard CCI protocols.[37] Animals received sustained release buprenorphine (1mg kg^{-1}) and were placed on a heating pad during recovery, at which time they were returned to their home cage and singly housed. Sham-operated animals were subjected to the same procedures described above, but did not receive an impact, while naïve animals were not subjected to surgical procedures.

2.3.2 Blood Sampling

The serum lipidome of rats was analyzed at 3- and 7-days following moderate CCI injury in order to identify potential biomarker candidates. During the afternoon, approximately 200 µL of whole blood was collected from a tail vein punctured by 20-gauge Precision Glide needles (Beckton Dickinson) and stored on ice. Whole blood samples were allowed to coagulate at room temperature for 45 minutes, and all sample collection followed literature guidelines for limiting the potential for hemolysis.[41,42] Samples were then centrifuged at 4 °C for 15 min at 2500 x g, and serum was collected in 50 µL aliquots and stored at -80 °C.

2.3.3 Sample Preparation

Prior to analysis, lipids and small non-polar metabolites were separated from proteins in blood using IPA for protein precipitation, shown to be advantageous over the Folch or Bligh and Dyer methods for a variety of experimental considerations.[43-46] For

protein precipitation purposes, serum samples were thawed on ice for 1 h and serum was mixed 1:3 v/v with IPA. Samples were centrifuged at 16,000 x g for 7 min, and the supernatant was collected. Samples were stored at -80 °C until analysis. LC-MS analysis confirmed excellent coverage of various expected lipid classes (Figure A1).

2.3.4 UPLC-MS Analysis

A Waters ACQUITY UPLC quaternary solvent manager system was employed for chromatographic separations. Both ionization modes utilized identical mobile phases, though different chromatographic gradients were employed (Table A1A). Mobile phase A was 40:60 water: acetonitrile (ACN) and mobile phase B was 10% ACN in IPA. Both mobile phases included 10 mM ammonium formate (Sigma Aldrich, >99.995%) and 0.1% formic acid (Fluka Analytical) additives to improve peak shape and ionization efficiency. All solvents used were of LC-MS grade and provided by Sigma Aldrich (IPA) or J.T. Baker (ACN). The column used was an ACQUITY UPLC BEH C18 1.7 μm, 2.1 x 50 mm, operated at 60°C, while samples were maintained at 5° C throughout the analysis. Injection volumes of 5μL and 10 μL were used in positive and negative ion modes, respectively. Run order was randomized, and samples were acquired in duplicate. A Waters Xevo G2 quadrupole time-of-flight (QTOF) mass spectrometer with an ESI source was used for lipidomic analysis of all samples. MS parameters are provided in the appendix (Table A1B). The mass spectrometer was calibrated with a sodium formate solution, and data were acquired in the 50-1200 Da range with leucine enkephalin used for lock mass correction. Data are available online at https://chorusproject.org/anonymous/download/experiment/-3567265606761364215 and at

http://dev.metabolomicsworkbench.org:22222/data/DRCCMetadata.php?Mode=Study&StudyID=ST000920.

Most MS/MS experiments were performed in the Xevo G2 QTOF mass spectrometer (4 different collision energies, ranging from 10 V to 40 V). For low abundance markers that required higher sensitivity, MS/MS experiments were performed in a Q-Exactive (QE) HF Orbitrap mass spectrometer (Thermo Fischer Scientific) at a normalized collision energy (NCE) setting of 10, 30 and 50, and combined into a single spectrum by the instrument software. Table A2 details the specific instrument used to acquire the MS/MS data for each respective lipid as well as the annotation of each species. Spectral interpretation of lipid fragmentation patterns was performed either manually or by comparison to entries in the Lipid Metabolites and Pathways Strategy (LIPID MAPS), human metabolome database (HMDB), and Metlin databases.[47-49] The LIPID MAPS MS/MS prediction tool for glycerophospholipids was also used for the assignment of fragment ion species.

2.3.5 Sample Size Calculation

Minimum sample size to achieve statistical significance was determined by *a priori* power analysis using G*Power 3.1 statistical software.[50] For each metabolomic feature, Cohen's effect size (d) was estimated at d=1 using pilot data, producing the desired statistical power ($1-\beta = 0.80$) and type I error probability ($\alpha = 0.05$) with a sample size of n=34.

2.3.6 Data Mining

Chromatographic alignment, de-isotoping, deconvolution, normalization, and peak picking were accomplished using Progenesis QI software. Sets of 1669 and 622 spectral

features, defined as unique pairs of RT and exact mass to charge ratio (*m/z*), were obtained for positive and negative ion modes, respectively. Filters were applied to remove peaks detected as background contaminants and peaks in which the instrumental variation, or the coefficient of variation measured (CV_m), approached the biological coefficient of variation (CV_b) through the use of solvent blanks and quality control (QC) pooled samples. Any features detected above the noise threshold in solvent blank runs or with high CV_m in pooled QC runs were removed from the datasets. Features detected in fewer than 75% of samples in TBI and control groups were also removed prior to binary classification. The remaining 727 feature abundances (413 positive and 314 negative mode) were exported as a single matrix combining both ionization modes to omniClassifier for multivariate analysis.

2.3.7 Feature Selection and Classification

Post-processed feature abundances were $\log_2$ normalized to create an approximately Gaussian distribution prior to binary classification. OmniClassifier was utilized to develop an initial model to predict TBI based on lipidomics data.[51] As a first approximation to model the data, sham-operated and naïve animals were collectively grouped as "controls" in a single class, while 3- and 7-day post-injury time points were collectively labeled as "TBI". This was done to increase the total number of samples in each class, prevent overfitting, and increase model statistical significance. Using nested cross-validation (CV), prediction models were optimized using four different classifiers bundled within omniClassifier: Bayesian, KNN, Logistic Regression and SVMs. Ten iterations of three-fold nested CV were applied to the training data to estimate prediction performance, resulting in 4x10x3 = 120 total tested models. Subsequently, non-nested CV

was applied to the training data to optimize a final prediction model. Blinding was utilized in the data analysis CV stage, where a subset of samples was removed from the training set, blinded and predicted for each tested model.

A single iteration of nested CV produced three prediction performance values, which were averaged into a single performance quantity. This entire process was repeated for ten iterations, resulting in ten averaged CV performance quantities. After nested CV, a final prediction model was chosen. When choosing a final prediction model, the same CV optimization procedure as previously used in the nested CV step was followed but applied to the entire training data set. Subsequently, the final model parameters were used to select features and train the classifier.

Each classifier was optimized over several parameters. Bayesian classifiers included nearest centroid, diagonal linear discriminant analysis, spherical discriminant, and uncorrelated discriminate classifiers.[52] KNN classifiers were optimized over ten values of K (K=1-10). The linear SVMs were optimized over ten cost values (i.e. 1 to 10). Feature selection was accomplished using the minimum redundancy, maximum relevance (mRMR) method, choosing optimal feature sizes from within the range of 1 to 100.[53] The mRMR feature selection method identified an optimal set of features that minimized the correlation among features while maximizing mutual information between features and class labels. Following omniClassifier analysis, more granular models were created using orthogonal partial least squares-discriminant analysis (oPLS-DA) for each of sham-operated or naïve vs. TBI samples (MATLAB, R2015a, The MathWorks, Natick, MA with PLS-Toolbox, version 8.0, Eigenvector Research, Inc., Manson, WA) with Venetian blinds CV.[54,55] Prior to oPLS-DA, features were autoscaled. Abundances of features with

significant changes (TBI vs. control) were analyzed at 3- and 7-days post-injury using a one-way analysis of variance (ANOVA) with $p < 0.05$ considered significant.

2.4 Development of a Lipid Biomarker Panel for the Classification of Moderate TBI

Overall, 2288 features were detected, this was and further reduced to 727 based on frequency criteria. PCA of this dataset (Figure 2.1A) showed that pooled samples grouped together and accurately represented the average composition of both TBI and non-injury (naïve + sham-operated) samples analyzed. Initially, each sample was projected into linear space so that the relationship across all variables could be visualized in two dimensions. However, the lack of distinct clustering in the PCA scores plot revealed that accurate discrimination of TBI would require the selection of specific features that directly reflected TBI pathophysiology using supervised classification approaches. We initially combined the injured groups in order to use robust binary classification schemes to find potential lipids that could distinguish injured from non-injured rats. Using a non-targeted lipidomics approach, we examined features that were able to distinguish TBI samples from controls. This feature set was then processed using a total of 120 multivariate omniClassifier models of controls (sham-operated + naïve) vs. TBI by testing a combination of various classifiers and comparing inner and outer CV values. In all cases, inner CV area under the curve (AUC) values approximately matched outer CV values, indicating lack of overfitting (Figure A2). Recursive selection within the 727-feature set simplified these classification models by reducing data dimensionality while preserving only features that resulted in high sensitivity and specificity of classification.

Table 2.1. Performance and selected features used for optimized models built with omniClassifier.

Classifier	Feature Selection Method	Number of Features	Cross-Validation Estimate, AUC (SD)	Performance on Whole Dataset, AUC	Features Selected (Using 1:727 Index)
Bayesian	mRMR-Difference	9	0.8019 (0.0618)	0.9653	24, 61, 140, 184, 271, 272, 377, 479, 665
K-nearest neighbors (K=10)	mRMR-Difference	31	0.8268 (0.0646)	0.9774	24, 41, 58, 61, 64, 103, 118, 128, 129, 140, 184, 185, 233, 245, 271, 272, 277, 289, 292, 314, 357, 377, 409, 479, 656, 665, 680, 698, 699, 702, 719
Logistic Regression	mRMR-Difference	17	0.8348 (0.0478)	1.0000	24, 41, 58, 61, 64, 140, 184, 245, 271, 272, 314, 377, 479, 656, 665, 699, 719
Linear Support Vector Machines (cost = 4)	mRMR-Difference	20	0.8404 (0.045)	1.0000	24, 41, 58, 61, 64, 118, 140, 184, 245, 271, 272, 314, 377, 409, 479, 656, 665, 680, 699, 719

Table 2.1 shows the performance of the best models produced by each of the four classifiers tested. All four models performed similarly well, with the number of features utilized ranging from 9 to 31 and AUC values ranging from 0.80 to 0.84 under CV. As expected, AUC performance on the whole dataset approached unity for these four best models, but the cross-validated AUC values were chosen as more representative of a scenario in which unknowns would be predicted. Interestingly, the smallest set of 9 features selected by the optimized Bayesian classifier using mRMR feature selection was conserved across all classifiers, lending support for the underlying biological basis of this multivariate

classification. The optimized KNN classification model, containing 31 metabolite features, was selected for chemical annotation of the features so as not to ignore any useful TBI biomarker that might reflect unique network level alterations. Of those 31 features, 5 eluted with the chromatographic solvent front where measured ion intensities are unreliable due to ion suppression effects.[56] As their removal from the multivariate model did not result in a significant decrease in classification accuracy, these features were excluded from further consideration. Following establishment of a subset of distinguishing features, we identified the molecules and examined changes in relative abundance at each of the post-injury time points.

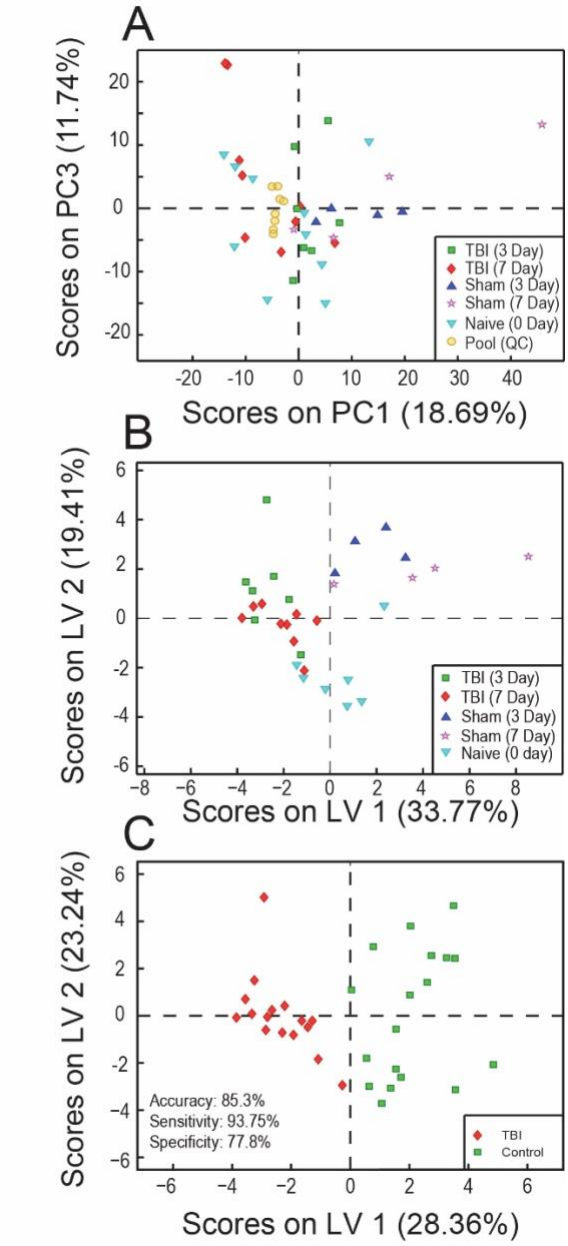

Figure 2.1: A) Principal component analysis (PCA) scores plot for the subset of 314 negative mode features obtained following filtering and prior to feature selection across each class. The distribution of samples in this plot reveals no clustering amongst samples. by class Pooled quality control samples, represented by yellow circles, clustered towards the center of the plot, indicating they are an accurate representation of the average sample analyzed. B) Orthogonal Partial Least Squares Discriminant Analysis (oPLS-DA) scores plot depicting clustering of samples separated into five classes by day of sample collection and injury status using the 26-feature model. Variance between classes is captured across the X-axis. C) oPLS-DA scores plot depicting clustering of samples separated into a binary model, with the y-axis acting as a separation boundary between classes. Samples are colored by the labels in the corresponding legends.

Figure 2.1B depicts an oPLS-DA scores plot for the optimized 26-feature lipid panel with all sample classes treated individually. Here, it becomes clear that the samples can be roughly split into two classes, with negative scores on latent variable (LV) 1 generally corresponding to TBI samples and positive scores on LV1 being more representative of controls, irrespective of day of collection. In a binary representation of the data, differences between all control samples and TBI samples were also modeled using oPLS-DA and leave-one-out CV (Figure 2.1C). Control samples separated from injured samples with no significant overlap, again with negative scores on LV1 corresponding to TBI samples and positive scores indicative of controls. The sensitivity, specificity and overall accuracy were 93.7 %, 77.8 % and 85.3 %, respectively. More detailed binary comparisons (sham-operated vs. TBI, naïve vs. TBI, all controls vs. TBI) were also performed using the same panel of 26 metabolites and oPLS-DA, a standard multivariate classification tool (Figure 2.2). The classification accuracy in all cases exceeded 90%, with a sensitivity of 93.8% and specificity of 87.5-100%. These results indicated that lipid alterations observed in the 26-feature panel can be attributed solely to TBI and were not a consequence of the surgical procedure.

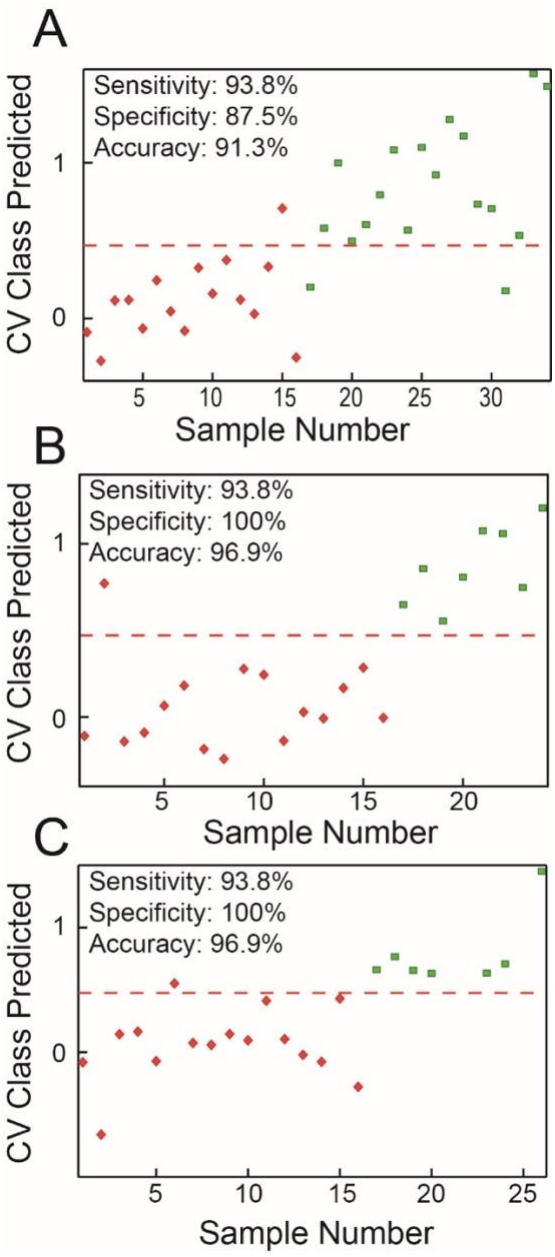

Figure 2.2: oPLS-DA cross validated class prediction plots based on the optimized 26 feature panel comparing A) sham + naïve controls vs. TBI, B) sham vs. TBI and C) naïve vs. TBI samples. For all plots, TBI samples are represented by red diamonds and correspond to a predicted class value of 0 while the various control samples are represented by green squares and correspond to a predicted value of 1. Accuracy, sensitivity and specificity values are given for each model. The red dashed line represents a decision boundary between classes. The oPLS-DA model details were as follows: A) 34 samples, venetian blinds CV, 5 splits, 3 latent variables (LVs); B) 24 samples, venetian blinds CV, 4 splits, 2 LVs; C) 26 samples, venetian blinds CV, 5 splits, 2 LVs.

2.5 Identification of Lipid Metabolites

With an average mass error of 1.4 ppm, the elemental formulae and head groups were determined for all but two lipids, and all species were annotated where possible. Table 2.2 details the identity of the lipids included in the 26-feature panel determined by both high-resolution mass spectrometry (HRMS) and MS/MS experiments, while Table A2 provides the level of confidence obtained for each identification. Two of the 26 species in the panel likely corresponded to a mixture of at least two lipids, which co-eluted in the UPLC dimension and were isobaric in the MS dimension, therefore being unavoidably co-isolated for MS/MS experiments. Distinction of these species was beyond the scope of this study, and would require an additional dimension of either liquid-phase or gas-phase separation, such as ion mobility.[57,58] Table 2.2 also depicts p-values and abundance fold changes (FC) for each species. Positive FC values correspond to species with increased abundance in injured samples, while negative values indicate higher abundance in controls. When considered univariately, 15 of the 26 lipid species showed p-values at or below 0.05 (p-value range=0.000354-0.0156) for a binary comparison between controls and TBI, though it must be taken into account that the panel as a whole was utilized for classification purposes, so the changes within an individual lipid species are less significant when alterations are investigated at a systems level. Of these 15 lipid species, 13 remained statistically significant when compared against time-matched sham controls only (naïve samples were removed from the control class) for p-value calculations, further verifying that the lipidome alterations observed were due to injury and not to surgery. Ionization efficiency varies widely between lipid classes, so only abundances of lipids belonging to the same class can be compared directly.[59] Calculation of absolute abundance values for

each lipid was beyond the scope of this paper, as it requires extraction of serum samples with all relevant internal standards.[60] This must therefore be performed prior to analysis and is better suited to targeted biomarker studies, which can be guided by our untargeted discovery analysis.[61]

Table 2.2. Annotation of lipids in 26-feature panel for the classification of moderate TBI. Retention time (RT), observed exact mass with Xevo instrument (and observed mass error), adduct, predicted elemental formulae, p-value comparing average abundances between all controls and TBI samples (and p-value comparing abundances between sham and TBI), and fold change (FC) values are included. Positive FC values correspond to species with increased abundance in injured animals, while negative values indicate higher concentrations in controls. Fatty acid chain information was included only when MS/MS experiments were possible, which required a minimum precursor ion abundance and no chemical overlaps with other species. SN1/SN2 stereochemistry was not determined. For those unidentified species, please refer to Table A2 for additional information on the identity of detected fragments. Abbreviations- PE: phosphatidylethanolamine; PC: phosphatidylcholine; Cer: Ceramide; DG: diacylglycerol; SM: sphingomyelin; PS: phosphatidylserine, PUA: polyunsaturated aldehyde, FFA: free fatty acid.

Feature Number	**RT (min)**	***m/z*** **Mass error (ppm)**	**Adduct**	**Elemental Formula**	**ID**	**p-value** **(p-value sham vs. TBI)**	**FC**
24	9.86	738.5081 0.27	[M-H]-	$C_{41}H_{74}NO_8P$	PE(20:4_16:0)	0.236 0.619	-1.58
41	5.38	303.2323 -2.31	[M-H]-	$C_{20}H_{32}O_2$	Arachidonic acid (AA)	0.0138 0.0134	1.35
58	11.32	666.6038 -0.60	$[M+HCO_2]^-$	$C_{40}H_{79}NO_3$	Cer(d18:1_22:0))	0.252 0.000168	-1.11
61	7.21	465.3035 -1.93	[M-H]-	$C_{27}H_{46}O_4S$	Cholesterol sulfate (CS)	0.00231 0.000971	-1.20
64	10.61	858.6225 -0.58	$[M+HCO_2]^-$	$C_{46}H_{88}NO_8P$	PC(20:2_18:0)	0.00280 **0.380**	-1.21
103	10.12	778.5594 -1.28	$[M+HCO_2]^-$	$C_{40}H_{80}NO_8P$	PC(16:0_16:0)	0.0606 0.0639	-1.50
118	10.35	742.5386 -0.81 -0.13	[M-H]- $[M-CH_3]^-$	$C_{41}H_{78}NO_8P$ $C_{42}H_{80}NO_8P$	PE(18:2_18:0) PC(18:2_16:0)	0.250 0.0763	-1.17
128	10.35	711.5221 -0.70	$[M+HCO_2]^-$	$C_{43}H_{70}O_5$	DG(22:6_18:1)	0.00169 6.92E-05	2.23
129	10.37	818.5912 -0.57	$[M+HCO_2]^-$	$C_{43}H_{84}NO_8P$	Not identified	0.0544 0.147	-1.18
245	0.54	262.8846	Not identified	Not identified	Not identified	0.00449 0.0235	2.88
271	10.02	709.5041 -1.13	$[M+HCO_2]^-$	$C_{43}H_{68}O_5$	DG(22:6_18:2)	0.000354 7.54E-06	2.49
272	5.91	329.2483 -0.91	[M-H]-	$C_{22}H_{34}O_2$	Docosapentaenoic acid (DPA)	0.00405 0.0001	2.59

Table 2.2 (continued).

277	10.47	687.5197 -1.16	$[M+HCO_2]^-$	$C_{41}H_{70}O_5$	DG(20:4_18:1)	0.00156 0.0057	2.61
289	5.02	283.2642 -0.35	$[M-H]^-$	$C_{18}H_{36}O_2$	FFA(18:0)	0.0153 0.000241	3.02
292	0.53	297.0985	Not identified	Not Identified	Not identified	0.0552 0.153	-10.8
314	1.48	295.2274 0.27	$[M-H]^-$	$C_{18}H_{32}O_3$	FFA(18:2 + 1 O)[c]	0.0560 0.0071	-2.55
357	9.35	813.617 6.64	$[M+NH_4]^+$	$C_{45}H_{82}NO_8P$	PE(18:0_22:4)	0.00835 **0.387**	-1.28
377	10.29	785.656 3.69	$[M+H]^+$	$C_{45}H_{89}N_2O_6P$	SM(d18:1/22:1))	0.00241 0.000247	-1.37
409	1.32	548.3713 0.36	$[M+H]^+$	$C_{28}H_{54}NO_7P$	LysoPC(20:2)	0.549 0.00147	-1.08
479	0.44	784.4746 -1.66	$[M+H]^+$	$C_{42}H_{74}NO_{10}P$	PS(16:0_20:4)	0.159 0.155	1.21
656	9.78	684.558 2.78	$[M+NH_4]^+$	$C_{43}H_{70}O_5$	DG(22:6_18:1)	0.00104 0.000213	2.67
665	10.93	746.5693 -0.13	$[M+H]^+$	$C_{41}H_{80}NO_8P$	Not identified	0.219 0.0492	-1.38
680	8.57	682.5402 -0.44	$[M+NH_4]^+$	$C_{43}H_{68}O_5$	DG(22:6_18:2)	0.000489 0.000125	2.60
698	7.14	822.60 -0.85	$[M+H]^+$	$C_{47}H_{84}NO_8P$	Not identified	0.370 0.0161	-1.36
699	0.92	582.3147 -0.17	$[M+2Na-H]^+$	$C_{26}H_{52}NO_8P$	LysoPC(18:2 + 1 O)	0.0144 0.0076	1.65
719	10.86	840.6465 -1.43	$[M+H]^+$	$C_{48}H_{90}NO_8P$	Not identified	0.0103 **0.426**	-2.65

[a] No matching database hits to expected fatty acid chain length from fragmentation experiments with PC headgroup.

[b] A co-eluting species at *m/z* 262.9005 was co-selected by the quadrupole in all attempted MS/MS experiments, preventing accurate annotation *via* fragmentation.

[c] The notation indicates that the position of the oxygen atom as well as the number of double bonds in the lipid structure are unclear at this stage. It could be an epoxide group or some other type of oxidized species.

Among the lipids identified as potential TBI biomarkers, PUFAs and PUFA-esterified DGs were found to increase in TBI samples. Also, a decrease in SM(d18:1_22:1) was observed in the TBI group, which was accompanied by a corresponding decrease in a related ceramide, Cer(d18:1_22:0). Injury-specific changes in abundance were also found for a variety of other membrane lipids (e.g. PCs, PEs, and a PS) as well as for CS. The PE membrane lipid containing esterified AA- PE(20:4_16:0)- was more abundant in controls, while the relative abundance of PS(20:4_16:0) was slightly increased in the TBI cohort following injury. Additionally, all PCs identified by the 26-feature model were of lower relative abundance in TBI samples, while the lysophosphatidylcholine (lysoPC) species observed showed an increase following injury.

In addition to the 26-lipid panel described in Table 2.2, other lipids were frequently selected by the 120 multivariate models built using omniClassifier but were not part of the optimum panels highlighted in Table 2.1. Figure A3 details the topmost 30 features in the 120 unique individual multivariate models based on their frequency of selection, which was related to the feature's ability to discriminate between classes. Only 7 features (#30, 34, 35, 227, 311, 475 and 701) were not covered in the 26-feature panel discussed above. Box plots and chemical annotations for the most significant additional features are shown in Figure A4. These were identified by both MS and MS/MS as eicosapentaenoic acid (EPA), DHA, lysoPE(20:4), PE(32:0), and PC(40:4).

2.6 Overview of Broad Changes in the Serum Lipidome

In order to visualize the entire set of relevant features simultaneously, a volcano plot was used to represent changes in individual species. Figure 2.3 provides a broad

overview of the most salient lipidome alterations following TBI as a function of p-value and fold change. Boundaries are drawn to illustrate features with FC absolute values > 2 and $p < 0.05$. Features in the upper left and upper right regions satisfy both of these requirements and are most likely to be good candidate biomarkers of TBI if a single species was more desirable, although it is known that biomarker panels are more robust than assays based on single species.[62,63] The lipids contained in the 26-feature model are indicated by red circles, with 9 of the 15 individually-significant features contained in those volcano plot regions. Additionally, most of the frequently selected features not in the panel, represented by blue X's in the plot, fell above the significance boundary, further validating the feature selection method. As shown, not all the selected features were significant or near significant individually; however, when combined into a multivariate panel, all species were critical to the accuracy of the classification.

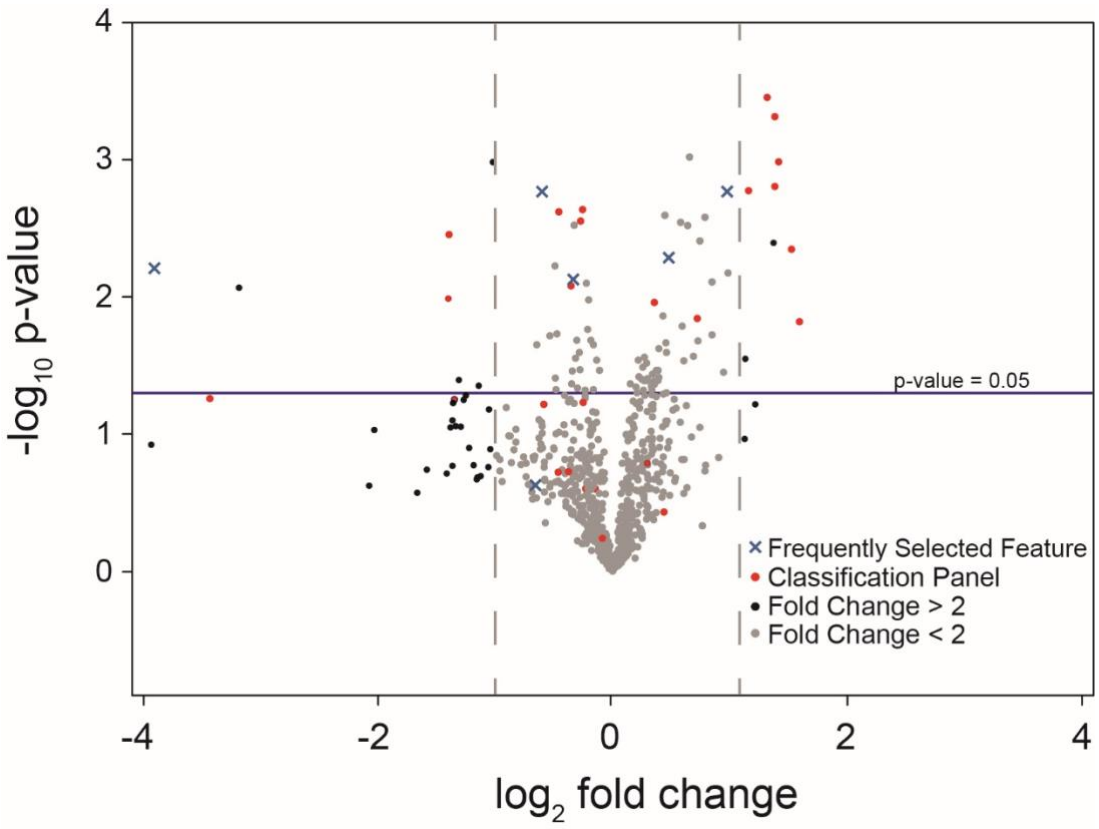

Figure 2.3: Volcano plot of processed metabolomic data set. Each point represents one feature. Features with fold change < 2 are colored in grey. Features in optimized classification panel are colored in red. Features frequently selected to build models but not in final classification panel are colored in blue. Positive fold change values correspond to increased abundance in TBI samples.

Box plots describing these trends in dysregulation and normalized relative abundances for a variety of lipid species from the classification panel are shown in Figure 2.4. As observed in panels A1-A3, FFA concentrations (18:0, 20:4 and 22:5) were all significantly elevated in TBI samples. The same trend held for DGs- DG(20:4_18:1) and DG(22:6_18:2)- as shown in panels A5 and A6. Panels B1-B3 illustrate decreases in abundance for CS as well for SM and PC species - SM(d18:1_22:1)) and PC(20:2_20:0).

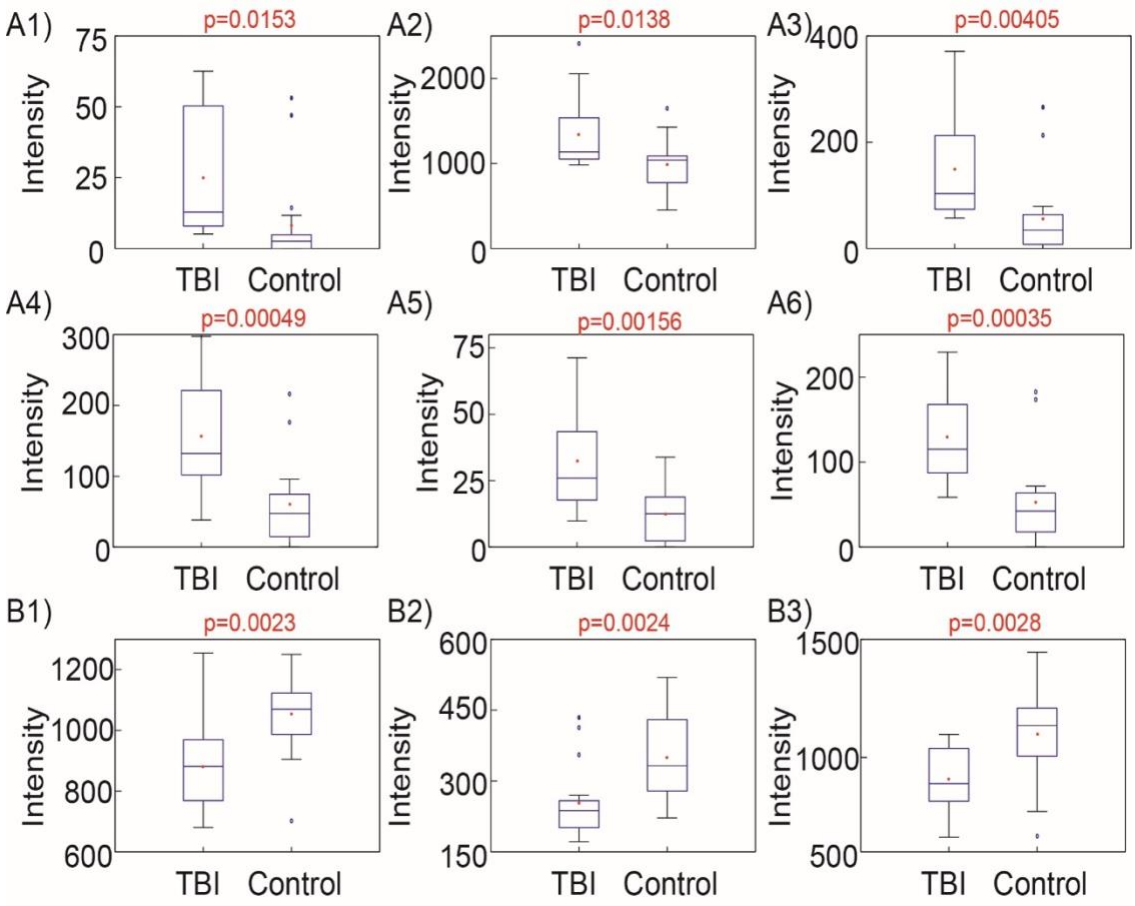

Figure 2.4: Example box plots showing significantly dysregulated species used by optimized model for classification of samples. A1-A6 show species that increased and B1-B3 show species that decreased following injury. A1) FFA 18:0, $[M-H]^-$ = 283.2644; A2) arachidonic acid, $[M-H]^-$ =303.2330; A3) docosapentaenoic acid, $[M-H]^-$ = 329.2483; A4) *m/z* = 262.8846; A5) DG(20:4_18:1), $[M+HCO_2]^-$ = 687.5197; A6) DG(22:6_18:2), $[M+HCO_2]^-$ = 709.5041; B1) Cholesterol Sulfate, $[M-H]^-$ = 465.3035; B2) SM(d18:1_22:1)), $[M+H]^+$ = 785.656; B3) PC(20:2_20:0), $[M+HCO_2]^-$ = 858.6225.

Altered lipids were subdivided into groups by describing their trend as increased, decreased, or no significant change at the 3- and 7-day time points following injury (Figure 2.5). No significant differences were observed compared to controls at either time point for five features, indicating that these alone are unlikely to translate to successful biomarkers. Approximately half (10/21) of the remaining features were significant across both time points when compared to controls, while 10 more showed significant differences at only 3- or 7-days post-injury (Figure 2.5A-B). Most features in the panel, all except for 2, did not show significant differences between 3 and 7 days, (Figure 2.5C). The remaining differences, however, could be attributed to reduced sample size for each pair-wise comparison or type I errors stemming from multiple comparisons. Additionally, many features showed temporal patterns supporting a return towards control levels at 7 days, warranting further study and inclusion of more acute time points to determine the time-course of biochemical changes following injury.

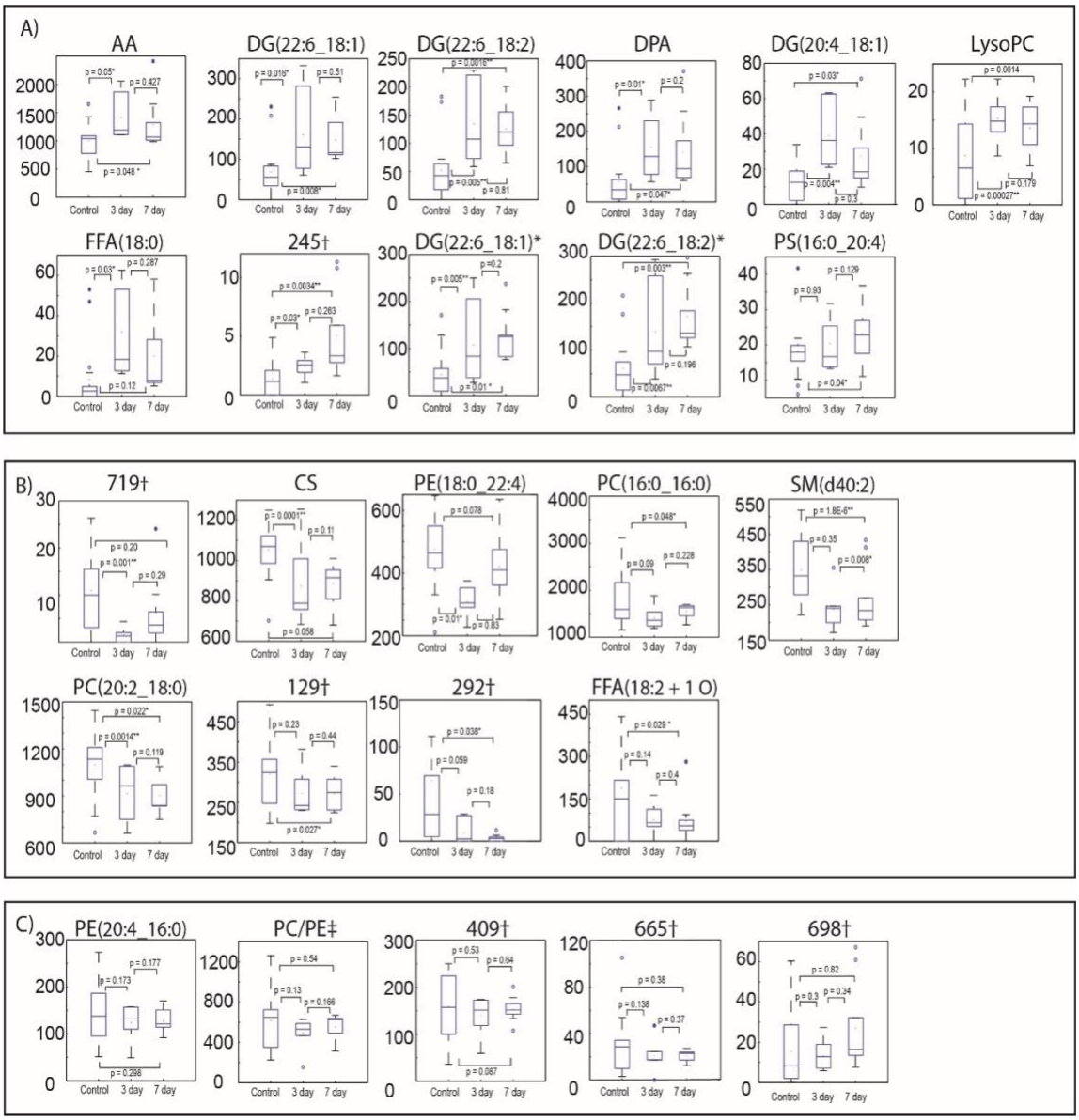

Figure 2.5: Boxplots showing time profile changes of samples at 0, 3 and 7 days following TBI. Features are divided into 3 groups: A) Features 14, 128, 271, 272, 277, 699, 289, 245, 656, 680 and 479 showed an initial increase following TBI; B) features 719, 61, 357, 103, 377, 64, 129, 292 and 314 that decreased following TBI and continued to decrease or started to return to baseline at 7 days; C) features 24, 118, 409, 665 and 698 that showed no significant differences between timepoints. †Not identified; *Adduct differences; ‡Corresponds to PE(18:2_18:0) and/or PC(18:2_16:0). See Table 2.2 for more information on lipids.

2.7 Discussion

We utilized a broadband, discovery approach to identify novel lipid biomarkers of moderate TBI in the serum of adult male rats at 3- and 7-days post-injury. These subacute time points correspond with ongoing secondary cell degradation, as well as the time-course of post-traumatic inflammatory and oxidative stress cascades.[31,64-70] Through the combination of HRMS methods and rigorous data-driven classification models (feature selection algorithms: Bayesian, KNN, Logistic Regression and SVMs), we determined a 26-feature lipid panel that consistently separated TBI samples from sham-operated and naïve controls with over 85% accuracy. Many of the lipids prominent in the panel were PUFAs and PUFA-containing DGs, as well as oxidized phospholipids, sphingolipids, and other lipophilic moieties. These dysregulated lipid species warrant further investigation and consideration for inclusion in a TBI biomarker panel. While it is expected that a biomarker panel will increase specificity over a single biomarker, 15 of the 26 lipids in the panel distinguished injury from control when considered individually, demonstrating the potential of this approach to identify TBI-specific changes in single lipid species.

2.7.1 Biological Relevance of the Identified Lipid Panel

Among the lipids identified as potential TBI biomarkers, PUFAs were found to increase after TBI. Specifically, FFAs such as FFA(18:0), FFA(20:4, AA), FFA(22:5, docosapentaenoic acid, DPA), and FFA(22:6, DHA) all showed significantly increased relative abundances following TBI, while the abundance of oxidized fatty acid species FFA(18:2 + 1 O) decreased. Similarly, elevated levels of AA have been found in rat serum following TBI using gas chromatography-mass spectrometry (GC-MS) at 1 and 5 days

post-injury.[71] FFA increases have also been observed in the rat brain following CCI[26] as well as in the CSF of TBI patients.[72,73]

An increase in FFAs is known to accompany cellular injury events such as uncoupling of oxidative phosphorylation, exacerbating the disruption of ion balance and aggregation of oxidative metabolites.[74] The disruption of calcium ion homeostasis in combination with energy depletion in the brain following injury leads to the activation of PLA_2 and PLC, which causes the release of FFAs from membrane phospholipids.[75,76] The activation of PLA_2 in particular causes the liberation of AA, DPA, EPA, DHA, and other FFAs, enabling their detection in serum post-TBI. Increases in phospholipase activity have been observed as early as 15 minutes post TBI,[77] and the levels of FFAs have been reported to remain elevated at least 35 days post-injury.[25] Evidence of fatty acid oxidation as well as disrupted amino acid metabolism has also been reported in patients presenting with severe blunt head trauma.[78].

While PUFAs are elevated following injury, FFA turnover is an essential process for membrane homeostasis and synaptogenesis,[79] and these changes may be associated with post-injury repair attempts. The downstream metabolites of AA have been cited as potential biomarkers of inflammation, albeit for both pro- and anti-inflammation cascades.[66] Specifically, AA is metabolized to eicosanoids through the COX pathway, as well to as anti-inflammatory lipoxins through the lipoxygenase (LOX) pathway, which are associated with the resolution phase of inflammation.[80]

Fatty acids can also undergo LP as a result of ROS and RNS imbalances once cleaved from membrane phospholipids, leading to the formation of α,ß-unsaturated aldehydes including MDA, 4-HNE and acrolein.[81] We observed a decreased abundance for

the oxidized FFA (18:2 + 1 O) and a lysoPC of the same species, lysoPC(18:2 + 1 O). The enzyme lipoprotein associated phospholipase A_2 (Lp-PLA_2) hydrolyzes oxidized phospholipids within LDL to generate oxidized lysoPC molecules, which are known to induce inflammation.[82] However, the resolution phase following injury is not reached if the oxygen supply in the brain is not re-established, possibly explaining the decrease in observed oxidized FFAs.[83] The decreased relative abundance of these oxidation products in TBI samples may thus indicate a lack of effective controlled clearance of damaged cellular membranes following TBI, possibly due to an imbalance in PUFA concentrations. Necrotic cell death also stimulates the release of ROS and cytokines, the activation of phospholipase and sphingomyelinase, and phospholipid hydrolysis, all of which occur in TBI.[84] Furthermore, the CNS has a high level of lipid content, providing abundant substrates for oxidative attack by ROS.[85] Neurons are particularly vulnerable to ROS due to reduced glutathione levels, with the high degree of polyunsaturation of brain lipids providing many sites for the propagation of LP reactions.[86]

We also found that PUFA-esterified DGs changed significantly following TBI. TBI stimulates the activation of phospholipases C and D, resulting in increased abundances of DGs.[87] In our study, DGs- specifically those containing PUFA residues (22:6 or 20:4)- were significantly increased in relative abundance following TBI. It has been shown previously that DGs in rat brains were increased immediately following CCI and remained elevated a month later compared to controls.[26]

While FFAs and DGs were increased in response to injury, all PCs and PEs identified in the classification panel were decreased in abundance after TBI. The majority of these lipids were esterified by PUFAs such as AA, including PE(20:4_16:0), PE

(22:4_18:0), and PC(20:2_18:0), which were all decreased in TBI samples, while the relative abundance of PS(20:4_16:0) was slightly increased. Although lipid species containing only saturated fatty acids followed the same trend, none achieved statistical significance individually.

A recent study showed decreased levels of cortical and cerebellar PCs and PEs following CCI in the rat, while hippocampal PC and PE levels were elevated. Levels of overall PC, PE, and SM were lower in plasma following injury, and ether PE levels were lower in the cortices and plasma of injured mice relative to controls.[24] In addition to preclinical evidence, phospholipid dysregulation has been observed in the CSF of human subjects following TBI. Clinical evidence for the disruption of CNS phospholipids has been observed within the first days following TBI, with PCs and PEs elevated to the highest concentration by day four.[88] Similarly, both PCs and PEs were dramatically increased as early as one day following TBI, though levels decreased with time for survivors, falling below control levels by day six.[89] Total PS concentrations were elevated at all measured time points, in agreement with the observed trend for the AA-containing PS molecule identified in the 26-feature panel above. Clinical evidence supports the initial increase of membrane phospholipids upon injury, followed by a decrease to levels below controls, likely indicative of ongoing hydrolysis of PC and PE species.[85] Activation of phospholipases results in the hydrolysis of PUFAs esterified to membrane phospholipids, leading to decreased concentrations of PUFA-containing PC and PEs. The same pathophysiology resulting in the increased formation of FFAs also leads to a decreased rate of phospholipid re-synthesis, and our results follow previous observations regarding phospholipid dysregulation following TBI.

Injury-specific changes in abundance were found for a variety of membrane lipids (e.g. PCs, PEs, and PSs) as well as for CS, which was significantly decreased in the TBI cohort. CS is an end product in the cholesterol metabolic pathway and may play a stabilizing role in cell membranes.[90] The decrease in CS may also indicate a possible disturbance in AA regulation, a vital pathway in the secondary injury cascade.[91] Additionally, while both cholesterol and CS play key roles in lipid organization, CS is often found in high abundance in DHA rich membranes.[92] DHA was increased following moderate injury, though CS was significantly decreased, potentially decreasing membrane permeability due to less efficient packing.

2.7.2 Limitations

There are some limitations to the present study that should be acknowledged. While we focused on time-points that are known to reflect secondary injury changes, exploration of earlier time points may help to guide biomarker panel development in the acute period for diagnostics measures. Furthermore, we did not examine possible correlations between biomarker levels and histopathological or behavioral changes post-TBI. While such correlation is not straightforward [93,94] it will be pertinent to examine histopathologic correlates. As the lipid panel is refined, it would also beneficial to study not only other outcome measures, but also how addition of other fluid biomarkers, such as GFAP or UCH_L1, might improve specificity and sensitivity of diagnosis.

Additional lipid changes after both experimental and clinical TBI have been observed. Gangliosides such as GM2, have been shown to increase in the hippocampus, thalamus and hypothalamus of mice following blast TBI, accompanied by a corresponding decrease in ceramides.[27] Brain CLs have been shown to be selectively oxidized following

TBI, [21,95,96] though none were detected in this study due to their low abundance in plasma resulting from localization within the mitochondrial membrane, as well as possible ion suppression effects.[97-99] Also DGs and CEs have been found to increase, while PCs, PEs, PIs, and cholesterol decrease in rat brains following CCI.[23] Phospholipids esterified with PUFAs have been found to increase in the CSF of TBI patients.[24] Similarly, levels were higher in patients with TBI who died within days after injury compared to those who survived.[89,100] The results of our study thus lend support to previously identified lipidome alterations resulting from TBI and introduce a host of new potential biomarker candidates warranting further validation.

2.8 Conclusion

In addition to providing novel lipid biomarker candidates for TBI, the untargeted nature of our study also provides an in-depth exploration of the metabolic processes in the subacute post-TBI period. Overall, many of the altered lipids are known to be involved in secondary injury pathways and would be expected to cross the BBB regardless of injury severity, increasing their likelihood of being detectable in serum, a readily accessible matrix with clinical relevance. The identified lipids may serve as prognostic biomarkers for TBI in the rat model, and it is expected that many of the same lipids could be detectable in both rodent and human blood. However, due to differences in the genome, proteome and subsequently the metabolome between rodents and humans, this specific diagnostic panel is unlikely to have direct clinical utility. Therefore, further discovery and validation studies are needed to assess the viability of this panel in detecting TBI in human patients. The metabolism of lipids is both complex and interwoven, but this study serves as a foundation

for future validation studies of TBI biomarkers. Comprehensive biomarker panels for TBI diagnosis and clinical management should consider inclusion of lipid-based molecules.

2.9 References

1 Faul, M., Xu, L., Wald, M. M. & Coronado, V. Traumatic Brain Injury in the United States. *Atlanta, GA: Centers for Disease Control and Prevention, National Center for Injury Prevention and Control* (2010).

2 Langlois, J. A., Rutland-Brown, W. & Wald, M. M. The epidemiology and impact of traumatic brain injury: a brief overview. *J Head Trauma Rehabil* **21**, 375-378 (2006).

3 Daneshvar, D. H., Nowinski, C. J., McKee, A. C. & Cantu, R. C. The epidemiology of sport-related concussion. *Clinics in sports medicine* **30**, 1-17 (2011).

4 Mondello, S. *et al.* The Challenge of Mild Traumatic Brain Injury: Role of Biochemical Markers in Diagnosis of Brain Damage. *Medicinal Research Reviews* **34**, 503-531, doi:10.1002/med.21295 (2014).

5 Bruns, J. & Hauser, W. A. The Epidemiology of Traumatic Brain Injury: A Review. *Epilepsia* **44**, 2-10, doi:10.1046/j.1528-1157.44.s10.3.x (2003).

6 Shear, D. A. *et al.* Severity profile of penetrating ballistic-like brain injury on neurofunctional outcome, blood–brain barrier permeability, and brain edema formation. *Journal of neurotrauma* **28**, 2185-2195 (2011).

7 Jennett, B. *et al.* Prognosis of patients with severe head injury. *Neurosurgery* **4**, 283-289 (1979).

8 Maas, A. I., Stocchetti, N. & Bullock, R. Moderate and severe traumatic brain injury in adults. *The Lancet Neurology* **7**, 728-741 (2008).

9 Ruff, R. Two decades of advances in understanding of mild traumatic brain injury. *The Journal of head trauma rehabilitation* **20**, 5-18 (2005).

10 Dash, P. K., Zhao, J., Hergenroeder, G. & Moore, A. N. Biomarkers for the diagnosis, prognosis, and evaluation of treatment efficacy for traumatic brain injury. *Neurotherapeutics* **7**, 100-114 (2010).

11 Pineda, J. A., Wang, K. K. & Hayes, R. L. Biomarkers of proteolytic damage following traumatic brain injury. *Brain Pathol* **14**, 202-209 (2004).

12 Plog, B. A. *et al.* Biomarkers of traumatic injury are transported from brain to blood via the glymphatic system. *J Neurosci* **35**, 518-526, doi:10.1523/JNEUROSCI.3742-14.2015 (2015).

13 Iliff, J. J. *et al.* A paravascular pathway facilitates CSF flow through the brain parenchyma and the clearance of interstitial solutes, including amyloid β. *Science translational medicine* **4**, 147ra111-147ra111 (2012).

14 Zhang, Z., Larner, S. F., Kobeissy, F., Hayes, R. L. & Wang, K. K. Systems biology and theranostic approach to drug discovery and development to treat traumatic brain injury. *Methods Mol Biol* **662**, 317-329, doi:10.1007/978-1-60761-800-3_16 (2010).

15 Csuka, E. *et al.* IL-10 levels in cerebrospinal fluid and serum of patients with severe traumatic brain injury: relationship to IL-6, TNF-α, TGF-β1 and blood–brain barrier function. *Journal of neuroimmunology* **101**, 211-221 (1999).

16 Kossmann, T. *et al.* Intrathecal and serum interleukin-6 and the acute-phase response in patients with severe traumatic brain injuries. *Shock* **4**, 311-317 (1995).

17 Viant, M. R., Lyeth, B. G., Miller, M. G. & Berman, R. F. An NMR metabolomic investigation of early metabolic disturbances following traumatic brain injury in a mammalian model. *NMR in Biomedicine* **18**, 507-516 (2005).

18 Pardridge, W. M. The blood-brain barrier: bottleneck in brain drug development. *NeuroRx* **2**, 3-14 (2005).

19 Davson, H. *An introduction to the blood-brain barrier*. (CRC Press, 1993).

20 Sheth, S. A., Iavarone, A. T., Liebeskind, D. S., Won, S. J. & Swanson, R. A. Targeted lipid profiling discovers plasma biomarkers of acute brain injury. *PLoS One* **10**, e0129735 (2015).

21 Ji, J. *et al.* Lipidomics identifies cardiolipin oxidation as a mitochondrial target for redox therapy of brain injury. *Nature neuroscience* **15**, 1407 (2012).

22 Hankin, J. A. *et al.* MALDI mass spectrometric imaging of lipids in rat brain injury models. *Journal of the American Society for Mass Spectrometry* **22**, 1014 (2011).

23 Roux, A. *et al.* Mass spectrometry imaging of rat brain lipid profile changes over time following traumatic brain injury. *Journal of neuroscience methods* **272**, 19-32 (2016).

24 Abdullah, L. *et al.* Lipidomic analyses identify injury-specific phospholipid changes 3 mo after traumatic brain injury. *FASEB J* **28**, 5311-5321, doi:10.1096/fj.14-258228 (2014).

25 Homayoun, P. *et al.* Delayed phospholipid degradation in rat brain after traumatic brain injury. *Journal of neurochemistry* **69**, 199-205 (1997).

26 Homayoun, P. *et al.* Cortical impact injury in rats promotes a rapid and sustained increase in polyunsaturated free fatty acids and diacylglycerols. *Neurochemical research* **25**, 269-276 (2000).

27 Woods, A. S. *et al.* Gangliosides and ceramides change in a mouse model of blast induced traumatic brain injury. *ACS chemical neuroscience* **4**, 594-600 (2013).

28 Kochanek, P. M. *et al.* Biomarkers of primary and evolving damage in traumatic and ischemic brain injury: diagnosis, prognosis, probing mechanisms, and therapeutic decision making. *Curr Opin Crit Care* **14**, 135-141, doi:10.1097/MCC.0b013e3282f5756400075198-200804000-00004] (2008).

29 Anthonymuthu, T. S., Kenny, E. M. & Bayir, H. Therapies targeting lipid peroxidation in traumatic brain injury. *Brain Res* **1640**, 57-76, doi:10.1016/j.brainres.2016.02.006 (2016).

30 McAllister, T. W. Neurobiological consequences of traumatic brain injury. *Dialogues Clin Neurosci* **13**, 287-300 (2011).

31 Singh, I. N., Sullivan, P. G., Deng, Y., Mbye, L. H. & Hall, E. D. Time course of post-traumatic mitochondrial oxidative damage and dysfunction in a mouse model of focal traumatic brain injury: implications for neuroprotective therapy. *Journal of Cerebral Blood Flow & Metabolism* **26**, 1407-1418 (2006).

32 Kimball, B. A. *et al.* Brain injury alters volatile metabolome. *Chemical senses* **41**, 407-414 (2016).

33 Schiess, R., Wollscheid, B. & Aebersold, R. Targeted proteomic strategy for clinical biomarker discovery. *Molecular oncology* **3**, 33-44 (2009).

34 Iannaccone, P. M. & Jacob, H. J. Rats! *Disease Models & Mechanisms* **2**, 206-210, doi:10.1242/dmm.002733 (2009).

35 Mondello, S. *et al.* Blood-based diagnostics of traumatic brain injuries. *Expert review of molecular diagnostics* **11**, 65-78 (2011).

36 White, T. E. *et al.* Gene expression patterns following unilateral traumatic brain injury reveals a local pro-inflammatory and remote anti-inflammatory response. *BMC genomics* **14**, 282 (2013).

37 Osier, N. & Dixon, C. E. The Controlled Cortical Impact Model of Experimental Brain Trauma: Overview, Research Applications, and Protocol. *Methods Mol Biol* **1462**, 177-192, doi:10.1007/978-1-4939-3816-2_11 (2016).

38 Kobeissy, F. H. *Brain neurotrauma: molecular, neuropsychological, and rehabilitation aspects*. (Crc Press, 2015).

39 Betancur, M. I. *et al.* Chondroitin Sulfate Glycosaminoglycan Matrices Promote Neural Stem Cell Maintenance and Neuroprotection Post-Traumatic Brain Injury. *ACS Biomater. Sci. Eng.* **3**, 420-430, doi:10.1021/acsbiomaterials.6b00805 (2017).

40 Gutowski, S. M. *et al.* Protease-degradable PEG-maleimide coating with on-demand release of IL-1Ra to improve tissue response to neural electrodes. *Biomaterials* **44**, 55-70 (2015).

41 Sharp, M. K. & Mohammad, S. F. Scaling of hemolysis in needles and catheters. *Annals of biomedical engineering* **26**, 788-797 (1998).

42 Lippi, G. *et al.* in *Seminars in thrombosis and hemostasis.* 565-575 (Thieme Medical Publishers).

43 Sarafian, M. H. *et al.* Objective set of criteria for optimization of sample preparation procedures for ultra-high throughput untargeted blood plasma lipid profiling by ultra performance liquid Chromatography–Mass spectrometry. *Analytical chemistry* **86**, 5766-5774 (2014).

44 Folch, J., Lees, M. & Sloane-Stanley, G. A simple method for the isolation and purification of total lipids from animal tissues. *J Biol chem* **226**, 497-509 (1957).

45 Bligh, E. G. & Dyer, W. J. A rapid method of total lipid extraction and purification. *Canadian journal of biochemistry and physiology* **37**, 911-917 (1959).

46 Pitkänen, A., Schwartzkroin, P. A. & Moshé, S. L. *Models of seizures and epilepsy*. 161-177 (Academic Press, 2005).

47 Fahy, E. *et al.* Update of the LIPID MAPS comprehensive classification system for lipids. *Journal of lipid research* **50**, S9-S14 (2009).

48 Smith, C. A. *et al.* METLIN: a metabolite mass spectral database. *Therapeutic drug monitoring* **27**, 747-751 (2005).

49 Wishart, D. S. *et al.* HMDB 3.0—the human metabolome database in 2013. *Nucleic acids research* **41**, D801-D807 (2012).

50 Faul, F., Erdfelder, E., Lang, A.-G. & Buchner, A. G* Power 3: A flexible statistical power analysis program for the social, behavioral, and biomedical sciences. *Behavior research methods* **39**, 175-191 (2007).

51 Phan, J. H., Kothari, S. & Wang, M. D. omniClassifier: a desktop grid computing system for big data prediction modeling. *Proceedings of the 5th ACM Conference on Bioinformatics, Computational Biology, and Health Informatics.* 514-523 (ACM).

52 Parry, R. M., Phan, J. H. & Wang, M. D. Win percentage: a novel measure for assessing the suitability of machine classifiers for biological problems. *BMC bioinformatics* **13**, S7 (2012).

53 Ding, C. & Peng, H. Minimum redundancy feature selection from microarray gene expression data. *Journal of bioinformatics and computational biology* **3**, 185-205 (2005).

54 Worley, B. & Powers, R. Multivariate Analysis in Metabolomics. *Curr Metabolomics* **1**, 92-107, doi:10.2174/2213235X11301010092 (2013).

55 Boccard, J. & Rutledge, D. N. A consensus orthogonal partial least squares discriminant analysis (OPLS-DA) strategy for multiblock Omics data fusion. *Analytica Chimica Acta* **769**, 30-39, doi:10.1016/j.aca.2013.01.022 (2013).

56 Annesley, T. M. Ion suppression in mass spectrometry. *Clinical chemistry* **49**, 1041-1044 (2003).

57 Kliman, M., May, J. C. & McLean, J. A. Lipid analysis and lipidomics by structurally selective ion mobility-mass spectrometry. *Biochim Biophys Acta* **1811**, 935-945, doi:10.1016/j.bbalip.2011.05.016 (2011).

58 May, J. C. & McLean, J. A. Advanced Multidimensional Separations in Mass Spectrometry: Navigating the Big Data Deluge. *Annu Rev Anal Chem (Palo Alto Calif)* **9**, 387-409, doi:10.1146/annurev-anchem-071015-041734 (2016).

59 Brügger, B., Erben, G., Sandhoff, R., Wieland, F. T. & Lehmann, W. D. Quantitative analysis of biological membrane lipids at the low picomole level by nano-electrospray ionization tandem mass spectrometry. *Proceedings of the National Academy of Sciences of the United States of America* **94**, 2339-2344 (1997).

60 Ivanova, P. T., Milne, S. B., Myers, D. S. & Brown, H. A. Lipidomics: a mass spectrometry based systems level analysis of cellular lipids. *Current opinion in chemical biology* **13**, 526-531 (2009).

61 Römisch-Margl, W. *et al.* Procedure for tissue sample preparation and metabolite extraction for high-throughput targeted metabolomics. *Metabolomics* **8**, 133-142 (2012).

62 Semmes, O. J. Defining the role of mass spectrometry in cancer diagnostics. *Cancer Epidemiol Biomarkers Prev* **13**, 1555-1557 (2004).

63 Robin, X. *et al.* PanelomiX: a threshold-based algorithm to create panels of biomarkers. *Advances in Integrative Medicine* **1**, 57-64 (2013).

64 Başkaya, M. K., Rao, A. M., Doğan, A., Donaldson, D. & Dempsey, R. J. The biphasic opening of the blood–brain barrier in the cortex and hippocampus after traumatic brain injury in rats. *Neuroscience letters* **226**, 33-36 (1997).

65 Ansari, M. A., Roberts, K. N. & Scheff, S. W. A time course of contusion-induced oxidative stress and synaptic proteins in cortex in a rat model of TBI. *Journal of neurotrauma* **25**, 513-526 (2008).

66 Ziebell, J. M. & Morganti-Kossmann, M. C. Involvement of pro- and anti-inflammatory cytokines and chemokines in the pathophysiology of traumatic brain injury. *Neurotherapeutics* **7**, 22-30, doi:10.1016/j.nurt.2009.10.016 (2010).

67 Soares, H. D., Hicks, R. R., Smith, D. & McIntosh, T. K. Inflammatory leukocytic recruitment and diffuse neuronal degeneration are separate pathological processes resulting from traumatic brain injury. *Journal of Neuroscience* **15**, 8223-8233 (1995).

68 Chen, S., Pickard, J. & Harris, N. Time course of cellular pathology after controlled cortical impact injury. *Experimental neurology* **182**, 87-102 (2003).

69 Cao, T., Thomas, T. C., Ziebell, J. M., Pauly, J. R. & Lifshitz, J. Morphological and genetic activation of microglia after diffuse traumatic brain injury in the rat. *Neuroscience* **225**, 65-75 (2012).

70 Licastro, F. *et al.* Peripheral inflammatory markers and antioxidant response during the post-acute and chronic phase after severe traumatic brain injury. *Frontiers in neurology* **7**, 189 (2016).

71 Yang, S. *et al.* Arachidonic acid: a bridge between traumatic brain injury and fracture healing. *Journal of neurotrauma* **29**, 2696-2705 (2012).

72 Pilitsis, J. G. *et al.* Free fatty acids in cerebrospinal fluids from patients with traumatic brain injury. *Neuroscience letters* **349**, 136-138 (2003).

73 Farias, S. E., Heidenreich, K. A., Wohlauer, M. V., Murphy, R. C. & Moore, E. E. Lipid mediators in cerebral spinal fluid of traumatic brain injured patients. *J Trauma* **71**, 1211-1218, doi:10.1097/TA.0b013e3182092c62 (2011).

74 Prins, M., Greco, T., Alexander, D. & Giza, C. C. The pathophysiology of traumatic brain injury at a glance. *Disease models and mechanisms* **6**, 1307-1315 (2013).

75 Wieloch, T. & Siesjo, B. K. Ischemic brain injury: the importance of calcium, lipolytic activities, and free fatty acids. *Pathol Biol (Paris)* **30**, 269-277 (1982).

76 McIntosh *et al.* gThe Dorothy Russell Memorial Lecture* The molecular and cellular sequelae of experimental traumatic brain injury: pathogenetic mechanisms. *Neuropathology and Applied Neurobiology* **24**, 251-267, doi:10.1046/j.1365-2990.1998.00121.x (1998).

77 Shohami, E., Shapira, Y., Yadid, G., Reisfeld, N. & Yedgar, S. Brain phospholipase A2 is activated after experimental closed head injury in the rat. *Journal of neurochemistry* **53**, 1541-1546 (1989).

78 Parent, B. A. *et al.* Use of metabolomics to trend recovery and therapy after injury in critically ill trauma patients. *JAMA surgery* **151**, e160853-e160853 (2016).

79 Da Silva, T. F., Sousa, V. F., Malheiro, A. R. & Brites, P. The importance of ether-phospholipids: a view from the perspective of mouse models. *Biochim Biophys Acta* **1822**, 1501-1508, doi:10.1016/j.bbadis.2012.05.014 (2012).

80 Needleman, P., Jakschik, B., Morrison, A. & Lefkowith, J. Arachidonic acid metabolism. *Annual review of biochemistry* **55**, 69-102 (1986).

81 Janero, D. R. Malondialdehyde and thiobarbituric acid-reactivity as diagnostic indices of lipid peroxidation and peroxidative tissue injury. *Free Radical Biology and Medicine* **9**, 515-540 (1990).

82 Zalewski, A., Nelson, J. J., Hegg, L. & Macphee, C. Lp-PLA2: a new kid on the block. *Clinical chemistry* **52**, 1645-1650 (2006).

83 Thomale, U.-W., Schaser, K., Kroppenstedt, S.-N., Unterberg, A. & Stover, J. F. in *Intracranial Pressure and Brain Biochemical Monitoring* 229-231 (Springer, 2002).

84 Morganti-Kossmann, M. C., Rancan, M., Stahel, P. F. & Kossmann, T. Inflammatory response in acute traumatic brain injury: a double-edged sword. *Current opinion in critical care* **8**, 101-105 (2002).

85 Adibhatla, R. M. & Hatcher, J. F. Role of Lipids in Brain Injury and Diseases. *Future Lipidol.* **2**, 403-422, doi:10.2217/17460875.2.4.403 (2007).

86 Tyurin, V. A. *et al.* Oxidative stress following traumatic brain injury in rats. *Journal of neurochemistry* **75**, 2178-2189 (2000).

87 Tang, X., Edwards, E. M., Holmes, B. B., Falck, J. R. & Campbell, W. B. Role of phospholipase C and diacylglyceride lipase pathway in arachidonic acid release and acetylcholine-induced vascular relaxation in rabbit aorta. *Am J Physiol Heart Circ Physiol* **290**, H37-45, doi:10.1152/ajpheart.00491.2005 (2006).

88 Pasvogel, A. E., Miketova, P. & Moore, I. M. K. Cerebrospinal fluid phospholipid changes following traumatic brain injury. *Biological research for nursing* **10**, 113-120 (2008).

89 Pasvogel, A. E., Miketova, P. & Moore, I. M. Differences in CSF phospholipid concentration by traumatic brain injury outcome. *Biological research for nursing* **11**, 325-331 (2010).

90 Banerjee, R. & Roy, A. The sulfotransferases of guinea pig liver. *Molecular pharmacology* **2**, 56-66 (1966).

91 Blache, D. Enhanced arachidonic acid and calcium metabolism in cholesteryl sulfate-enriched rat platelets. *Journal of lipid mediators and cell signalling* **13**, 127-138 (1996).

92 Schofield, M., Jenski, L. J., Dumaual, A. C. & Stillwell, W. Cholesterol versus cholesterol sulfate: effects on properties of phospholipid bilayers containing docosahexaenoic acid. *Chemistry and physics of lipids* **95**, 23-36 (1998).

93 Mondello, S. *et al.* Insight into pre-clinical models of traumatic brain injury using circulating brain damage biomarkers: Operation brain trauma therapy. *Journal of neurotrauma* **33**, 595-605 (2016).

94 Ringger, N. C. *et al.* A novel marker for traumatic brain injury: CSF αII-spectrin breakdown product levels. *Journal of neurotrauma* **21**, 1443-1456 (2004).

95 Bayir, H. *et al.* Selective early cardiolipin peroxidation after traumatic brain injury: an oxidative lipidomics analysis. *Annals of Neurology* **62**, 154-169, doi:10.1002/ana.21168 (2007).

96 Sparvero, L. J. *et al.* Mass-spectrometry based oxidative lipidomics and lipid imaging: applications in traumatic brain injury. *Journal of neurochemistry* **115**, 1322-1336 (2010).

97 Cheng, H. *et al.* Shotgun Lipidomics Reveals the Temporally Dependent, Highly Diversified Cardiolipin Profile in the Mammalian Brain: Temporally Coordinated Postnatal Diversification of Cardiolipin Molecular Species with Neuronal Remodeling†. *Biochemistry* **47**, 5869-5880 (2008).

98 Levine , J. S., Branch , D. W. & Rauch , J. The Antiphospholipid Syndrome. *New England Journal of Medicine* **346**, 752-763, doi:10.1056/NEJMra002974 (2002).

99 Marinetti, G., Erbland, J. & Stotz, E. Phosphatides of pig heart cell fractions. *Journal of Biological Chemistry* **233**, 562-565 (1958).

100 Kay, A. D. *et al.* Remodeling of cerebrospinal fluid lipoprotein particles after human traumatic brain injury. *Journal of neurotrauma* **20**, 717-723 (2003).

CHAPTER 3: ACUTE PHASE SERUM LIPIDOME ALTERATIONS IN A RODENT MODEL OF CLOSED-HEAD MILD TRAUMATIC BRAIN INJURY

3.1 Abstract

Following the development of a high accuracy multivariate classification panel to detect moderate traumatic brain injury at the post-acute phase (t= 3-7 days), we proposed to study a mild injury model at an earlier acute time point (t=24 h). Using a matched pair study design to improve statistical power, a panel of 16 lipid metabolites was developed with a classification accuracy of 88.5%, a modest improvement from the previous study despite the use of a less complex metabolite panel (reduction of the number features utilized for classification) and the occurrence of a milder form of injury in which the average effect size of lipid alterations was reduced. These promising results demonstrate the feasibility of utilizing non-targeted lipidomics to detect mild, concussive events in serum samples. MS/MS analysis of the target panel reveals similar trends with respect to alterations in lipid classes to those observed in the first study of moderate TBI, here indicating that phosphatidylcholines (PCs) were increased in TBI samples, while a lysoPC was decreased in abundance compared to controls. Again, cholesterol sulfate was identified as a biomarker candidate, exhibiting a significant (1.27-fold) decrease in abundance across mTBI samples, while a DHA-containing CE showed a relative increase (1.48-fold). Time-matched sham controls were included to indicate that changes in lipid profiles were a direct consequence of the injury. Control samples including pre-injury baseline, sham baseline, and sham 24-hour samples were nearly identical experimentally, except for the time and

method of collection as well as total duration of anesthesia exposure. Specificity must still be demonstrated in other co-occurring environments to be applicable to return to play considerations (e.g. stress, exercise, inflammatory diseases, or orthopedic injury).

3.2 Introduction

3.2.1 Traumatic Brain Injury Epidemiology

The widespread occurrence of TBI in the military, general public and athletics has led to heightened awareness of an ongoing public health crisis, in which more than 50 million injuries are estimated to occur worldwide each year.[1] Including both direct and indirect healthcare expenses, the total economic burden of brain injuries exceeds $400 billion USD annually, accounting for approximately 0.5% of the global output.[2,3] TBI is especially prevalent in young adults, as more than 30% of people have experienced some form of TBI by age 25, while more than half of the world's population will sustain a TBI at some point in their lifetime.[1,4] TBI is also the leading cause of mortality in young adults and is among the leading causes of injury related death and disability across all populations.[5]

TBI is typically stratified into three broad categories (mild, moderate, and severe) based on a patient's level of consciousness using the GCS.[6] However, this simple grading scheme fails to capture the heterogeneity associated with different primary and secondary injury mechanisms. Variance within the affected clinical population, including age, sex, and genetic differences as well as previous history of injury, may also have an influence on outcome.[7,8] Until recently, most research focused on severe TBI, which accounts for only approximately 3% of the documented injuries worldwide. However more than 70-90% of TBI occurrences are classified as mild, or mTBI. Synonymous with concussions,

these milder injuries were initially viewed as insignificant, with patients being discharged immediately without any recommended follow up.[9] However, it is now understood that even mild brain trauma can lead to significant neurological alterations, post-traumatic amnesia, and other concussive symptoms, which may persist for days, weeks or even years in some instances.[10,11] Mild brain injuries are often diagnosed based on the presence of these subjective self-reported symptoms, which has led to many going undetected or unreported.[12] Thus, a substantial gap remains between basic science efforts and clinical implementation of more objective injury assessments in the setting of mTBI. Concerted research efforts must be focused on the study of individual responses in the midst of heterogeneity in order to develop diagnostic tools capable of providing objective measures of brain injury status.

3.2.2 The Use of Biomarkers for TBI Diagnostics

Blood-based biomarkers are gaining traction as a possible solution to this problem, as they have the potential to objectively monitor injury status and provide a key to understanding the pathophysiological responses to TBI.[13,14] Biomarkers can be measured in a variety of sample sources. For TBI, the ideal sample type would be the brain tissue directly affected by injury, but since this can only be sampled post-mortem, other clinically relevant sample sources must be explored. CSF is the fluid source closest to the tissue and bathes the brain and spinal cord. However, collection of CSF is not commonly clinically feasible and can be a painful procedure. Therefore human samples can be especially difficult to obtain.[15] Additionally, available CSF volume and total lipid concentration in CSF are low in comparison to other readily available biological

matrices.[16] Thus blood, either serum or plasma, is the ideal sample type for biomarker studies, as it can be easily collected in both animal and human subjects.

The majority of existing biomarker research has focused on a few brain-specific proteins and peripheral markers of BBB dysfunction that are up-regulated as a consequence of brain injury.[17] For example, tau protein is expressed in axons, and concentrations in ventricular CSF have been shown to correlate well with lesion size and clinical outcome following TBI.[18,19] Without adequate clearance, aggregates of misfolded proteins, composed primarily of tau and amyloid-beta (Aβ) that have been associated with the onset of AD and chronic traumatic encephalopathy (CTE), form in the brain. Thus, TBI may be a risk factor for the development of neurogenerative disorders due to the resulting buildup of such proteins.[20] GFAP is also cited within the literature as a candidate biomarker for the diagnosis of TBI, as astroglial cells produce more GFAP in response to brain injury, while levels of the protein do not spike without brain injury even when other injuries are present.[21] Recent research efforts have successfully utilized the combination of multiple markers into a single panel to improve sensitivity and specificity of diagnosis, as Banyan Biomarkers took a major step forward when their Brain Trauma Indicator, a panel of UCH-L1 and GFAP, gained FDA approval for determining the need for CT scan in the presence of injury.[22]

Peripheral markers of BBB disruption have also been suggested as biomarkers of TBI, the most commonly cited being CSF/serum albumin ratio.[23] The elevation of this ratio indicates that albumin has passed from the blood to CSF.[17] While an increase in this ratio has been discovered in cases of severe TBI, similar alterations have not been observed in studies of mTBI, indicating a lack of BBB breach.[24,25] Thus, in cases of

mTBI, BBB efflux transporters are likely required for brain-specific biomarkers including proteins to reach systemic circulation, perhaps explaining the lack of pre-clinical to clinical translation within existing protein biomarkers to date.

Lipid biomarker research is more limited but offers promising leads as well. Recently, a panel of 6 lipids was shown to discriminate between athletes with TBI and non-injured teammates at <6 h, 2d, 3d, and 7d post-mTBI.[26] The ability of these 6 lipids to classify injury in both the initial college athlete cohort as well as a separate independent cohort indicates the utility of lipid biomarkers to detect changes associated with TBI and make predictive assessments of TBI using objective methods. Additionally, a number of targeted studies have looked at changes in gangliosides, ceramides, and SMs as these lipids are much more highly concentrated in the CNS.[27,28] Increases in circulating FFAs and DGs have also been shown to occur as a consequence of TBI.[29,30] Previously, using non-targeted lipidomics in a rodent TBI model, we identified a panel of 26 lipid metabolites capable of differentiating moderate TBI serum samples from controls.[31] In this study, we aimed to utilize the same methods to determine which lipids are affected at the onset of mild, closed-head TBI.

3.3 Methods and Materials

3.3.1 Injury and Blood Sampling

All procedures involving animals were performed according to the guidelines set forth in the Guide for the Care and Use of Laboratory Animals (U.S. Department of Health and Human Services, Pub no. 85-23, 1985) and were approved by the Georgia Institute of Technology Institutional Animal Care and Use Committee (protocol #A15088). The study was not pre-registered. Male Sprague-Dawley rats (8 weeks old;

Charles River) were kept on a 12-h light–dark cycle, and food and water were available *ad libitum*. Thirty-eight animals weighing between 300 and 450 g were randomly assigned to the following groups using a computer-based randomization algorithm: (1) TBI, n=30 and (2) sham (no injury, n=8). The 30 TBI animals were further subdivided into four groups based on the type of foam used to support the head during injury: (1) closed-cell (C, n=7), (2) polyurethane (P, n=8), (3) yellow generic in-house foam (Y, n=7) and (4) Marmarou (M, n=8). A pre-procedure baseline was taken just before injury (during isoflurane exposure), such that each sample was acquired in matched pairs (0 and 24 h). Sham-control animals were employed as time-matched controls to ensure that the differences in lipid metabolite abundances were due primarily to injury status rather than anesthesia exposure duration or other confounding effects.

Mild, closed-head injury was induced using a CCI device (Pittsburgh Precision Instruments, Pittsburgh, PA). Rats were anesthetized (induction, 5% isoflurane; maintenance 2-3% isoflurane) prior to all procedures, and injury was induced 30 s after removal of the isoflurane supply. A pneumatic piston fitted with a 1.6cm diameter silicone tip (Yield House Industries) impacted the dorsal surface of the head directly above the center of the cortex (head displacement = 5 mm, velocity=5 m/s, duration=100 ms), modifying literature protocols to simulate mTBI insult.[32,33,34] Animals were placed on a heating pad during recovery, after which they were singly housed in their home cage. Sham-control animals were subjected to the same procedures described above but did not receive an impact.

For baseline samples, approximately 200 µL of whole blood was collected during the afternoon from the tail vein punctured by 22-gauge Precision Glide needles (Beckton

Dickinson) and stored on ice. The matched pair 24 h samples were collected directly from the heart upon sacrifice. Whole blood samples were allowed to coagulate at room temperature for 45 min., and all sample collection followed literature guidelines for limiting the potential for hemolysis.[35,36] To isolate the lipophilic portion of the serum lipidome, sample preparation was conducted as previously described.[31]

3.3.2 UPLC-MS Analysis

Reversed-phase chromatography was employed to separate the components of serum using a Waters Acquity UPLC quaternary solvent manager system using previously established methods for LC separation and MS acquisition settings.[31] Solvents and additives were obtained from Fisher Chemical (ACN), Honeywell (IPA), CovaChem (formic acid, LC-MS grade) and Sigma Aldrich (ammonium formate, purity > 99.995%).

Tandem MS experiments were performed in a QE HF mass spectrometer (Thermo Fischer Scientific) using three distinct NCE values (10, 30 and 50), which were then averaged and combined into a single spectrum. Spectral interpretation of lipid fragmentation patterns was performed either manually or by comparison to entries in the LIPID MAPS, HMDB, and Metlin databases.[37-39] Lipid Search software was also used in order to verify identifications.[40] Additionally, for low abundance metabolites, a more sensitive instrument was required to obtain pertinent MS/MS information. These experiments were conducted on a Thermo IDX mass spectrometer with the instrument programmed to perform a full scan every second and internal mass calibration activated. During free injection time, the instrument was programmed to target ions of interest, as determined by the use of an inclusion list containing pertinent adducts of the target ions. The method utilized both Orbitrap (OT) and ion trap (IT) detectors, while OT data

collection was given priority. If an ion in the inclusion list was detected, it was fragmented by higher-energy collisional dissociation (HCD) and the fragment ions were measured in the OT. Then the parent was fragmented by Collision-induced dissociation (CID) and the ions were measured in the OT. If time permitted, the second priority scan was initiated, and the targeted parent ion was fragmented by CID while the ions were collected in the IT. HCD and orbitrap DDA data were collected with an isolation window of 1.2 *m/z*, resolution of 15,000, and collision energy of 10, 30, and 50, which were again averaged into a single spectrum. CID data were acquired at a collision energy of 32 V with the same isolation window and resolution.

3.3.3 Data Mining

Chromatographic alignment, de-isotoping, deconvolution, normalization, and peak picking were accomplished using Progenesis QI software. Sets of 1805 and 826 spectral features, defined as unique pairs of retention time (RT) and exact mass to charge ratios (*m/z*) corresponding to unidentified lipid metabolites, were obtained from positive and negative ion mode data, respectively. Filters were applied to remove peaks detected as background contaminants and peaks in which the instrumental variability exceeded 20% through the use of solvent blanks and pooled QC samples.[41] Features detected in fewer than 75% of samples in both TBI and control groups were also removed prior to binary classification. The relative abundances for the remaining 841 features (564 positive mode and 277 negative mode) were exported as a single matrix combining both ionization modes into MATLAB (R2018b, The MathWorks, Natick, MA with PLS-Toolbox, version 8.2.1, Eigenvector Research, Inc., Manson, WA) for multivariate analysis.

3.3.4 Feature Selection and Classification

The procedure for multivariate feature selection is described in Figure 3.1. Briefly, a matrix was created containing the relative feature abundances across each sample. A scheme was developed within MATLAB using the iPLS-DA internal feature selection algorithm, which selected the single feature that minimized cross-validation error (CVE) and iteratively added features until an optimized model was developed. To begin, the 62 samples were randomly stratified into random CV sets, using 7 or 8 data splits. This way, a portion of the data were used to select features, while others were withheld to cross-validate the predictive model. The use of random subsets CV ensured that different samples were used for the feature selection process as well as for the external CV step in each model built, an effort to avoid overfitting the data, a common problem that commonly plagues PLS-DA studies.[42,43] Each iteration of the process generated a model comprised of approximately 5-10 features with classification accuracy approaching 90%. The features used to build all 20 of these models were then sorted by frequency of selection and the most commonly selected features were retained within the optimized classification model.

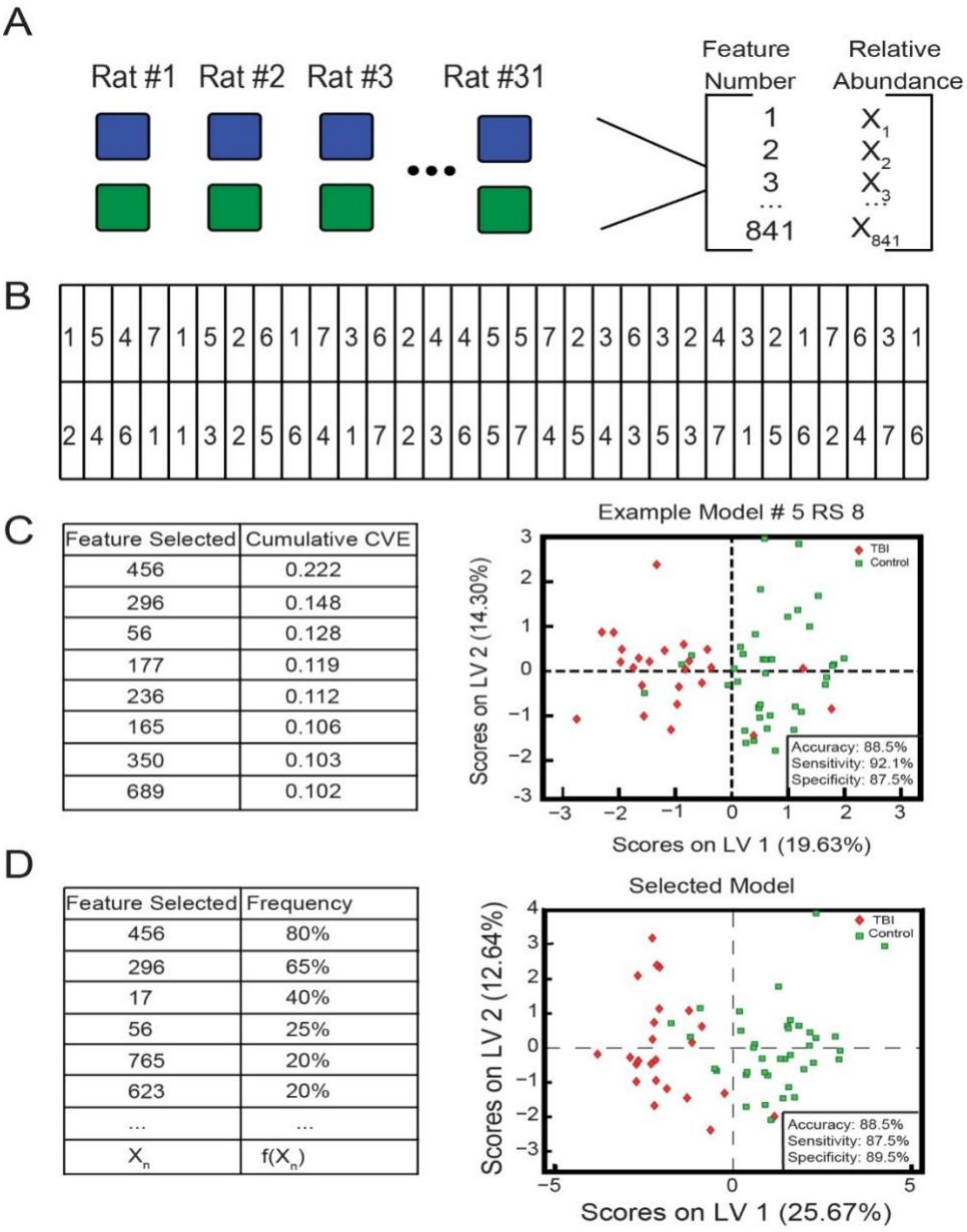

Figure 3.1: Schematic overview of the feature selection process for determining an optimized classification model used to differentiate TBI samples (red) from controls (green). A) Matched pair data (n=31) were imported into Matlab as a 62x841 matrix containing relative feature abundances for each sample. B) Samples were randomly stratified into 7 or 8 data splits so that a different portion of the data were withheld to build each model using random subsets cross-validation. C) Using the iPLS-DA feature selection algorithm, a classification model was built by iteratively adding the feature that contributed to the lowest total error of cross-validation. This process was repeated 10 times using 7 data splits and 10 times using 8 data splits. D) The features selected most frequently within the 20 classification models were combined to build an optimized classification panel consisting of 16 total features.

3.4 Results

3.4.1 Preliminary Data Overview

The serum lipidome of 38 Sprague-Dawley rats was analyzed at 24 h post-injury following closed-head CCI injury in order to identify potential biomarker candidates of mTBI, with each animal's pre-injury baseline sample serving as a matched pair control. During sample processing, two samples (Y7 baseline and M4 baseline) were discarded following rupture of the Eppendorf tube in the centrifugation process. Five additional samples (C7 baseline, C2 post-injury, C3 post-injury, Y1 baseline and S8 post-anesthesia) were noted for possible evidence of hemolysis, and these samples were excluded as outliers during analysis using T_2 and Q residual values to identify outliers in the multivariate analysis. Therefore, the matched pair samples associated with the above were all also excluded in order to maintain a robust matched pair study design, leaving a total of 62 samples for analysis (31 baseline control samples and 31 24 h post-injury samples with the distribution of animals within groups as described in Table 3.1.

Table 3.1. Experimental design for subset of 31 animals including number of animals (n) sampled per group and the density of each different type foam subtype.

Foam Type	n	Foam Density
Closed-cell (C)	4	0.046 g/cm3
Marmarou (M)	7	0.017 g/cm3
Polyurethane (P)	8	0.036 g/cm3
Yellow (Y)	5	0.031 g/cm3
Sham (no injury)	7	N/A
Total	31	

All anticipated classes of lipids were detectable as determined by the use of base peak intensity chromatograms (BPI, Figure 3.2). However, no differences in the abundance of these lipids were observed within the BPI traces when sorted by type of sample (TBI, matched-pair baseline control or sham), indicating that advanced multivariate techniques were necessary for the discrimination of TBI samples from controls. Overall, 2631 features with signal intensity above background were detected, and this total was further reduced to 841 based on filtering criteria. These features were imported into MATLAB, in order to determine which lipids were most critical to the accurate distinction of mTBI serum samples from controls.

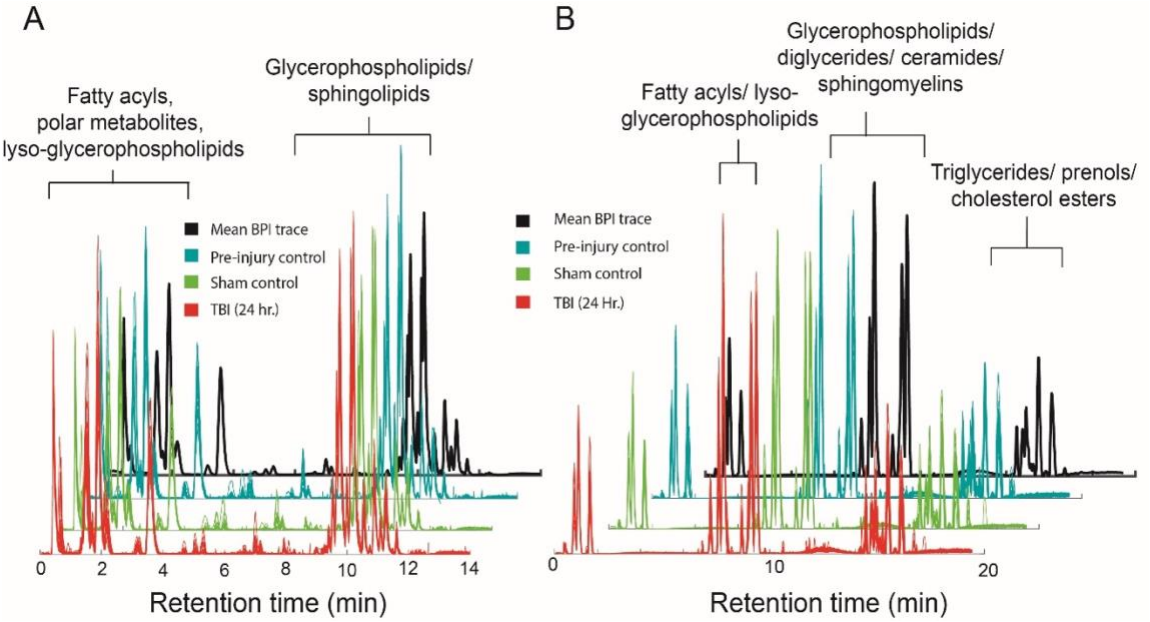

Figure 3.2: Offset base peak intensity (BPI) traces for aligned chromatographic separations of rodent serum samples in A) negative ionization mode and B) positive ionization mode. Colors correspond to individual sample subtypes: TBI samples are colored in red, pre-injury control samples are colored in light blue, and sham control samples are colored in green. The top black trace corresponds to a mean BPI trace of all samples analyzed during the experiment. Lipid classes are labeled by anticipated time of elution, and the classes of lipids labeled above correspond to the retention time across the mean BPI trace.

3.4.2 Development of Multivariate Models for the Classification of Mild Traumatic Brain Injury

PCA of the lipidomics dataset indicated that the effect of mTBI was relatively more subtle than what was detected in Chapter 2 (Figure 3.3A). While TBI samples trended towards negative scores on principal component one, there was still broad overlap between TBI and control samples using unsupervised techniques on the entire set of features. For supervised classification, in which class information was incorporated into the data, an oPLS-DA model was created using the relative abundances of all features to attempt to classify TBI samples from all controls (Figure 3.3B). This multivariate model performed with an overall accuracy of 83.9%, specificity of 92.1% and sensitivity of 70.8%. While this model performed well in terms of overall accuracy, it had a tendency to underperform in the ability to accurately predict TBI samples, as numerous false negatives were produced in the initial classification. In the field of concussion diagnostics, there is a tendency to underestimate the existence of mTBI due to lack of perceived symptoms (i.e. false negative). However, it is safer to overestimate (i.e. false positive) the number of injuries than risk subsequent injury due to second impact syndrome, which could lead to post-concussive symptoms.[44,45] Therefore, future iterations were optimized to select just those features which contributed to the improved classification sensitivity and overall accuracy, leading to the development of a classification panel containing 16 unique lipid metabolites which were capable of classifying mTBI samples from controls with an accuracy of 88.5%, sensitivity of 87.5%,

and specificity of 89.5% (Figure 3.3C). The features contained within this classification panel are included in Table 3.2.

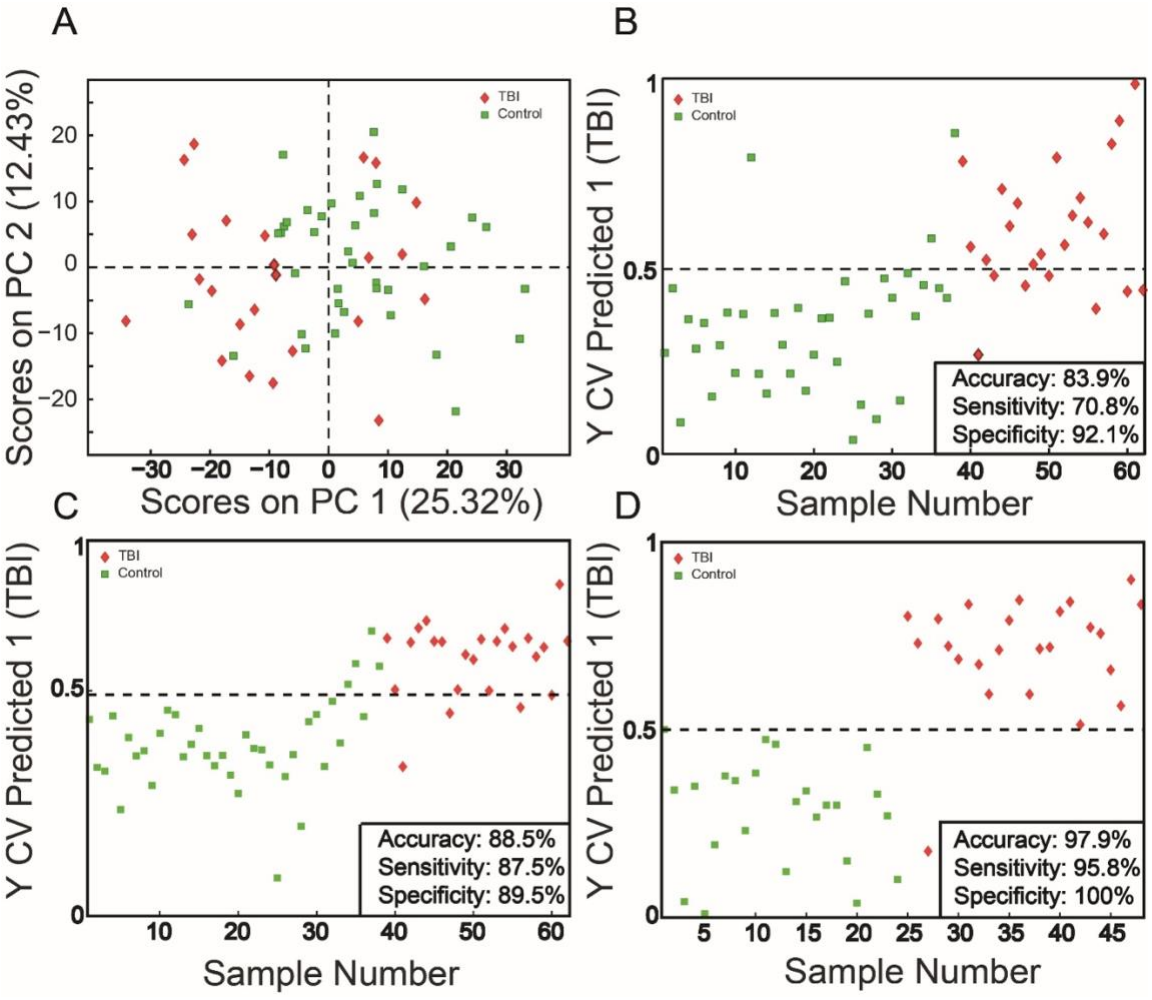

Figure 3.3: Classification model performance comparisons with and without feature selection illustrating accuracies of developed classification models to used discriminate between TBI samples, represented by red diamonds, and control samples, represented by green squares. A) PCA scores plot containing all features; B) oPLS-DA model containing all features; C) oPLS-DA scores plot for 16 feature model showing performance of classification of all 62 samples, including sham controls. Sample numbers 1-24 correspond to baseline control samples, 25-38 indicate sham control samples, and 39-62 represent TBI samples; D) oPLS-DA model showing performance of 16 feature classification model on 48 matched pair samples, excluding shams. Sample numbers 1-24 correspond to baseline control samples and 25-48 represent TBI samples. For plots A-C, the line at 0.5 on the y-axis represents the decision boundary between TBI samples and control samples.

3.4.3 Performance of the Classification Models

When the same model was used to classify TBI samples against only their matched pair baseline control samples, a model with accuracy of 97.9%, sensitivity of 95.8%, and specificity of 100% was generated, indicating that much of the CVE stemmed from the misidentification of sham control samples in the multivariate classification scheme. While this may be attributed in part to overfitting of the data, or non-injury related differences within sample subtypes, it is further evidence that pre-injury baseline samples offer the clearest path to identification of mTBI following injury.

Additionally, much of the power of the multivariate classification model was due to only differences in a handful of these 16 features. Comparing loadings, levels of significance and fold changes between sample types, the panel of 16 could be reduced to a simpler model including only 5 lipid metabolites capable of classifying mTBI with nearly the same accuracy (Figure 3.4). While this simpler model again performed very well on the matched pair samples, accurately predicting 47/48 samples (Figure 3.3D), it also had a tendency to misclassify a number of the sham samples as injuries. In this and other similar prediction models, each of the multivariate models systematically misclassified the 24 h sham samples, performing with approximately 50% accuracy on this subgroup.

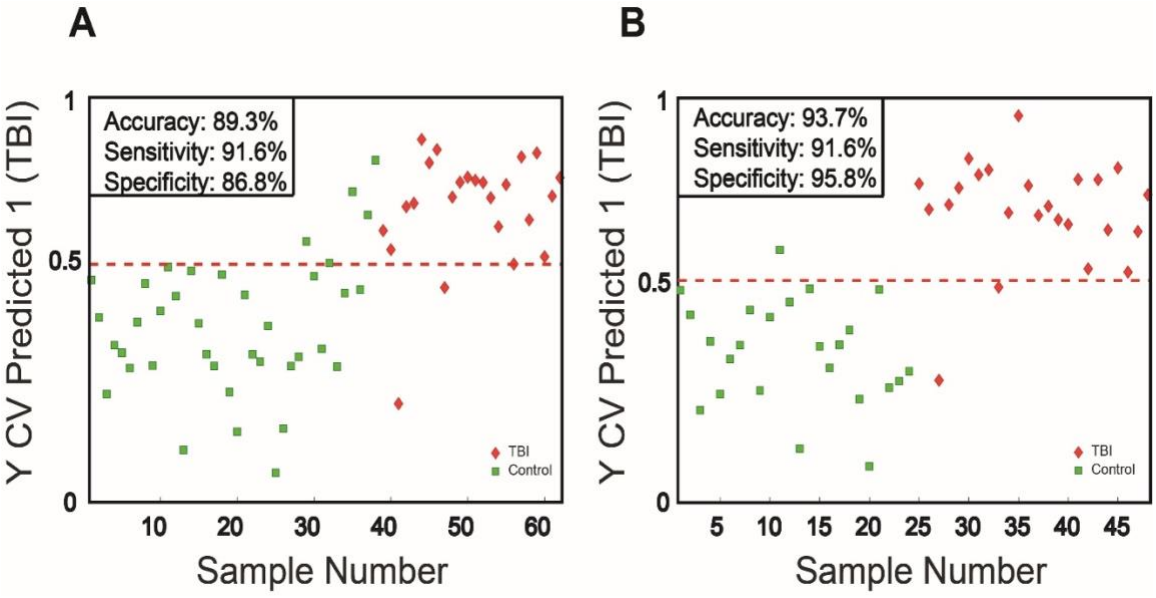

Figure 3.4: Performance of the 5-feature oPLS-DA model. Performance accuracy of developed classification models to discriminate between TBI samples, represented by red diamonds, and control samples, represented by green squares. A) oPLS-DA model for 5 feature model, including only features 56, 380, 448, 456, and 623, showing performance of classification of all 62 samples, including sham controls. Sample numbers 1-24 correspond to baseline control samples, 25-38 indicate sham control samples, and 39-62 represent TBI samples; B) oPLS-DA model showing performance of 5-feature classification model on 48 matched pair samples, excluding shams. Sample numbers 1-24 correspond to baseline control samples and 25-48 represent TBI samples. The line at 0.5 on the y-axis represents the decision boundary between TBI samples and control samples.

3.4.4 Possible Confounding Factors

The inability of the multivariate classification model to accurately predict the 24 h sham samples as controls may be attributed to a number of confounding factors. The effect size of mTBI on the features was small compared to previously published data on moderate TBI.[31] Thus, minor differences may also exist within the sham samples that affected the serum lipidome with a similar effect size to that of the mild injury. Isoflurane was used to anesthetize rats during collection of blood, and this has been shown to affect

the metabolome as well, inducing changes in protein phosphorylation with durations as low as 30 minutes.[46] Use of isoflurane as an anesthetic also led to increased concentrations of lactate and glutamate in the rodent hippocampus and parietal cortex compared to animals anesthetized with propofol, though these increases were independent of blood lactate concentrations.[47] Additionally, plasma samples of patients sedated with propofol showed different metabolic profiles when compared to patients treated with etomidate. The primary differences observed included a general decrease in metabolite concentrations due to slowed metabolism while under anesthesia, decreased branched amino acids such as leucine and isoleucine coupled to increased ketones such as acetone, acetoacetate and 3-hydroxybutyrate, while others could be attributed to differences in drugs administered to patients, such as cefuroxime, an antibiotic.[48] Prolonged exposure to sevoflurane, another anesthetic agent, has also been shown to alter lipid metabolism, leading to disruption of cellular membranes and subsequent neuronal dysfunction and damage in developing brains.[49,50] Therefore in studies utilizing anesthetic agents, the distinction between association of brain injury with lipidome alterations must be interpreted in light of the potential confounding effects of anesthesia exposure.

Additionally, the collection of the baseline sample and subsequent matched pair sample, at 24 h for sham and mTBI, were done *via* different procedures, as the 24 h samples were collected from the heart upon sacrifice of the animal. Though differences in circulating blood should have normalized by this time, it is possible that the method or time of collection contributed to more similarities within the lipidome of 24 h sham and TBI samples than their baselines, which again favors the collection of pre-injury

baselines samples for later comparison to injuries, as has been done in other biomarker studies.[51,52]

While the foam was initially intended to provide support for the head during injury, it also may have served the purpose of cushioning the skull from impact by absorbing and dampening some of the force directed by the pneumatic piston. Due to the densities and cell structures of the foams, the dispersion of forces was unique to each foam subtype. If the foam support sufficiently dissipated the force of impact, the presence of injury in these TBI samples would be partially mitigated and such samples may be modeled more similarly as sham controls. To investigate this hypothesis, we temporarily changed the class membership of the samples taken from each foam type from TBI to control, generating new classification models to see how cross-validated accuracy was affected.

For three of the foams (Marmarou, closed-cell, and polyurethane), this led to a dramatic decrease in performance accuracy of the 5-lipid model (0.174, 0.219, and 0.203 CVE respectively), indicating that the samples were still correctly predicted as TBI, as they were subsequently misclassified in each of the newly generated multivariate models. However, yellow, in-house lab foam showed similar classification accuracy in both cases (Figure 3.5). Alteration of class membership of TBI samples to controls from the yellow foam group adjusted the separation boundary between classes and improved classification accuracy of 24 h sham samples. While overall performance was slightly decreased (89.3% to 87.5%), this indicates that the effect on the selected lipids was even more subtle than the mTBI induced across the remainder of the foam types.

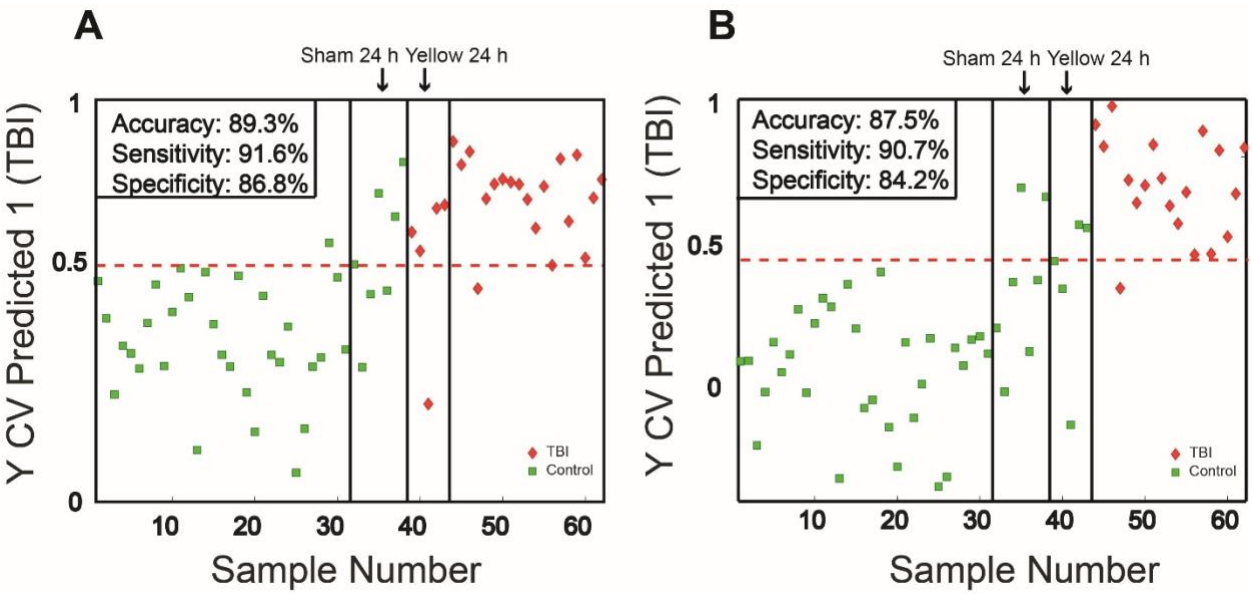

Figure 3.5. Cross-validated class prediction values using 5-lipid classification model when yellow foam TBI samples are defined as A) TBI (class = 1) and B) control (class = 0). Sample numbers 1-24 correspond to baseline control samples, 25-38 indicate sham control samples, and 39-62 represent TBI samples.

3.4.5 Disruption of Cholesterol Metabolic Pathways

While the combination of multiple lipids into a multivariate classification panel led to the accurate distinction of TBI and control samples, changes on the univariate level can be mapped to known pathophysiology, helping to explain the importance of the features used for classification. For instance, a significant decrease ($p < 1.0E-9$) in the level of CS was observed across TBI samples. CS, a sterol sulfate present in human plasma in µg/mL levels as well as in tissue including the epidermis, plays a stabilizing role in cellular membranes and serves as a precursor in the synthesis of other sulfonated adrenal steroids such as pregnenolone sulfate.[53,54] Levels of plasma CS may increase by an order of magnitude in association with disease states such as cirrhosis of the liver and hypothyroidism.[55,56] CS has been shown to have a significant on lipid metabolism, acting

via a number of mechanisms including inhibiting the esterification of cholesterol.[57] Conversely, decreased supply of both cholesterol and sulfate have been associated with impaired autophagy and insulin resistance.[58] The observed decrease in CS in this study (FC = -1.27) followed the same trend as previously observed in the study of moderate TBI in rodents, and was of a slightly higher magnitude (FC = -1.20 for the moderate TBI study).[31] These findings indicate that CS may also be potential novel biomarker of TBI ranging across multiple severities. Additionally, a significant increase ($p < 1.5E-4$) in the abundance of the DHA-containing cholesteryl ester CE(22:6) was observed following mTBI (Figure 3.6). Similar trends have been discovered in the rodent brain following TBI induced by CCI, revealing that CE(22:6) and other CEs were not detected in control brains but were increased in the injury site at timepoints corresponding decreases in cholesterol in the same region (3 and 7 days).[59] One hypothesis for the increased formation of CEs stems from a lack of CS in the brain following injury, which fails to inhibit of the esterification reactions forming CEs, leading to increased circulation of these lipids in the serum. Thus, these dietary lipids may also serve a purpose as biomarkers of TBI.

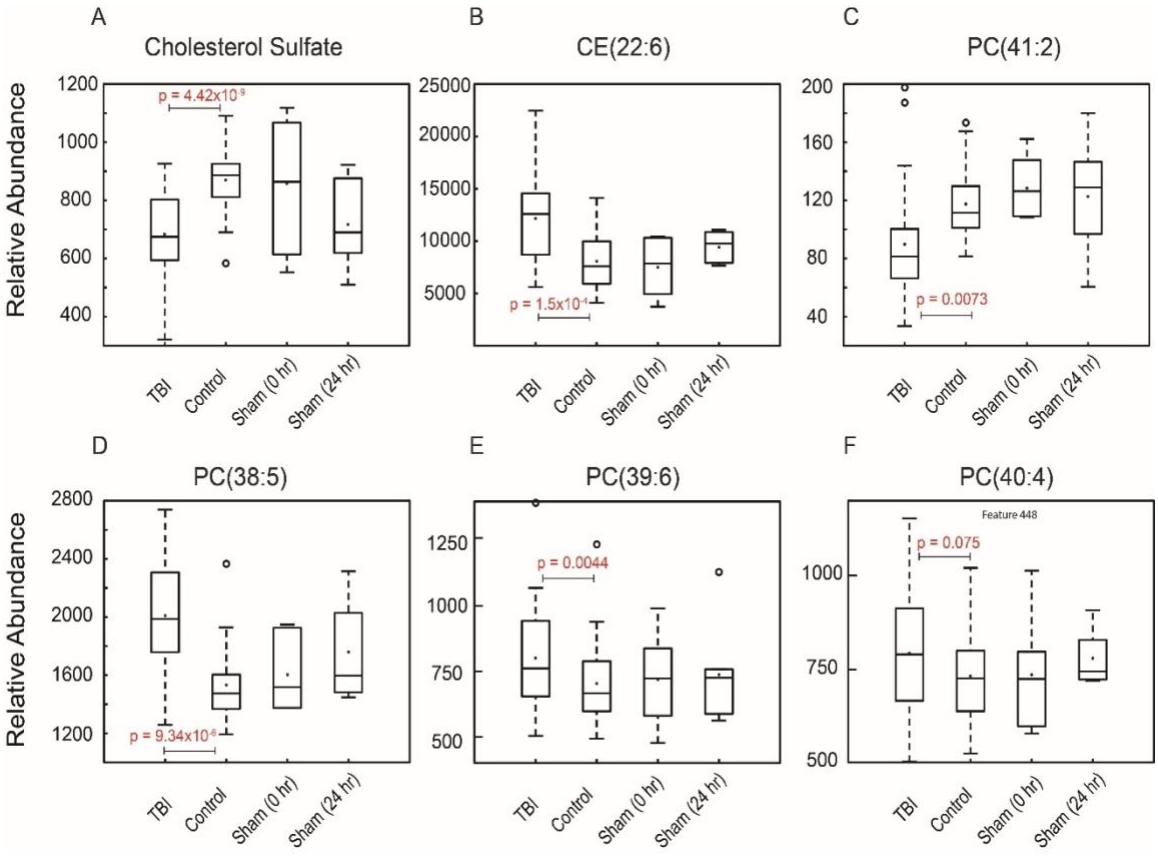

Figure 3.6: Boxplots of selected features from 16-lipid classification panel showing relative abundances corresponding to: A) Cholesterol Sulfate: $[M-H]^-$ = 465.3035; B) CE(22:6): $[M+NH_4]^+$ = 706.6345; C) PC(41:2): $[M+H]^+$ = 856.6821; D) PC(38:5): $[M+H]^+$ = 808.5873; E) PC(39:6): $[M+H]^+$ = 820.5851; F) PC(40:4), $[M+H]^+$ = 838.632.. Dots in the center of the boxes indicate the mean while the line represents the median value for each sample subtype; p-values were calculated as matched pairs.

3.4.6 Dysregulation of Membrane Phospholipids

The boxplots in Figure 3.6 also show the distribution of changes in membrane phospholipids, specifically PUFA-containing PCs. The largest decrease was observed for PC(38:6), though all four species showed related decreases in abundance following TBI. Two of the lipids, PC(41:2) and PC(39:6) are not expected to be found in large quantities endogenously, as they represent odd chain fatty acid (OCFA)-containing lipids. Other

PUFA-containing PCs such as PC(18:1_22:6), PC(20:0_20:5) and PC(18:0_22:4) showed non-significant increases, indicating that systemic alterations of the membrane lipids was not observed. Decreased abundance of PUFA-containing PCs was previously related to increased hydrolysis of these lipids, which also led to increased formation of associated FFAs and lysoPCs. Here, AA and lysoPC(22:4) were both decreased, suggesting that mTBI does not simply lead to lower magnitude changes in the serum lipidome, but that novel metabolic alterations are induced, at least at the early timepoint studied here (24 h).

3.4.7 Limitations

A number of limitations within the experimental design must be acknowledged. Tandem MS experiments were employed in order to identify which lipid species were associated with the induction of mTBI. Due to experimental difficulties including low ion abundances of the selected features and inadequate separation of some lipid classes, including ceramides, a few of the features were not identified. For these species, a characteristic headgroup or elemental formula is listed, where possible. Where MS/MS data were collected, the esterified fatty acids chains are listed. The lipid biomarkers included within the classification panel may also represent markers of general inflammation, so their specificity to the brain or brain injury must be determined in future experiments.[60] This would require a study of lipid fluxes between brain and blood, which is assumed to operate primarily *via* the BBB, but could also include glymphatic clearance and other efflux routes.[61,62]

Additionally, some lipids containing OCFAs are expected to be present based on the precursor mass and adducts determined, as in PC(41:2) and PC(17:0_22:6). While ECFAs compose >99% of all fatty acids present in plasma, four OCFAs, C15:0, C17:0,

C17:1 and C23:0, also exist in small but detectable amounts.[63,64] These OCFAs have been hypothesized to originate primarily from dietary fats, specifically dairy, due in part to high levels of their production by rumen microbial fermentation.[65,66] It is now believed that altered metabolic pathways may also allow for the production of such OCFAs endogenously. Fatty acids are normally metabolized by β-oxidation, but an alternative mechanism (α-oxidation) is necessary when fatty acids cannot undergo β-oxidation, as in the case of β-branched chain fatty acids.[67] When the α-oxidation process acts on straight chain fatty acids, OCFAs may be produced.[68,69] OCFAs increase membrane fluidity and have been found in lower levels in AD patients, indicating their potential utility as biomarkers in TBI, which operates *via* similar mechanisms of neurodegeneration.[70,71] Tandem MS experiments confirmed the fatty acyl chains of PC(17:0_22:6).

Table 3.2: Identification of candidate biomarkers and annotation of lipids in 16-feature panel for the classification of mTBI.
Feature number, retention time (RT), observed exact mass (*m/z*) with Xevo instrument mass error, observed adduct, predicted elemental formulae, p-value for differences between matched pair control (MPC) and TBI samples, and fold change (FC) values are included. Positive FC values correspond to species with increased relative abundances in injured animals, while negative values indicate higher relative abundances in controls. SN1/SN2 stereochemistry was not determined.
PC: phosphatidylcholine; Hex: hexose; Cer: Ceramide; CE: cholesteryl ester; TG: triacylglycerol.

Feature Number	**RT (min)**	***m/z*** **Mass error (ppm)**	**Adduct**	**Elemental Formula [N]**	**ID**	**p-value** (TBI vs MPC)	**FC** (TBI/MPC)
17	1.05	311.1684 N/A	N/A	N/A	Not identified	0.078	-1.65
56	7.18	465.3035 -1.93	[M-H]-	$C_{27}H_{46}O_4S$	Cholesterol Sulfate (CS)	$4.42*10^{-9}$	-1.27
102	9.57	876.5729 --3.54	$[M+HCO_2]^-$	$C_{48}H_{82}NO_8P$	PC(18:1_22:6)	0.249	-1.06
244	11.29	698.6297 -1.00	$[M+HCO_2]^-$	$C_{41}H_{83}NO_4$	Cer*	$3.70*10^{-5}$	-1.21
249	11.34	856.6874 1.05	$[M+HCO_2]^-$	$C_{48}H_{93}NO_8$	HexCer(d18:1_24:0)	0.385	1.08
253	11.44	706.6345 -1.42	$[M+HCO_2]^-$	$C_{43}H_{83}NO_3$	Cer*	0.161	-1.11
296	14.43	714.6206 3.26	$[M+NH_4]^+$	$C_{49}H_{76}O_2$	CE(22:6)	$1.53*10^{-4}$	1.48
307	10.69	864.6488 1.27	$[M+H]^+$	$C_{50}H_{90}NO_8P$	PC(20:0_22:5)	0.182	1.15
324	7.26	844.5282 3.43	$[M+K]^+$	$C_{46}H_{80}NO_8P$	PC(16:0_22:6)	$2.2*10^{-4}$	1.24
380	9.49	808.5873 2.72	$[M+H]^+$	$C_{46}H_{82}NO_8P$	PC(16:0_22:5) PC(18:1_20:4)	$9.34*10^{-6}$	1.27
448	10.68	838.6312 -0.95	$[M+H]^+$	$C_{48}H_{88}NO_8P$	PC(18:0_22:4)	0.075	1.07
456	12.42	856.6821 3.62	$[M+H]^+$	$C_{49}H_{94}NO_8P$	PC(41:2)	0.00727	1.31
579	7.72	820.5823 -3.41	$[M+H]^+$	$C_{47}H_{82}NO_8P$	PC(17:0_22:6)	0.0044	1.12
608	16.04	940.833 0.21	$[M+NH_4]^+$	$C_{60}H_{106}O_6$	TG(57:5)	$5.48*10^{-5}$	-1.32
623	2.72	305.2463 -3.91	$[M+H]^+$	$C_{20}H_{32}O_2$	Arachidonic Acid (AA)	$1.01*10^{-6}$	-2.63
764	1.77	572.3689 -3.84	$[M+H]^+$	$C_{30}H_{54}NO_7P$	LysoPC(22:4)	$3.19*10^{-8}$	-1.93

3.5 Conclusion

Non-targeted lipidomic techniques were utilized to identify a number of novel biomarker candidates for the identification of mTBI in rodent serum samples using a matched pair study design. A multivariate classification model was built that was capable of discriminating mTBI from control samples with close to 90% using only the relative abundances of a panel 16 lipids. A model generated using a subset of 5 of these lipids performed with nearly equivalent accuracy, indicating that many of the initial lipids identified were not critical to the classification accuracy of the model. Among the univariate changes observed within the species selected to build the classification panel, cholesterol sulfate was decreased in TBI samples, while a DHA-containing cholesterol ester was increased in the TBI cohort, indicating that cholesterol metabolic pathways play a role in injury pathophysiology. Additionally, membrane lipids, primarily PCs containing PUFAs, were generally of higher relative abundance in the TBI samples. The robust matched pair study design enabled high classification accuracy due to the use of pre-injury baseline controls; however, these experiments must be replicated to determine if statistical overfitting contributed in part to the high accuracy of classification. Additionally, a similar study involving the use of human samples to identify which specific lipids are capable of detecting the presence of mTBI would be more clinically relevant, as differences exist within the lipidomic profile of rodent and human serum that would invariably lead to altered patterns of lipid metabolism following injury.

3.6 References

1 Maas, A. I. R. Traumatic brain injury: integrated approaches to improve prevention, clinical care, and research. *The Lancet Neurology* **16**, 987-1048, (17) (2017).

2 Feigin, V. L. *et al.* Incidence of traumatic brain injury in New Zealand: a population-based study. *The Lancet Neurology* **12**, 53-64, (2013).

3 James, S. L. *et al.* Global, regional, and national burden of traumatic brain injury and spinal cord injury, 1990–2016: a systematic analysis for the Global Burden of Disease Study 2016. *The Lancet Neurology* **18**, 56-87 (2019).

4 McKinlay, A. *et al.* Prevalence of traumatic brain injury among children, adolescents and young adults: prospective evidence from a birth cohort. *Brain injury* **22**, 175-181 (2008).

5 Majdan, M. *et al.* Epidemiology of traumatic brain injuries in Europe: a cross-sectional analysis. *The Lancet Public Health* **1**, e76-e83 (2016).

6 Teasdale, G. & Jennett, B. Assessment of coma and impaired consciousness: a practical scale. *The Lancet* **304**, 81-84 (1974).

7 Bazarian, J. J., Blyth, B., Mookerjee, S., He, H. & McDermott, M. P. Sex differences in outcome after mild traumatic brain injury. *Journal of neurotrauma* **27**, 527-539 (2010).

8 Giza, C. C., Prins, M. L., Hovda, D. A., Herschman, H. R. & Feldman, J. D. Genes preferentially induced by depolarization after concussive brain injury: effects of age and injury severity. *Journal of neurotrauma* **19**, 387-402 (2002).

9 Ruff, R. Two decades of advances in understanding of mild traumatic brain injury. *The Journal of head trauma rehabilitation* **20**, 5-18 (2005).

10 Mittenberg, W., Canyock, E. M., Condit, D. & Patton, C. Treatment of post-concussion syndrome following mild head injury. *Journal of clinical and experimental neuropsychology* **23**, 829-836 (2001).

11 Ryan, L. M. & Warden, D. L. Post concussion syndrome. *International review of psychiatry* **15**, 310-316 (2003).

12 Te Ao, B. J. *Measuring the economic cost of traumatic brain injury (TBI) in New Zealand: a cost-of-illness study*, Auckland University of Technology, (2014).

13 Dash, P. K., Zhao, J., Hergenroeder, G. & Moore, A. N. Biomarkers for the diagnosis, prognosis, and evaluation of treatment efficacy for traumatic brain injury. *Neurotherapeutics* **7**, 100-114 (2010).

14 Kulbe, J. R. & Geddes, J. W. Current status of fluid biomarkers in mild traumatic brain injury. *Experimental neurology* **275**, 334-352 (2016).

15 Boon, J., Abrahams, P., Meiring, J. & Welch, T. Lumbar puncture: anatomical review of a clinical skill. *Clinical Anatomy: The Official Journal of the American Association of Clinical Anatomists and the British Association of Clinical Anatomists* **17**, 544-553 (2004).

16 Irani, D. N. *Cerebrospinal fluid in clinical practice*. (Elsevier Health Sciences, 2009).

17 Kim, H. J., Tsao, J. W. & Stanfill, A. G. The current state of biomarkers of mild traumatic brain injury. *JCI insight* **3** (2018).

18 Franz, G. *et al.* Amyloid beta 1-42 and tau in cerebrospinal fluid after severe traumatic brain injury. *Neurology* **60**, 1457-1461 (2003).

19 Zemlan, F. P. *et al.* C-tau biomarker of neuronal damage in severe brain injured patients: association with elevated intracranial pressure and clinical outcome. *Brain research* **947**, 131-139 (2002).

20 Edwards III, G., Moreno-Gonzalez, I. & Soto, C. Amyloid-beta and tau pathology following repetitive mild traumatic brain injury. *Biochemical and biophysical research communications* **483**, 1137-1142 (2017).

21 Pelinka, L. E. *et al.* Glial fibrillary acidic protein in serum after traumatic brain injury and multiple trauma. *Journal of Trauma and Acute Care Surgery* **57**, 1006-1012 (2004).

22 Bazarian, J. J. *et al.* Serum GFAP and UCH-L1 for prediction of absence of intracranial injuries on head CT (ALERT-TBI): a multicentre observational study. *The Lancet Neurology* **17**, 782-789, (2018).

23 Zetterberg, H., Smith, D. H. & Blennow, K. Biomarkers of mild traumatic brain injury in cerebrospinal fluid and blood. *Nature Reviews Neurology* **9**, 201 (2013).

24 Csuka, E. *et al.* IL-10 levels in cerebrospinal fluid and serum of patients with severe traumatic brain injury: relationship to IL-6, TNF-α, TGF-β1 and blood–brain barrier function. *Journal of neuroimmunology* **101**, 211-221 (1999).

25 Zetterberg, H. *et al.* Neurochemical aftermath of amateur boxing. *Archives of neurology* **63**, 1277-1280 (2006).

26 Fiandaca, M. S. *et al.* Plasma metabolomic biomarkers accurately classify acute mild traumatic brain injury from controls. *PloS one* **13**, e0195318 (2018).

27 Sheth, S. A., Iavarone, A. T., Liebeskind, D. S., Won, S. J. & Swanson, R. A. Targeted lipid profiling discovers plasma biomarkers of acute brain injury. *PLoS One* **10**, e0129735 (2015).

28 Woods, A. S. *et al.* Gangliosides and ceramides change in a mouse model of blast induced traumatic brain injury. *ACS chemical neuroscience* **4**, 594-600 (2013).

29 Homayoun, P. *et al.* Cortical impact injury in rats promotes a rapid and sustained increase in polyunsaturated free fatty acids and diacylglycerols. *Neurochemical research* **25**, 269-276 (2000).

30 Pilitsis, J. G. *et al.* Free fatty acids in cerebrospinal fluids from patients with traumatic brain injury. *Neuroscience letters* **349**, 136-138 (2003).

31 Hogan, S. R. *et al.* Discovery of Lipidome Alterations Following Traumatic Brain Injury via High-Resolution Metabolomics. *Journal of proteome research* **17**, 2131-2143 (2018).

32 Kobeissy, F. H. *Brain neurotrauma: molecular, neuropsychological, and rehabilitation aspects*. (Crc Press, 2015).

33 Dixon, C. E., Clifton, G. L., Lighthall, J. W., Yaghmai, A. A. & Hayes, R. L. A controlled cortical impact model of traumatic brain injury in the rat. *Journal of neuroscience methods* **39**, 253-262 (1991).

34 Jamnia, N. *et al.* A clinically relevant closed-head model of single and repeat concussive injury in the adult rat using a controlled cortical impact device. *Journal of neurotrauma* **34**, 1351-1363 (2017).

35 Sharp, M. K. & Mohammad, S. F. Scaling of hemolysis in needles and catheters. *Annals of biomedical engineering* **26**, 788-797 (1998).

36 Lippi, G. *et al.* in *Seminars in thrombosis and hemostasis.* 565-575 (Thieme Medical Publishers).

37 Fahy, E. *et al.* Update of the LIPID MAPS comprehensive classification system for lipids. *Journal of lipid research* **50**, S9-S14 (2009).

38 Smith, C. A. *et al.* METLIN: a metabolite mass spectral database. *Therapeutic drug monitoring* **27**, 747-751 (2005).

39 Wishart, D. S. *et al.* HMDB 3.0—the human metabolome database in 2013. *Nucleic acids research* **41**, D801-D807 (2012).

40 Taguchi, R. & Ishikawa, M. Precise and global identification of phospholipid molecular species by an Orbitrap mass spectrometer and automated search engine Lipid Search. *Journal of Chromatography A* **1217**, 4229-4239 (2010).

41 Piccoli, S., Sauer, J. & Amur, S. in *FDA Public Workshop: Scientific and Regulatory Considerations for the Analytical Validation of Assays Used in the Qualification of Biomarkers in Biological Matrices. Washington, DC, USA.* 14-15.

42 Hawkins, D. M. The problem of overfitting. *Journal of chemical information and computer sciences* **44**, 1-12 (2004).

43 Rodríguez-Pérez, R., Fernández, L. & Marco, S. Overoptimism in cross-validation when using partial least squares-discriminant analysis for omics data: a systematic study. *Analytical and bioanalytical chemistry* **410**, 5981-5992 (2018).

44 Wetjen, N. M., Pichelmann, M. A. & Atkinson, J. L. Second impact syndrome: concussion and second injury brain complications. *Journal of the American College of Surgeons* **211**, 553-557 (2010).

45 Willer, B. & Leddy, J. J. Management of concussion and post-concussion syndrome. *Current treatment options in neurology* **8**, 415-426 (2006).

46 Kohtala, S. *et al.* Brief isoflurane anesthesia produces prominent phosphoproteomic changes in the adult mouse hippocampus. *ACS chemical neuroscience* **7**, 749-756 (2016).

47 Makaryus, R. *et al.* The metabolomic profile during isoflurane anesthesia differs from propofol anesthesia in the live rodent brain. *Journal of Cerebral Blood Flow & Metabolism* **31**, 1432-1442 (2011).

48 Ghini, V. *et al.* Metabolomics profiling of pre-and post-anesthesia plasma samples of colorectal patients obtained via Ficoll separation. *Metabolomics* **11**, 1769-1778 (2015).

49 Wang, C. *et al.* Lipidomics reveals a systemic energy deficient state that precedes neurotoxicity in neonatal monkeys after sevoflurane exposure. *Analytica chimica acta* **1037**, 87-96 (2018).

50 Wang, C. *et al.* Lipid profiling as an effective approach for identifying biomarkers/adverse events associated with pediatric anesthesia. *Toxicology and applied pharmacology* **354**, 191-195 (2018).

51 Meier, T. B. *et al.* Prospective assessment of acute blood markers of brain injury in sport-related concussion. *Journal of neurotrauma* **34**, 3134-3142 (2017).

52 Shahim, P. *et al.* Blood biomarkers for brain injury in concussed professional ice hockey players. *JAMA neurology* **71**, 684-692 (2014).

53 Huang, Y., Eid, K. & Davignon, J. Cholesteryl sulfate; measurement with β-sitosteryl sulfate as an internal standard. *Canadian journal of biochemistry* **59**, 602-605 (1981).

54 Strott, C. A. & Higashi, Y. Cholesterol sulfate in human physiology what's it all about? *Journal of lipid research* **44**, 1268-1278 (2003).

55 Tamasawa, N., Tamasawa, A. & Takebe, K. Higher levels of plasma cholesterol sulfate in patients with liver cirrhosis and hypercholesterolemia. *Lipids* **28**, 833-836 (1993).

56 van Doormaal, J. J. *et al.* Increase of plasma and red cell cholesterol sulfate levels in induced hypothyroidism in man. *Clinica chimica acta* **155**, 195-200 (1986).

57 Nakagawa, M. & Kojima, S. Effect of cholesterol sulfate and sodium dodecyl sulfate on lecithin-cholesterol acyltransferase in human plasma. *The Journal of Biochemistry* **80**, 729-733 (1976).

58 Seneff, S., Lauritzen, A., Davidson, R. & Lentz-Marino, L. Is endothelial nitric oxide synthase a moonlighting protein whose day job is cholesterol sulfate synthesis? Implications for cholesterol transport, diabetes and cardiovascular disease. *Entropy* **14**, 2492-2530 (2012).

59 Roux, A. *et al.* Mass spectrometry imaging of rat brain lipid profile changes over time following traumatic brain injury. *Journal of neuroscience methods* **272**, 19-32 (2016).

60 Wallace, M. *et al.* Relationship between the lipidome, inflammatory markers and insulin resistance. *Molecular bioSystems* **10**, 1586-1595 (2014).

61 Plog, B. A. *et al.* Biomarkers of traumatic injury are transported from brain to blood via the glymphatic system. *Journal of Neuroscience* **35**, 518-526 (2015).

62 Iliff, J. J. *et al.* A paravascular pathway facilitates CSF flow through the brain parenchyma and the clearance of interstitial solutes, including amyloid β. *Science translational medicine* **4**, 147ra111-147ra111 (2012).

63 Kochanek, P. M. *et al.* Biomarkers of primary and evolving damage in traumatic and ischemic brain injury: diagnosis, prognosis, probing mechanisms, and therapeutic decision making. *Current opinion in critical care* **14**, 135-141 (2008).

64 Hodson, L., Skeaff, C. M. & Fielding, B. A. Fatty acid composition of adipose tissue and blood in humans and its use as a biomarker of dietary intake. *Progress in lipid research* **47**, 348-380 (2008).

65 Brevik, A., Veierød, M., Drevon, C. & Andersen, L. Evaluation of the odd fatty acids 15: 0 and 17: 0 in serum and adipose tissue as markers of intake of milk and dairy fat. *European journal of clinical nutrition* **59**, 1417 (2005).

66 Vlaeminck, B., Fievez, V., Cabrita, A., Fonseca, A. & Dewhurst, R. Factors affecting odd-and branched-chain fatty acids in milk: A review. *Animal feed science and technology* **131**, 389-417 (2006).

67 Mannaerts, G. P., Van Veldhoven, P. P. & Casteels, M. Peroxisomal lipid degradation via β-and α-oxidation in mammals. *Cell biochemistry and biophysics* **32**, 73-87 (2000).

68 Foulon, V. *et al.* Breakdown of 2-hydroxylated straight chain fatty acids via peroxisomal 2-hydroxyphytanoyl-coa lyase a revised pathway for the α-oxidation of straight chain fatty acids. *Journal of Biological Chemistry* **280**, 9802-9812 (2005).

69 Kondo, N. *et al.* Identification of the phytosphingosine metabolic pathway leading to odd-numbered fatty acids. *Nature communications* **5**, 5338 (2014).

70 Johnson, V. E., Stewart, W. & Smith, D. H. Traumatic brain injury and amyloid-β pathology: a link to Alzheimer's disease? *Nature Reviews Neuroscience* **11**, 361 (2010).

71 Adibhatla, R. M. & Hatcher, J. in *Lipids in health and disease* 241-268 (Springer, 2008).

CHAPTER 4: *KARENIA BREVIS* ALLELOPATHY COMPROMISES THE LIPIDOME, MEMBRANE INTEGRITY, AND PHOTOSYNTHETIC EFFICIENCY OF COMPETITORS

Portions reprinted with permission from:
Poulin, R. X., Hogan, S., Poulson-Ellestad, K. L., Brown, E., Fernández, F. M., & Kubanek, J. (2018). Karenia brevis allelopathy compromises the lipidome, membrane integrity, and photosynthesis of competitors. *Scientific Reports*, *8*(1), 9572.

4.1 Abstract

Karenia brevis is a bloom-forming species of algae that can reduce the growth of phytoplankton competitors through the release of allelopathic chemicals. The sub-lethal effects of allelopathy on competitors vary based on patterns of cohabitation, as some species such as *Asterionellopsis glacialis* may have developed an evolved resistance during periods of co-occurrence with *K. brevis* while other non-resistant competitors such as *Thalassiosira pseudonana*, having had no such previous exposure, show diminished cell membrane integrity and reduced photosynthetic capabilities in addition to reduced growth rates when grown in the presence of *K. brevis*. Lipidomics, the study of all lipid metabolites contained within an organism, can be a useful tool to understanding the changes associated with allelopathy. Here, MS- and NMR-based lipidomics experiments identified a variety of fatty acids, phospholipids, glycolipids, sulfolipids and amino acid-related metabolites as significantly dysregulated as a result of *K. brevis* exposure. Mapping these changes to systems pathways may be critical in understanding and preventing the devastating effects of exposure to the red tide on both marine and human life.

4.2 Background

4.2.1 Bloom Forming Algae

The accumulation of high concentrations of microscopic algae that release or exude toxic compounds leads to the formation of harmful algal blooms (HABs), which pose a threat to marine and ultimately human life due to transfer of these toxins up the food chain.[1] One such dinoflagellate, *Karenia brevis*, often forms blooms in the Gulf of Mexico and the Southeastern Atlantic Ocean. As the pigments contained within these phytoplankton cause a red color to form within the water, these dense congregations of *K. brevis* are commonly referred to as red tides.[2] *K. brevis* releases a suite of polyether neurotoxins called brevetoxins.[3] Shellfish and filter-feeding organisms can accumulate high concentrations of these toxins, ingestion of which causes neurotoxic shellfish poisoning.[4] Exposure to these toxins can thus be fatal and often leads to massive fish kills in marine ecosystems.[5]

4.2.2 Impact of *K. Brevis* Allelopathy

Additionally, when *K. Brevis* forms HABs, it is able to out compete or exclude other plankton species through allelopathy, the release of chemicals that inhibit the growth of competitors.[6] However, brevetoxins have not been shown to be responsible for such effects.[7] Instead, allelopathic compounds are suggested to be unstable aromatic or unsaturated hydrocarbons, possibly derived from fatty acids, though complete characterization has eluded researchers to date.[8] As *K. brevis* allelopathy results in sub-lethal changes within competitors including suppressed growth rates, diminished photosynthetic activity and reduced membrane integrity, the response to allelopathic stress can be studied within living competitors, making this an attractive target for

metabolomic analysis.[9] Metabolomics provides an instantaneous view of all the small molecule metabolites contained within an organism and reflects the chemical transformation of such metabolites caused by isolated treatment effects.[10] Determining which metabolites are most affected by *K. brevis* allelopathy may thus provide insight into the mechanisms responsible for such physiological responses.

4.2.3 Changes Discovered in the Polar Metabolome of Marine Phytoplankton

Previously, proteomic and metabolomic analysis was conducted in order to compare the responses within the polar metabolome of two distinct competitors to *K. brevis* exposure.[11] One competitor, *Asterionellopsis glacialis,* cohabitates in geographical regions with *K. brevis* and has likely developed a resistance to exposure in order to survive. Other competitors such as *Thalassiosira pseudonana* have had no such periods of co-occurrence and therefore may be more susceptible to *K. brevis* allelopathy. As hypothesized, *T. pseudonana* cell extracts showed altered levels of protein expression indicating increased cell membrane permeability, inhibited osmoregulation, decreased photosynthetic capability and increased levels of oxidative stress.[11] In addition, increased synthesis and β-oxidation of fatty acids and significant changes in concentrations of a few vital lipid membrane constituents were also discovered, indicating that effects of *K. brevis* allelopathy may also extend to the lipophilic portion of the diatom metabolome.

4.2.4 The Use of Lipidomics to Discover Changes in the Non-Polar Metabolome

The objectives of this study thus were to determine which specific lipids in *T. pseudonana* were significantly altered as a consequence of *K. brevis* exposure and to determine how this response differed from that of *A. glacialis*. Using established lipidomics techniques to assess variations in the response of competitors *A. glacialis* and

T. pseudonana to *K. brevis* allelopathy, several lipids were identified through high-resolution mass spectrometry (HRMS) and tandem MS techniques that relate to hypothesized physiological changes induced by interactions with *K. brevis*. Based on the complementary nature of the techniques, NMR was also used to characterize changes within a different subset of lipophilic compounds in the diatoms of interest.

The exclusive study of lipid metabolites, referred to as lipidomics, is a newly expanding field under the umbrella of metabolomics.[12] Lipids play keys roles in cellular physiology, regulating processes such as signal transduction, energy storage, and membrane integrity.[13] Like plants, marine phytoplankton contain a unique mix of lipids, distinct from those typically observed in mammallian cells.[14] Commonly occuring lipids such as triacylglycerols (TGs), FFAs and polyunsaturated aldehydes (PUAs) in addition to a vairety of phospholipids such as PEs, PCs, and PGs have been found in these organisms.[14,15] Marine plankton also contain a diverse family of other polar glycerolipids, the most abundant class of lipids in the sea, that compose the bulk of eukaryotic microbial cell membranes.[16] These include glycolipids such as monogalactosyldiacylglycerols (MGDGs), digalactosyldiacylglycerols (DGDGs) and sulfoquinovosyldiacylglycerols (SQDGs) as well as betaine lipids such as diacylglyceryl trimethyl homoserines (DGTSs), diacylglyceryl hydroxymethyl trimethyl-β-alanines (DGTAs), and diacylglyceryl carboxyhydroxymethylcholines (DGCCs). The range of concentrations of these polar glycerolipids in the ocean is relatively small, spanning the order of hundreds to thousands of pmol/L.[14]

A total of nine distinct classes of polar glycerolipids thus exist within marine phytoplankton, primarily derived from FFAs, which have previsouly served as

biomarkers in ocean science research.[17,18] More recently, it has been discovered that changes in concentrations of lipids such as sulfolipids and betaine lipids may serve as indicators of nutrient induced stress in conditions when sources of phosphorus, nitrogen or sulfur are limited.[19,20,21] ROS also serve as source of stress in biological systems including plants. Developed to identify and annotate products of ROS stress in diatoms, the lipid and oxylipin biomarker screening through adduct hierarchy sequences (LOBSTAHS) database served as a useful tool for identifying the diverse array of lipids found within the studied marine diatoms and was critical in identifying metabolic changes brought about by such stressors.[15]

4.3 Experimental Methods

4.3.1 Preparation of Cellular Extracts

Changes within polar metabolites of diatoms undergoing stress from competition with *K. brevis* were previously reported by Poulson-Ellestad *et al.* (2014), with growth of diatom cultures and exposure to *K. brevis* as previously described.[11] For the subsequent analysis of non-polar metabolites, lipid metabolites within dried extracts were dissolved in a biphasic mixture of 9:10:15 water/methanol/chloroform to induce phase separation. The more lipophilic layer was removed and washed twice with 9:10 water/methanol, dried and stored at -80° C until analysis. For the current work, the lipid-soluble fractions were analyzed by ^{1}H NMR spectroscopy and UPLC-MS metabolomics. The cellular extracts of all samples were reconstituted in 200 µL IPA prior to MS analysis. Methods for NMR sample preparation and data acquisition can be found within the published manuscript, as previously reported.[22]

4.3.2 UPLC-MS Data Collection

Lipid extracts (n=13 per group) were reconstituted in 200 µL IPA. Quantitative metabolomics data were acquired using a Waters Xevo G2 QTOF mass spectrometer. The instrument was operated in negative mode ESI with a capillary voltage of -2.0 kV and a sampling cone voltage of 30 V. The source temperature of 90 °C was maintained throughout the experiment. Nitrogen was used as a desolvation gas at 250 °C with a flow rate of 600 L/h. The mass spectrometer was calibrated across the 50-1200 Da mass range using a sodium formate solution. Leucine enkephalin was infused at a flow rate of 2 µL/min and acquired as a lockmass correction. Run order was randomized and samples were acquired in duplicate. Pooled QC samples were acquired after every twelfth sample injection to monitor instrumental drift and minimize batch effects.

Chromatographic separation was accomplished using a Waters Acquity UPLC quaternary solvent manager system fitted with a Waters ACQUITY UPLC BEH C18 column (1.7-µm particle size, 2.1 × 50 mm), with an injection volume of 10 µL. The column was operated at 60 °C, while the autosampler tray was maintained at 5 °C. Mobile phase A contained 40:60 water: ACN and mobile phase B contained 10% ACN in IPA. A flow rate of 300 µL/min was used with the following gradient: 0-1 min, 70% B; 1-3 min, 75% B; 3-6 min, 80% B; 6-10 min, 90% B; 10-14 min, 100% B. Both mobile phases included 10 mM ammonium formate (Sigma Aldrich, >99.995%) and 0.1% formic acid (Fluka Analytical) additives to improve peak shape and ionization efficiency. All solvents used were of LCMS grade and provided by OmniSolv (water, ACN) or Honeywell (IPA).

4.3.3 UPLC-MS Data Processing

Data were imported into Progenesis QI for chromatographic alignment, de-isotoping, adduct deconvolution, normalization, and peak picking. Peaks detected in the sample blanks at greater than 10% of the average sample intensity were removed as potential contaminants. The corresponding normalized intensities across each sample for every feature, defined as a temporarily unidentified *m/z* and RT pair, were imported into MATLAB for multivariate analysis.

4.3.4 Multivariate Statistical Analysis

Prior to multivariate modeling, NMR and MS spectral data were preprocessed. PCA and oPLS-DA models were generated to investigate the effect of *K. brevis* allelopathy on algal lipidomes (MATLAB and PLS Toolbox, version 8.1, Eigenvector research). Spectral features with discriminatory power in NMR-based models were annotated using HMDB and Chenomx Profiler while MS-based features were annotated using LOBSTAHS, Kyoto Encyclopedia of Genes and Genomes (KEGG), LIPID MAPS, and Metlin databases[15,23-27]. Pooled extracts of each species were used to collect 2D NMR spectral data including: correlation spectroscopy (COSY), heteronuclear single quantum coherence (HSQC), and heteronuclear multiple bond correlation spectroscopy (HMBC) to aid in annotation.

PCA and oPLS-DA plots were constructed using PLS Toolbox version 8.1 in Matlab. For PLS-DA, plots were orthogonalized such that the maximum variance between classes was produced across the first LV, with all other LVs explaining within class variance. Data were autoscaled and the model containing the fewest LVs that produced the lowest cross-validated error was selected. Venetian blinds CV was

employed with six data splits for analysis of treatment/control effects of each cell type, while eight data splits were used when comparing all samples (n=61) including pooled QCs. Significant peaks, defined as $p<0.05/n$ (number of features) were identified using a 2-tailed t-test with unequal variance following the use of the Bonferroni correction for multiple comparisons.

4.3.5 Metabolite Annotation

Tandem MS experiments were performed on Thermo Q-Exactive HF quadrupole-Orbitrap mass spectrometer using the top 10 Data-dependent acquisition (DDA) method to select and fragment all ions of interest with resolution=30,000, automatic gain control (AGC) = 1e5, maximum injection time = 30 ms, and a stepped NCE ranging from 10 to 50.

All features with significant differences between control and treatment groups within each cell type were analyzed by MS/MS to elucidate structure. Following adduct analysis, elemental formulae were determined based on exact mass and isotopic distribution. Features with exact masses corresponding to matches in the LOBSTAHS database were tentatively identified, with identities confirmed by matching headgroup fragments and fatty acid chains from the MS/MS spectra to tentative identities.[15] For those features without LOBSTAHS matches, identifications were performed by hand using known lipid fragmentation patterns and cross-checked against other the KEGG, Metlin and LIPID MAPS databases.[25-27]

4.4 Results

4.4.1 MS Analysis Reveals Broad Changes in Phytoplankton Lipidome

MS-based analysis was conducted in negative mode using a Waters Xevo G2-QTOF mass spectrometer operated with an electrospray ionization source. Use of negative ionization mode enabled the detection of a wide variety of fatty acids, primary fatty acid amides (PFAAs), and a number of sulfolipids, which included SQDGs and other lipids containing sulfate functional groups. Polar glycolipids such as MGDGs and DGDGs were also detected and identified in negative ionization mode. Although easier to ionize in positive mode, PCs and PEs were detected here as formate adducts $[M+HCO_2]^-$, and the use of negative mode allowed for the precise annotation of esterified fatty acid chains in the detected lipids of interest.

A total of 13 samples from each of four groups were analyzed: *T. pseudonana* control, *T. pseudonana* treatment, *A. glacialis* control and *A. glacialis* treatment. Treatment groups were exposed to *K. brevis* allelopathy for six days, while control samples remained unexposed. A total of 1546 features detected within all samples, including pooled QCs, were imported into Matlab to conduct qualitative interpretation of the alterations within the lipidomes of each phytoplankton competitor. PCA is an unsupervised analysis technique that reduces dimensionality in the data in order to visualize multivariate matrices in a linear space.[28] It can be helpful in observing clustering patterns in the data without the potential overfitting imposed by imparting class information. A number of interesting trends can be visualized by decomposing the data into lower dimensional space, with each sample represented by a single point in a PCA scores plot. First, pooled QC samples, obtained by alloquoting an equivalent portion of

each sample contained within the study, were resampled over the duration of the experiment. As expected, these samples, represented by pink stars in Figure 4.1, clearly clustered together towards the center of the scores plot, indicating the reliablity of the analysis conducted over time. Next, clear distinction between the lipidomic profile of the two species was seen, with *T. pseudonana* samples possessing negative scores on PC1 and *A. glacialis* samples having positive scores on PC1. More interestingly, the two classes of *T. pseudonana* samples clustered distinctly from each other, with control samples exhibiting negative scores on PC2 while treatment samples showed a distinct trend towards positive scores. No such separation existed for the *A. glacialis* samples, with both treatment and control samples generally overlapped, indicating that changes within the *T. pseudonana* lipidome were far more pronounced than those within *A. glacialis*.

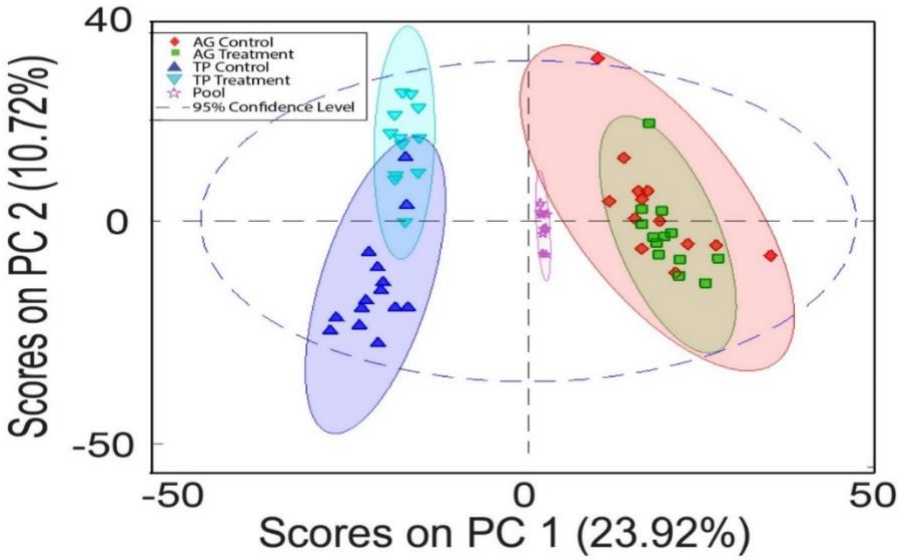

Figure 4.1: Principal Component Analysis (PCA) scores plot prior to feature selection. Pools, closely clustered together in the center of the plot, were successful representations of the combination of all classes of samples analyzed and can be used for quality control purposes. No initial separation of *A. glacialis* treatment (green square) and *A. glacialis* control (red diamond) samples was observed. A clear separation of *T. pseudonana* treatment (light blue) and *T. pseudonana* control (dark blue) samples could easily be approximated by the blue ellipses. This indicates that larger differences exist in the response of the *T. pseudonana* lipidome to *K. brevis* exposure.

4.4.2 Comparison of Lipidomic Changes Within Individual Phytoplankton Species

Peak lists were also processed and compiled separately for each of the two model systems being investigated in order to distinguish between features that were unique to each species. A total of 320 features were detected in *T. pseudonana* samples, following filters to remove low abundance, high variance, and contaminant peaks detected within experiments, while 358 were detected in the cellular extracts *A. glacialis*. Using univariate techniques to assess the extent of lipidomic variation caused by exposure to *K. brevis*, changes within 171 of the 320 species detected in the *T. pseudonana* lipidome

were considered statistically significant ($p < 0.05$) compared to only 91 of the 358 peaks detected in *A glacialis* samples. Applying the Bonferonni correction for multiple comparisons, the difference in response of each species' respective lipidome was even more pronounced. While almost half (80/171) of the features remained statistically significant ($p < 0.05/n$) in *T. pseudonana* samples, only 6 of the 91 features found in *A. glacialis* samples remained above this same threshhold. The identifications for significantly altered metabolites are included in Tables 4.1 and 4.2 respectively. Additionally, of those 6, all were contained within the set of 80 statistically significant peaks in the *T. pseudonana* samples, indicating that lipidomic changes within *T. pseudonana* samples were more pronounced, and that the negative effects of allelopathy could be understood by studying the lipidomic changes assocaited exclusivly within this single competitor.

Table 4.1: Identification of metabolites from *T. pseudonana* whose concentrations are significantly altered when exposed to *K. brevis*. Observed *m/z* and mass error (ppm), adduct, elemental formula, and molecular composition (full fatty acid chain information) are provided where possible. Fold change (FC) values are positive when relative abundance of metabolite increased when *T. pseudonana* was exposed to allelopathy. Annotation confidence (conf.) ranges from 1-3. Confidence level 1: observed MS/MS data consistent with predicted spectrum AND LOBSTAHS exact mass match to corresponding lipid class; 2: observed MS/MS data consistent with predicted spectrum; 3: observed exact mass match to LOBSTAHS database and/or partial MS/MS structural determination.
* Fold change value uncertain due to extremely low concentration of metabolites in control samples

m/z error (ppm)	Adduct	Elemental Formula	ID	FC	p-value	Conf.	Lipid Class
563.3986 0.71	[M-H]-	$C_{30}H_{60}O_7S$	Tetradecanoyl Sulfohydroxy-palmitic acid	>25*	2.39E-05	2	Other (sulfur containing)
577.4146 1.39	[M-H]-	$C_{31}H_{62}O_7S$	Myristoyl sulfohydroxy-heptadecanoic acid	>25*	3.83E-06	2	Other (sulfur containing)
591.4308 2.20	[M-H]-	$C_{32}H_{64}SO_7$	Pentadecanoyl sulfohydroxy-heptadecanoic acid	>25*	1.88E-06	2	Other (sulfur containing)
379.2148 7.12	[M-H]-	$C_{21}H_{32}O_6$	FFA(21:5 + 4 O)	>25*	4.25E-5	3	Free fatty acid
607.4243 1.81	[M-H]-	$C_{32}H_{64}O_8S$	Pentadecanoyl sulfohydroxy-heptadecanoic acid	>25*	2.77E-5	2	Other (sulfur containing)
619.4249 0.81	[M-H]-	$C_{33}H_{64}SO_8$	Hydroxy-pentadecanoyl sulfooleic acid	>25*	1.96E-05	2	Other (sulfur containing)
572.4354 0.87	[M-H]-	$C_{32}H_{63}NO_5S$	Pentadecanoyl sulfate heptadecenamide	>25*	5.77E-07	2	Other (sulfur containing)
367.2127 1.63	[M-H]-	$C_{20}H_{32}O_6$	FFA(20:4 + 4 O)	>25*	2.75E-05	3	Free fatty acid
575.4356 1.91	[M-H]-	$C_{32}H_{64}O_6S$	Pentadecanoyl sulfoheptadecanoic acid	>25*	4.38E-07	2	Other (sulfur containing)
592.4942 0.17	[M-H]-	$C_{36}H_{67}NO_5$	*N*-heptadecenoic acid oleamide	>25*	3.82E-06	2	Fatty acid amide

Table 4.1 (continued).

665.5117 **3.31**	[M-H]-	$C_{35}H_{74}N_2O_7S$	Hexadecenoyl *N*-sulfanediol dihydroxy-nonadecanediamide	>25*	3.04E-06	2	Other (sulfur containing)
257.2125 **3.11**	[M-H]-	$C_{15}H_{30}O_3$	FFA(15:0 + 1 O)	>25*	7.05E-05	3	Free fatty acid
616.4615 **0.65**	[M-H]-	$C_{34}H_{67}NO_6S$	*N*-sulfo, *N*-pentadecanoyl nonadecanamide	>25*	1.0E-08	2	Other (sulfur containing)
561.4194 **0.89**	[M-H]-	$C_{31}H_{62}O_6S$	Myristoyl sulfo-heptadecanoic acid	>25*	1.9E-06	2	Other (sulfur containing)
787.5583 **0.76**	$[M+HCO_2]^-$	$C_{42}H_{78}O_{10}$	MGDG(33:1)	20.	8.84E-06	3	Monogalactosyldiacylglycerol
574.4516 **1.91**	[M-H]-	$C_{32}H_{65}NO_5S$	Pentadecanoyl sulfate heptadecanamide	14	9.71E-08	2	Other (sulfur containing)
578.4790 **1.04**	[M-H]-	$C_{35}H_{65}NO_5$	*N*-palmitoleic acid oleamide	8.5	2.14E-06	2	Fatty acid amide
564.4639 **1.95**	[M-H]-	$C_{34}H_{63}NO_5$	*N*-pentadecenoic acid oleamide	7.1	7.94E-07	2	Fatty acid amide
566.4792 **1.41**	[M-H]-	$C_{34}H_{65}NO_5$	*N*-pentadecanoic acid oleamide	7.0	6.79E-08	2	Fatty acid amide
686.4778 **1.75**	[M-H]-	$C_{37}H_{70}NO_8P$	PE(16:1_16:1)	6.5	3.54E-05	1	Phosphatidylethanolamine
550.4480 **1.64**	[M-H]-	$C_{33}H_{61}NO_5$	*N*-pentadecenoic acid heptadecanamide	5.8	9.45E-06	2	Fatty acid amide
682.5090 **1.47**	[M-H]-	$C_{39}H_{73}NO_6S$	*N*-sulfo, *N*-octadecanoyl heneicosanamide	5.5	4.23E-05	2	Other (sulfur containing)
651.4958 **3.68**	[M-H]-	$C_{34}H_{72}N_2O_7S$	Pentadecenoyl *N*-sulfanediol dihydroxy-nonadecanediamide	3.3	3.48E-04	2	Other (sulfur containing)
653.5117 **3.37**	[M-H]-	$C_{34}H_{74}N_2O_7S$	Pentadecanoyl *N*-sulfanediol dihydroxy-nonadecanediamide	1.7	0.0276	2	Other (sulfur containing)
793.5113 **3.53**	[M-H]-	$C_{41}H_{78}O_{12}S$	SQDG(16:0_16:0)	-2.0	5.05E-05	1	Sulfoquinovosyldiacylglycerol

Table 4.1 (continued).

763.4646 **1.83**	[M+HCO_2]-	$C_{41}H_{66}O_{10}$	MGDG(16:3_16:3)	-2.1	4.05E-05	1	Monogalactosyldiacylglycerol
791.4988 **0.38**	[M-H]-	$C_{41}H_{76}O_{12}S$	SQDG(16:0_16:1)	-2.2	4.52E-05	1	Sulfoquinovosyldiacylglycerol
771.5272 **1.04**	[M+HCO_2]-	$C_{41}H_{74}O_{10}$	MGDG(16:1_16:1)	-2.5	2.6E-06	1	Monogalactosyldiacylglycerol
719.4879 **1.39**	[M-H]-	$C_{38}H_{73}O_{10}P$	PG(16:0_16:1)	-2.6	4.89E-07	1	Phosphatidylglycerol
737.4527 **1.63**	[M-H]-	$C_{37}H_{70}O_{12}S$	SQDG(14:0_14:0)	-2.6	7.99E-08	1	Sulfoquinovosyldiacylglycerol
779.4988 **0.38**	[M-H]-	$C_{40}H_{76}O_{12}S$	SQDG(15:0_16:0)	-2.6	7.16E-06	1	Sulfoquinovosyldiacylglycerol
813.4798 **3.07**	[M-H]-	$C_{43}H_{74}O_{12}S$	SQDG(16:0_18:4)	-2.7	1.79E-06	1	Sulfoquinovosyldiacylglycerol
765.4723 **1.44**	[M-H]-	$C_{42}H_{71}O_{10}P$	PG(16:1_20:5)	-2.8	2.33E-02	1	Phosphatidylglycerol
769.5111 **0.39**	[M+HCO_2]-	$C_{41}H_{72}O_{10}$	MGDG(16:0_16:3)	-2.8	1.30E-03	1	Monogalactosyldiacylglycerol
977.5477 **0.20**	[M+HCO_2]-	$C_{51}H_{80}O_{15}$	DGDG(16:3_20:5)	-2.8	1.07E-02	1	Digalactosyldiacylglycerol
759.4368 **1.19**	[M-H]-	$C_{39}H_{68}O_{12}S$	SQDG(14:0_16:3)	-2.9	1.42E-02	1	Sulfoquinovosyldiacylglycerol
751.4681 **1.20**	[M-H]-	$C_{38}H_{72}O_{12}S$	SQDG(14:0_15:0)	-3.1	2.93E-08	1	Sulfoquinovosyldiacylglycerol
765.4796 **3.53**	[M-H]-	$C_{39}H_{74}O_{12}S$	SQDG(14:0_16:0)	-3.2	1.69E-08	1	Sulfoquinovosyldiacylglycerol
691.4565 **1.30**	[M-H]-	$C_{36}H_{69}O_{10}P$	PG(14:0_16:1)	-3.2	9.85E-07	1	Phosphatidylglycerol
819.5268 **0.49**	[[M+HCO_2]-	$C_{45}H_{74}O_{10}$	MGDG(16:1_20:5)	-3.3	9.7E-05	1	Monogalactosyldiacylglycerol
791.4989 **0.51**	[M-H]-	$C_{41}H_{76}O_{12}S$	SQDG(14:0_18:1)	-2.2	4.52E-05	1	Sulfoquinovosyldiacylglycerol
745.5114 **1.61**	[M+HCO_2]-	$C_{39}H_{72}O_{10}$	MGDG(14:0_16:1)	-3.6	2.05E-06	1	Monogalactosyldiacylglycerol

Table 4.1 (continued).

748.5145 **2.14**	[M+HCO_2]-	$C_{38}H_{74}NO_8P$	PC(14:0_16:1)	-3.7	2.59E-06	1	Phosphatidylcholine
761.4489 **3.41**	[M-H]-	$C_{39}H_{70}O_{12}S$	SQDG(14:0_16:2)	-3.9	9.06E-06	1	Sulfoquinovosyldiacylglycerol
799.4681 **1.13**	[M-H]-	$C_{42}H_{72}O_{12}S$	SQDG(15:0_18:4)	-3.9	7.44E-05	1	Sulfoquinovosyldiacylglycerol
743.4965 **2.69**	[M+HCO_2]-	$C_{39}H_{70}O_{10}$	MGDG(14:0_16:2)	-4.0	1.75E-05	1	Monogalactosyldiacylglycerol
802.5609 **1.37**	[M+HCO_2]-	$C_{42}H_{80}NO_8P$	PC(16:1_18:1) / PC(16:0_18:2)	-4.0	9.41E-06	1	Phosphatidylcholine
907.5639 **0.33**	[M+HCO_2]-	$C_{45}H_{82}O_{15}$	DGDG(14:0_16:1)	-4.0	4.9E-06	1	Digalactosyldiacylglycerol
762.5017 **35.1**	[M+HCO_2]-	$C_{39}H_{76}NO_8P$	PC(15:0_16:1)	-4.0	8.47E-06	3	Phosphatidylcholine
822.5293 **0.24**	[M+HCO_2]-	$C_{44}H_{76}NO_8P$	PC(16:1_20:5)	-4.1	4.57E-08	1	Phosphatidylcholine
841.5108 **3.92**	[M-H]-	$C_{45}H_{78}O_{12}S$	SQDG(36:4)	-4.2	1.24E-05	3	Sulfoquinovosyldiacylglycerol
935.5961 **1.28**	[M+HCO_2]-	$C_{47}H_{86}O_{15}$	DGDG(16:0_16:1)	-4.2	1.8E-07	1	Digalactosyldiacylglycerol
757.4210 **1.06**	[M-H]-	$C_{39}H_{66}O_{12}S$	SQDG(14:0_16:4)	-4.4	5.19E-06	1	Sulfoquinovosyldiacylglycerol
820.5129 **0.61**	[M+HCO_2]-	$C_{44}H_{74}NO_8P$	PC(16:2_20:5)	-4.4	3.36E-06	1	Phosphatidylcholine
583.3129 **1.89**	[M-H]-	$C_{30}H_{48}O_{11}$	MGDG(21:4+1 O)	-4.5	1.23E-06	3	Monogalactosyldiacylglycerol
773.5427 **0.78**	[M+HCO_2]-	$C_{41}H_{76}O_{10}$	MGDG(16:0_16:1)	-4.5	8.48E-07	1	Monogalactosyldiacylglycerol
795.5265 **0.13**	[M+HCO_2]-	$C_{43}H_{74}O_{10}$	MGDG(16:0_18:4)	-4.5	6.45E-06	1	Monogalactosyldiacylglycerol
829.4763 **1.09**	[M-H]-	$C_{43}H_{74}O_{13}S$	SQDG(34:4 + 1 O)	-4.8	0.000138	3	Sulfoquinovosyldiacylglycerol
818.4976 **0.24**	[M+HCO_2]-	$C_{44}H_{72}NO_8P$	PC(16:3_20:5) / PC(18:4_18:4)	-5.1	2.69E-07	1	Phosphatidylcholine

Table 4.1 (continued).

850.5604 **0.00**	$[M+HCO_2]^-$	$C_{46}H_{80}NO_8P$	PC(18:1_20:5)	-5.3	4.66E-06	1	Phosphatidylcholine
870.5292 **0.11**	$[M+HCO_2]^-$	$C_{48}H_{76}NO_8P$	PC(20:5_20:5)	-5.3	6.87E-07	1	Phosphatidylcholine
796.5138 **1.13**	$[M+HCO_2]^-$	$C_{42}H_{74}NO_8P$	PC(14:0_20:5) / PC(16:1_18:4)	-6.3	3.49E-07	1	Phosphatidylcholine
824.5454 **0.85**	$[M+HCO_2]^-$	$C_{44}H_{78}NO_8P$	PC(16:0_20:5)	-6.4	1.25E-08	1	Phosphatidylcholine
896.5448 **0.11**	$[M+HCO_2]^-$	$C_{50}H_{78}NO_8P$	PC(20:5_22:6)	-6.7	3.46E-07	1	Phosphatidylcholine
800.5449 **0.25**	$[M+HCO_2]^-$	$C_{42}H_{78}NO_8P$	PC(16:0_18:3)	-6.9	4.77E-05	1	Phosphatidylcholine
798.5286 **0.63**	$[M+HCO_2]^-$	$C_{42}H_{76}NO_8P$	PC(16:0_18:4)	-7.8	5.7E-05	1	Phosphatidylcholine
844.5135 **0.12**	$[M+HCO_2]^-$	$C_{46}H_{74}NO_8P$	PC(18:4_20:5)	-8.5	1.41E-05	1	Phosphatidylcholine
848.5448 **0.12**	$[M+HCO_2]^-$	$C_{46}H_{78}NO_8P$	PC(18:2_20:5) / PC(16:1_22:6)	-8.5	5.3E-06	1	Phosphatidylcholine
821.5427 **1.46**	$[M+HCO_2]^-$	$C_{45}H_{76}O_{10}$	MGDG(36:5)	-9.3	2.82E-06	3	Monogalactosyldiacylglycerol
843.5266 **0.24**	$[M+HCO_2]^-$	$C_{47}H_{74}O_{10}$	MGDG(18:3_20:5)	-11	6.0E-05	1	Monogalactosyldiacylglycerol

Table 4.2: Identification of metabolites from *A. glacialis* showing significantly altered relative concentrations when exposed to *K. brevis.* Observed *m/z* and associated mass error (ppm), adduct, elemental formula, and molecular composition (full fatty acid chain information) are provided where possible. Fold change (FC) values are positive when relative abundance of metabolite increased when *A. glacialis* was exposed to allelopathy. Annotation confidence (Conf.) ranges from 1-3. Confidence level 1: observed MS/MS data consistent with predicted spectrum AND LOBSTAHS exact mass match to corresponding lipid class; 2: observed MS/MS data consistent with predicted spectrum; 3: observed exact mass match to LOBSTAHS database and/or partial MS/MS structural determination.

m/z **error (ppm)**	Adduct	Elemental Formula	ID	FC	p-value	Conf.	Lipid Class
591.4308 **2.37**	[M-H]-	$C_{32}H_{64}SO_7$	Pentadecanoyl sulfohydroxy-heptadecanoic acid	4.9	4.24E-06	2	Other (sulfur containing)
607.4243 **1.81**	[M-H]-	$C_{32}H_{64}O_8S$	Pentadecanoyl sulfodihydroxy-heptadecanoic acid	4.9	1.66E-05	2	Other (sulfur containing)
616.4615 **0.65**	[M-H]-	$C_{34}H_{67}NO_6S$	*N*-sulfo, *N*-pentadecanoyl nonadecanamide	13.8	5.55E-05	2	Other (sulfur containing)
578.4790 **1.04**	[M-H]-	$C_{35}H_{65}NO_5$	*N*-palmitoleic acid oleamide	12.2	7.2E-06	2	Fatty acid amide
651.4958 **3.68**	[M-H]-	$C_{34}H_{72}N_2O_7S$	Pentadecenoyl *N*-sulfanediol dihydroxy-nonadecanediamide	12.5	1.42E-05	2	Other (sulfur containing)
653.5117 **3.37**	[M-H]-	$C_{34}H_{74}N_2O_7S$	Pentadecanoyl *N*-sulfanediol dihydroxy-nonadecanediamide	16.4	4.57E-05	2	Other (sulfur containing)

These same observations held true when interpreting oPLS-DA plots of both MS and NMR data for each of the two studied species (Figure 4.2). oPLS-DA is a powerful supervised classification tool, useful for maximizing the separation of two or more distinct classes using multivariate data dimensionality reduction.[29] Optimized models incorporating data obtained from both MS and NMR showed that treatment and control samples from each of the two species studied could in fact be separated with a high degree of accuracy. However, the distinction between *T. pseudonana* treatment and control samples was more prounounced, as LV1 explained 79.2% of the variance within samples for MS data, while LV1 only captured 21.9% of the variance within *A. glacialis* samples analyzed by MS. Additionally, the classification model separating *T. pseudonana* treatment and control samples, built using the 80 significant features previously discussed, perfomed with 100% accuracy, sensitivty and specificity, in comparison to 88.5%, 92.3%, and 84.6% for the MS-based *A. glacialis* model, respectively. Similar patterns were observed within the NMR classification models, again indicative of a resistance to allelopathy evolved within *A. glacialis* dinoflaggellates.

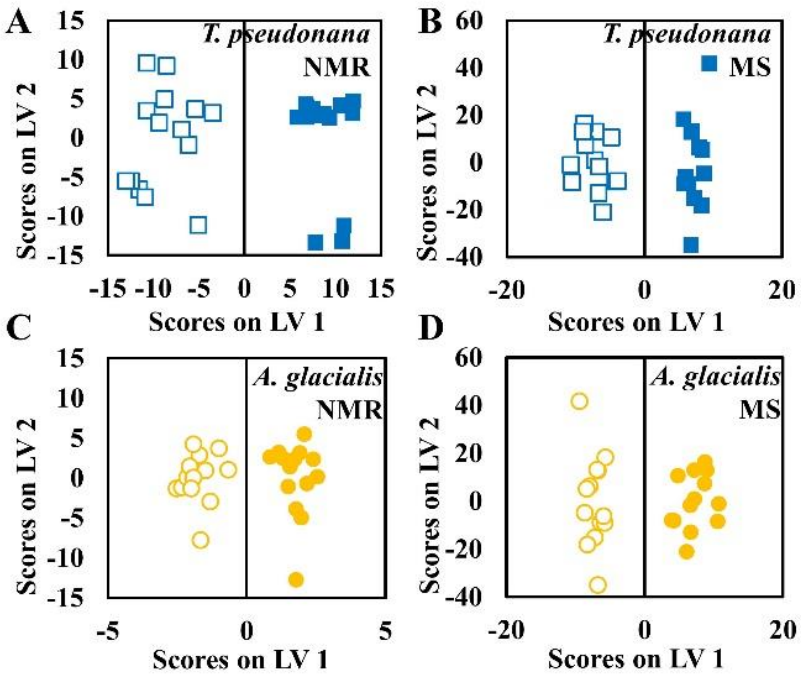

Figure 4.2: oPLS-DA models reveal that lipidomes of *T. pseudonana* and *A. glacialis* are disrupted by *Karenia brevis* allelopathy. Filled symbols represent lipidomes of algae exposed to *K. brevis* through molecule-permeable but cell impermeable membranes, empty symbols represent lipidomes from unexposed algae (controls). oPLS-DA model generated from A) $_1$H NMR spectral data and B) from UPLC-MS metabolic features from lipidomes of *T. pseudonana* (blue squares). oPLS-DA model generated from C) $_1$H NMR spectral data and D) from UPLC-MS metabolic features from lipidomes of *A. glacialis* (yellow circles). NMR data were collected and interpreted and figure produced by Dr. Remington Poulin.[22]

4.4.3 Identification of Altered Lipid Species within *T. Pseudonana*

The direction of change for these features was visualized using a volcano plot (Figure 4.3). Volcano plots are intended to give a broad overview of the association between p-value and fold change (FC) for datasets containing a large number of variables, with the highly significant points with large FCs appearing in the upper left and upper right corners of the plot. Here it was clear that a vast majority of the *A. glacialis*. data remained below the significance threshold, while many *T. pseudonana* features were

highly significant. Allelopathy led to reductions in relative abundances for a total of 47 of these features within *T. pseudonana* samples, while the remaining 33 statistically significant features were increased within the treatment group as a result of exposure. All six of the significantly altered features detected within *A. glacialis* samples displayed increased relative abundances in the treatment group, though the relative FC was generally less than that observed for the same features detected in *T. pseudonana* samples (Table 4.2). This evidence supports the hypothesis that *A. glacialis* has evolved a pattern of resistance to *K. brevis* allelopathy, as displayed by the relatively minor changes observed within the lipidome of this species following exposure to *K. brevis*. Meanwhile, a substantial fraction of all lipids found within *T. pseudonana* were statistically different upon treatment with *K. brevis*, and the changes within the lipidome of this competitor may help explain the broad physiological changes caused by exposure to *K. brevis* allelopathy.

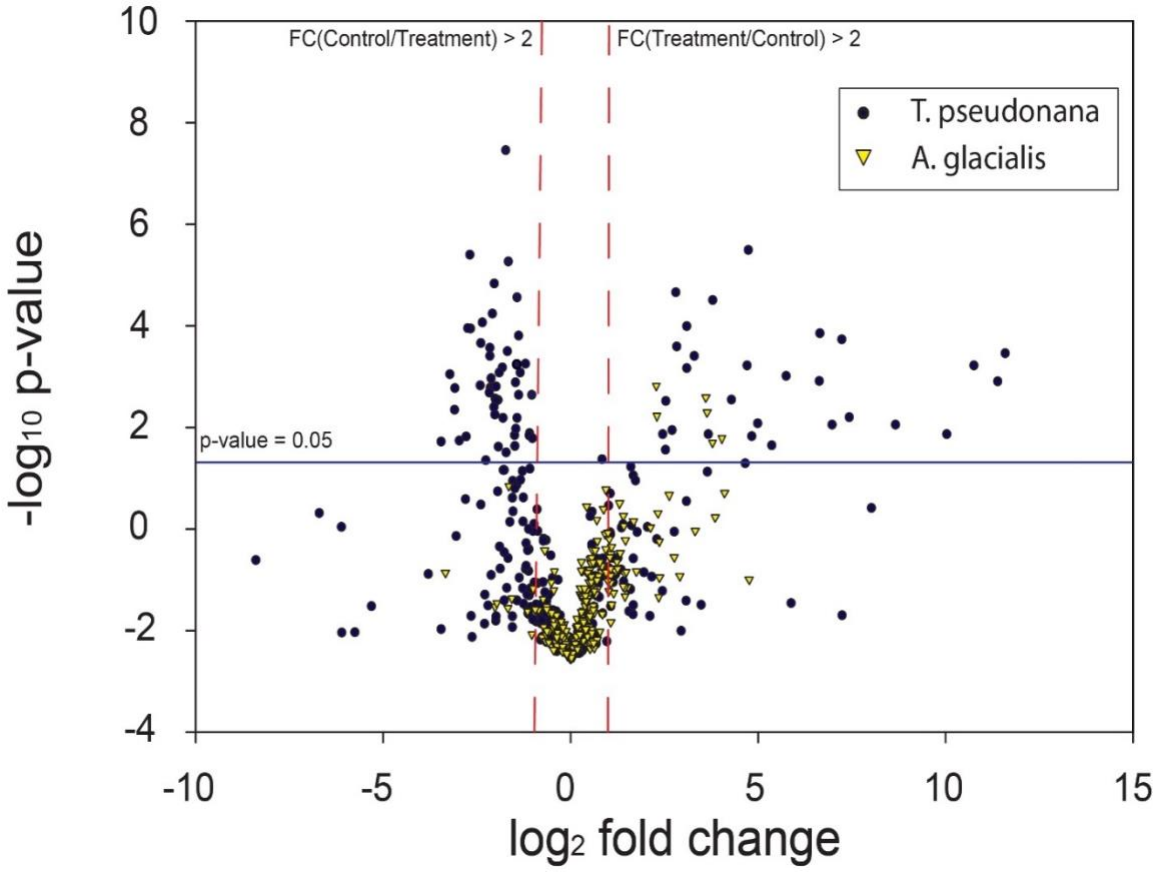

Figure 4.3: Volcano plot summarizing the differences in the lipidomic responses of *T. pseudonana* (blue) and *A. glacialis* (yellow) when exposed to *K. brevis* allelopathy. The relative abundances of 80 metabolites were significantly different ($p < 0.05$ after Bonferroni correction) in *T. pseudonana* samples upon exposure to *K. brevis* allelopathy. Red lines indicate $\log_2$ fold differences of ±1.

Of the 80 species identified to be significantly dysregulated in cell extracts of *T. pseudonana*, a total of 70 lipid metabolites were confidently identified using tandem MS fragmentation patterns, class specific characteristic headgroup fragments and fatty acid chain lengths (see Table 4.1 for full annotation). These lipid species belonged to nine classes, with each class generally showing the same trend regardless of fatty acid chain length (Table 4.3). Therefore lipid class was far more correlated with physiological effects associated with allelopathy than was fatty acid chain length.

T**able 4.3**: Lipid classes identified by MS-based oPLS-DA model as having significantly different concentrations in *T. pseudonana* based upon exposure to *K. brevis* allelopathy. Common adducts detected, the number of detected compounds, and the average fold change (FC) are included for each lipid class. The average FC is an average of the individual FCs for each lipid identified in a class. Classes of lipids identified include: phosphatidylcholines (PCs), phosphatidylethanolamines (PEs), phosphatidylglycerols (PGs), sulfoquinovosyldiacylglycerols (SQDGs), digalactosyldiacylglycerols (DGDGs), monogalactosyldiacylglycerols (MGDGs), primary fatty acid amides (PFAAs), free fatty acids (FFAs), and non-SQDG sulfontated lipids (SULF).

Lipid Class	Adduct Detected	# Chemical Species	Average FC
PC	$[M+HCO_2]^-$	15	-5.8
SQDG	$[M-H]^-$	14	-3.3
DGDG	$[M+HCO_2]^-$	3	-3.3
PG	$[M-H]^-$	3	-2.9
MGDG	$[M+HCO_2]^-$	12	-2.8
PE	$[M+HCO_2]^-$	1	6.5
PFAA	$[M-H]^-$	5	25
FFA	$[M-H]^-$	3	>25*
SULF	$[M-H]^-$	14	>25*

*Fold change value uncertain due to extremely low concentration of metabolites in control samples

Each class of lipid was identified by a characteristic neutral loss or parent ion scan, often indicative of the lipid headgroup. Previous studies have identified and quantified these classes of lipids using diagnostic scans in positive mode,[14] but the use of negative mode allowed for the distinction of isobaric lipids by exact fatty acid composition, giving rise to a weath of information about underlying chemisty related to metabolomic changes within phytoplankton. PCs, PEs and PGs were identified using the characteristic headgroup fragments of 224.07, 196.04 and 227.03 Da respectively. MGDGs and DGDGs each contained a minor peak at 235.08 Da and were distinguished by the number of attached sugar molecules and exact mass, while SQDGs contained a

unique fragment at 225.01 Da. PFAAs were tentatively identified by the presence of a 74.02 Da fragment, while sulfolipids showed a characteristic 80.96 Da fragment representing the HSO_3^- ion. FFAs were identified with exact mass only and matched to the LOBSTAHS database.[15]

4.4.4 Alterations in Free Fatty Acids and Related Small Molecules

Fatty acids are small molecules found within cells that play a role in energy production and serve as intermediates in metabolism. A basic building block of more complex lipids, they exist as free carboxylic acids or may be esterified as in wax esters, phospholipids, and other similar molecules.[30] Following exposure to *K. brevis*, the relative abundance of three fatty acids, each containing some degree of oxidation, was dramatically increased (FC > 25) within *T. pseudonana* cell extracts. The largest increase was observed for FFA(21:5 + 4 O), which showed a 1000-fold increase due to minimal initial relative abundance found within the control samples. Fatty acid amides, consisting of an acyl chain and carboxamide group, are formed from the conversation of a fatty acid and an amine and often play a role in cell signaling.[31,32] Ammonium is likely the source of nitrogen in such metabolic reactions.[33] For all non-sulfur containing PFAAs, a similarly large increase was observed. A nearly 100-fold increase was observed for one species (n-heptadecenoic acid oleamide), while the four other molecules identified showed more modest increases in relative abundance (average FC = 7.1).

4.4.5 Identified Sulfolipid Alterations

The term sulfolipid has been used to describe compounds containing sulfonic acid ($C\text{-}SO_3H$) functional groups, and sulfolipids have been discovered within all photosynthetic organisms.[34] Two main types of sulfur-containing molecules exist in such

organisms: alkyl sulfates and SQDGs.[35] The alkyl sulfates observed in the cellular extracts of *T. pseudonana* largely consisted of molecules with a sulfonated fatty acid or alcohol esterified to another fatty acid. A total of 14 species within this class (SULF, or non-SQDG sulfonated lipids) were significantly different in *K. brevis* treated samples. Each of the compounds within this class exhibited large increases in relative abundance (FC > 25). Conversely, SQDGs showed a moderate decrease in relative abundance resulting from *K. brevis* exposure (FC = -3.3), and all 14 statistically significant SQDGs identified were more abundant in *T. pseudonana* control samples than in the treatment group. SQDGs compose a minor level of lipids found within the thylakoid membrane of chloroplasts in marine plankton.[36] They are involved in the maintenance of photosystem II activity, and the observed decrease in SQDGs may be associated with the decrease in photosynthetic efficiency which has been observed within competitors exposed to *K. brevis* allelopathy.[9] The changes may also be the result of nutrient induced stress conditions brought about by sulfur deficiency.[37]

4.4.6 *K. Brevis* Exposure Leads to Lower Levels of Phospholipids

Dramatic changes in phospholipid concentrations were also observed in *T. pseudonana* samples resulting from exposure to *K. brevis* allelopathy. Phospholipids including PCs, PEs and PGs are all lipids commonly found in cellular membanes. In this study, compared to *T. pseudonana* cells grown in culture alone, the number of cells with damaged membranes was increased as a result of co-culture with *K. brevis*, indicating that allelopathy decreased the permeability of cell membranes.[22] The large decrease in PCs (FC = -5.8) and moderate decrease in PGs (FC = -2.9) was likely associated with the observed decrease in membrane integrity. A single PE species, PE(16:1_16:1), was found

to be significantly increased in the treatment group. However, PCs and PGs were more prone to systems level alterations than were PEs, indicating that changes within these two classes of phospholipids may be associated with the observed alterations in cell membrane permeability.

4.4.7 Allelopathy Also Leads to Significant Alterations in Glycolipids

Similarly, decreased abundance of MGDGs (FC = -2.8) and DGDGs (FC = -3.3) was also observed within *T. pseudonana* cell extracts following *K. brevis* exposure. These are the most abundant lipids in chloroplast membranes, over 80%. Thus, decreased concentrations of these lipids is likely associated with the decreased photosynthetic activity observed in these experiments. The increased membrane permeability could also be a result of decreased MGDGs and DGDGs, which compose over 80% of total lipid content in chloroplasts.[36]

4.4.8 NMR Identifies Complementary Alterations within *T. Pseudonana*

A wealth of complementary information can be obtained by incorporating orthogonal techniques such as NMR into metabolomics experiments. In addition to the lipids identified above, NMR metabolomics led to the discovery of aconitic acid, malonic acid, methyl guanidine, *N*-acetyl cysteine, and *N*-acetyl glutamine as compounds whose concentration was significantly suppressed in *T. pseudonana* samples by *K. brevis* allelopathy.[22] Aconitic acid is an intermediate in the tricarboxylic acid (TCA) cycle, while malonic acid is an intermediate in fatty acid synthesis. The decrease in relative abundance of these metabolites may be explained by increased catabolism of these molecules as starting materials and intermediates or reduced anabolism.[38,39] The suppression of three methylated and acylated amino acids also suggests the alteration of

amino acid metabolism induced by allelopathy. None of these five compounds could be identified using MS-based analysis, highlighting the highly complementary nature of information obtained by these techniques.

4.5 Conclusion

Initial exposure to the red tide dinoflaggellate *K. brevis* resulted in substantial changes within the lipidome of *T. pseudonana* cell extracts, as determined by the use of MS and NMR as complementary analytical techniques. Meanwhile, smaller often insigificant changes were observed in *A. glacialis*, likely based on the development of an evolved resistence in this competitor due to previous periods of co-habitation with *K. brevis*, reducing the effects of allelopathy. The study of the lipidomic response in *T. pseudonana* cell extracts may give rise to a more thorough understanding of the effects of allelopathy on non-resistent competitors, which displayed reduced growth rates, reduced cell membrane integrity, and decreased photosynthetic activity as a result of exposure. Significant decreases in complex lipids such as PCs, PGs, MGDGs, DGDGs and SQDGs were observed, while the relative abundance of a variety of smaller lipid metabolites including fatty acids, PFAAs and sulfolipids was increased in *T. pseudonana* treatment samples. Ultimately, these systems level alterations offer unique insight into the metabolic changes associated with *K. brevis* allelopathy in both resistant and non-resistant phytoplankton competitors.

4.6 References

1 Pierce, R. H. & Henry, M. Harmful algal toxins of the Florida red tide (Karenia brevis): natural chemical stressors in South Florida coastal ecosystems. *Ecotoxicology* **17**, 623-631 (2008).

2 Glibert, P. M., Anderson, D. M., Gentien, P., Granéli, E. & Sellner, K. G. The global, complex phenomena of harmful algal blooms. (2005).

3 Landsberg, J., Flewelling, L. & Naar, J. Karenia brevis red tides, brevetoxins in the food web, and impacts on natural resources: Decadal advancements. *Harmful Algae* **8**, 598-607 (2009).

4 Landsberg, J. The role of harmful algal blooms in shellfish disease. *Journal of Shellfish Research* **16**, 350 (1997).

5 Baden, D. G., Rein, K. S. & Gawley, R. E. in *Molecular Approaches to the Study of the Ocean* 487-514 (Springer, 1998).

6 Wardle, D. A., Karban, R. & Callaway, R. M. The ecosystem and evolutionary contexts of allelopathy. *Trends in ecology & evolution* **26**, 655-662 (2011).

7 Kubanek, J., Hicks, M. K., Naar, J. & Villareal, T. A. Does the red tide dinoflagellate Karenia brevis use allelopathy to outcompete other phytoplankton? *Limnology and Oceanography* **50**, 883-895 (2005).

8 Prince, E. K., Poulson, K. L., Myers, T. L., Sieg, R. D. & Kubanek, J. Characterization of allelopathic compounds from the red tide dinoflagellate Karenia brevis. *Harmful Algae* **10**, 39-48 (2010).

9 Prince, E. K., Myers, T. L., Naar, J. & Kubanek, J. Competing phytoplankton undermines allelopathy of a bloom-forming dinoflagellate. *Proceedings of the Royal Society B: Biological Sciences* **275**, 2733-2741 (2008).

10 Patti, G. J., Yanes, O. & Siuzdak, G. Innovation: Metabolomics: the apogee of the omics trilogy. *Nature reviews Molecular cell biology* **13**, 263 (2012).

11 Poulson-Ellestad, K. L. *et al.* Metabolomics and proteomics reveal impacts of chemically mediated competition on marine plankton. *Proceedings of the national academy of sciences* **111**, 9009-9014 (2014).

12 Griffiths, W. J. & Wang, Y. Mass spectrometry: from proteomics to metabolomics and lipidomics. *Chemical Society Reviews* **38**, 1882-1896 (2009).

13 Van Meer, G., Voelker, D. R. & Feigenson, G. W. Membrane lipids: where they are and how they behave. *Nature reviews Molecular cell biology* **9**, 112 (2008).

14 Popendorf, K. J., Fredricks, H. F. & Van Mooy, B. A. Molecular ion-independent quantification of polar glycerolipid classes in marine plankton using triple quadrupole MS. *Lipids* **48**, 185-195 (2013).

15 Collins, J. R., Edwards, B. R., Fredricks, H. F. & Van Mooy, B. A. LOBSTAHS: an adduct-based lipidomics strategy for discovery and identification of oxidative stress biomarkers. *Analytical chemistry* **88**, 7154-7162 (2016).

16 Van Mooy, B. A. & Fredricks, H. F. Bacterial and eukaryotic intact polar lipids in the eastern subtropical South Pacific: water-column distribution, planktonic sources, and fatty acid composition. *Geochimica et Cosmochimica Acta* **74**, 6499-6516 (2010).

17 Bossio, D. A. & Scow, K. Impacts of carbon and flooding on soil microbial communities: phospholipid fatty acid profiles and substrate utilization patterns. *Microbial ecology* **35**, 265-278 (1998).

18 Zelles, L. Fatty acid patterns of phospholipids and lipopolysaccharides in the characterisation of microbial communities in soil: a review. *Biology and fertility of soils* **29**, 111-129 (1999).

19 Benning, C. Biosynthesis and function of the sulfolipid sulfoquinovosyl diacylglycerol. *Annual review of plant biology* **49**, 53-75 (1998).

20 Van Mooy, B. A., Rocap, G., Fredricks, H. F., Evans, C. T. & Devol, A. H. Sulfolipids dramatically decrease phosphorus demand by picocyanobacteria in oligotrophic marine environments. *Proceedings of the National Academy of Sciences* **103**, 8607-8612 (2006).

21 Van Mooy, B. A. *et al.* Phytoplankton in the ocean use non-phosphorus lipids in response to phosphorus scarcity. *Nature* **458**, 69 (2009).

22 Poulin, R. X. *et al.* Karenia brevis allelopathy compromises the lipidome, membrane integrity, and photosynthesis of competitors. *Scientific reports* **8**, 9572 (2018).

23 Wishart, D. S. *et al.* HMDB 3.0—the human metabolome database in 2013. *Nucleic acids research* **41**, D801-D807 (2012).

24 Weljie, A. M., Newton, J., Mercier, P., Carlson, E. & Slupsky, C. M. Targeted profiling: quantitative analysis of 1H NMR metabolomics data. *Analytical chemistry* **78**, 4430-4442 (2006).

25 Kanehisa, M. The KEGG database. *silico simulation of biological processes* **247**, 91-103 (2002).

26 Fahy, E. *et al.* Update of the LIPID MAPS comprehensive classification system for lipids. *Journal of lipid research* **50**, S9-S14 (2009).

27 Smith, C. A. *et al.* METLIN: a metabolite mass spectral database. *Therapeutic drug monitoring* **27**, 747-751 (2005).

28 Wold, S., Esbensen, K. & Geladi, P. Principal component analysis. *Chemometrics and intelligent laboratory systems* **2**, 37-52 (1987).

29 Westerhuis, J. A., van Velzen, E. J., Hoefsloot, H. C. & Smilde, A. K. Multivariate paired data analysis: multilevel PLSDA versus OPLSDA. *Metabolomics* **6**, 119-128 (2010).

30 Murphy, R. C. & Axelsen, P. H. Mass spectrometric analysis of long-chain lipids. *Mass spectrometry reviews* **30**, 579-599 (2011).

31 Farrell, E. K. *et al.* Primary fatty acid amide metabolism: conversion of fatty acids and an ethanolamine in N18TG2 and SCP cells. *Journal of lipid research* **53**, 247-256 (2012).

32 Divito, E. B. & Cascio, M. Metabolism, Physiology, and Analyses of Primary Fatty Acid Amides. *Chemical Reviews* **113**, 7343-7353, doi:10.1021/cr300363b (2013).

33 Sugiura, T. *et al.* Enzymatic synthesis of oleamide (cis-9, 10-octadecenoamide), an endogenous sleep-inducing lipid, by rat brain microsomes. *IUBMB Life* **40**, 931-938 (1996).

34 Benson, A. in *Advances in lipid research* Vol. 1 387-394 (Elsevier, 1963).

35 Harwood, J. in *Lipids: Structure and Function* 301-320 (Elsevier, 1980).

36 Devaiah, S. P. *et al.* Quantitative profiling of polar glycerolipid species from organs of wild-type Arabidopsis and a PHOSPHOLIPASE Dα1 knockout mutant. *Phytochemistry* **67**, 1907-1924 (2006).

37 De Kok, L. J., Abrol, Y. P. and Ahmad, A. Sulphur in plants. *Ann Bot* **93**, 343-343, doi:10.1093/aob/mch047 (2004).

38 Krebs, H. & Eggleston, L. Metabolism of acetoacetic acid in animal tissues. *Nature* **154**, 209-210 (1944).

39 Wakil, S. J. A malonic acid derivative as an intermediate in fatty acid synthesis. *Journal of the American Chemical Society* **80**, 6465-6465 (1958).

CHAPTER 5: CONCLUSIONS, IMPACT, AND OUTLOOK

5.1 Abstract

The primary focus of this thesis centers around the examination of lipids to aid in the diagnosis, prognosis, and mechanistic understanding of traumatic brain injury (TBI). Lipids are important signaling molecules and play a critical role in energy storage as well as membrane structure and organization. Using mass spectrometry (MS) based methods to perform non-targeted metabolomic experiments with a focus on extraction of lipid metabolites, a rodent model is investigated to explore the feasibility of developing lipid biomarker panels to classify injury post-hoc across multiple severities. The developed methods are then used to study another biological system in order to show the broad applicability of lipidomics by investigating the effect of *Karenia brevis* allelopathy on two phytoplankton competitors. Additionally, suggestions for potential future directions of the projects and improvements upon experimental limitations are included within this chapter.

5.2 Use of High-Resolution Mass Spectrometric Metabolomics to Determine Lipidome Alterations Following Traumatic Brain Injury of Differential Severity

5.2.1 Summary of Accomplishments

In order to measure the changes in relative abundances of circulating serum lipids resulting from the induction of TBI in rats, a CCI device was used to generate moderate TBI in rats. A subsequent study utilized the same techniques to detect differences in

serum abundances in the setting of mTBI. Protocols for the extraction of serum lipids were established and multivariate modeling techniques were used to classify TBI and to discover potential novel biomarker candidates of TBI. The developed LC-MS methods were used to separate, detect, identify and provide relative quantification for many unique lipid metabolites that may ultimately serve as biomarkers of TBI.

In the first study, thirty-four animals weighing 300-400 g were randomly assigned to the following groups: (1) naïve (n=10), (2) sham-operated (n= 8; n=4, 3 days post-surgery; n=4, 7 days post-surgery), and (3) controlled cortical TBI (TBI, n= 16; n=7, 3 days post-injury; n=9, 7 days post-injury). A panel of 26 metabolites was created using omniClassifier to conduct rigorous feature selection across four unique classifiers (Bayesian, K-nearest neighbors, logistic regression and support vector machines), which performed classification of injured vs. non-injured samples with 85% accuracy.[1] Both inner and outer cross-validation were utilized to avoid overfitting. Using the same 26-feature model, binary comparisons of sham-operated vs TBI and naïve vs. TBI each performed with greater than 90% accuracy, indicating that the serum lipidome alterations were associated directly with injury and were not attributable to another confounding factor. Some minor differences in lipid abundances existed between the 3- and 7- day timepoints, though injury was the main discriminating factor, not time of sampling.

Several trends could be observed based on the classes of lipids selected for inclusion in the multivariate classification panel. Increases in all measured and identified FFAs such as AA, DHA and EPA as well as corresponding decreases in a variety of membrane phospholipids such as PE(20:4_16:0), PE(18:0_22:4), and PC(20:2_18:0) were observed. These changes were likely the result of the activation of phospholipase

A_2, which causes the liberation of AA, DHA, EPA and other FFAs from membrane phospholipids. An increase in DGs was also observed, specifically those containing PUFA residues (22:6 or 20:4). TBI is known to stimulate the activation of phospholipases C and D, resulting in increased abundances of PUFA-containing DGs.[2] Finally, the relative concentration of cholesterol sulfate (CS), a unique metabolite in the cholesterol and steroid hormone biosynthesis pathway, was decreased following induction of TBI.

A follow-up study was conducted to determine how the severity of injury affected serum lipidome alterations stemming from mTBI. Using a closed-head injury model, the same CCI device was used to induce mTBI in another cohort of adult male Sprague-Dawley rats using a matched pair study design (n=30). A separate multivariate classification panel was generated to distinguish between mTBI and control samples, which performed with an accuracy of 88.5%, sensitivity of 87.5%, and specificity of 89.5%. While the majority of features selected within the two classification panels were different, CS was selected as a novel biomarker of injury in both studies of mild and moderate TBI, displaying a significant decrease in the TBI cohort.

5.2.2 Moving Forward

The work presented in chapters 2 and 3 demonstrates the utility of lipids as biomarkers for the detection of TBI in the serum of rodents across multiple injury severities. Additional studies are warranted to independently validate the proposed biomarkers and to address several limitations within the design of experiments. The following studies are recommended in order to fully characterize the lipidomic alterations stemming from TBI:

1. The work contained within this thesis focused on the development of a lipid-based biomarker panel for the diagnosis of TBI in a homogeneous cohort of adult male Sprague-Dawley rats. While the use of this population minimized the number of independent variables being examined experimentally, it did not capture the heterogeneity of the population incurring TBI clinically. Future studies must consider how the lipidomic response to TBI varies based on sex, strain, and age of the animals to account for inherent population heterogeneity. Additionally, the use of orthopedic controls (i.e. musculoskeletal injuries), or control subjects with injuries to tissues other than the brain, is needed to demonstrate whether the alterations in serum lipids associated with TBI stem from biochemical changes within the brain or general inflammation.[3]

2. While it has been demonstrated that the abundances of certain lipid species are altered following TBI, this association does not indicate the source (i.e. brain or peripheral tissues) of these biochemical changes. For example, if the source was the brain molecules would have to exit the brain to be detectable in the blood. The BBB normally acts to prevent diffusion of molecules between the brain and the blood, but this membrane has been shown to be disrupted, particularly in the case of severe TBI.[4] Increased permeability of the BBB has also been shown in cases of mTBI, though such changes are often much shorter in duration.[5] Additionally, lipophilic molecules may diffuse through an intact BBB, though proteins require alternative transport mechanisms for the clearance of molecular effectors into systemic circulation.[6,7]

Lacking lymphatic circulation, the brain instead possesses a glial lymphatic (glymphatic) system, which has recently been investigated as a means of clearance for proteins.[8] Therefore, future studies must investigate the nature of efflux of potential

biomarkers of TBI in order to determine whether their clearance is *via* BBB-only transport or potentially through multiple efflux routes.[9] For example, pilot studies were conducted in which injection of small volumes of AlexaFluor594 dye, a small fluorescent tracer, into the lateral ventricle, were subsequently detected in the blood 30 min after injection using high resolution MS. While these experiments demonstrated the utility of this approach to examine efflux of surrogate biomarkers, they must be further expanded upon. We have also examined tracer efflux using IR imaging of lymph and peripheral circulation, which allows us to measure the kinetics of tracers and determine if the route is brain to lymph to blood, or directly into the blood. Alexis Pulliam, a graduate student in Dr. LaPlaca's research group, has begun experiments investigating the glymphatic system as a potential clearance route for molecules from the brain. Determining the major efflux pathways of lipid effectors from the brain to blood would help to establish how these markers reach systemic circulation and aid in questions regarding specificity.

In order to determine the efflux routes for biomarker clearance, the sampling of different biological fluids must be incorporated into the experimental design. Measuring the concentrations of biomarkers, or specified molecular effectors that model biomarker candidates, in CSF, interstitial fluid (ISF), saliva, urine and blood could enable the development of a closed-system model accounting for total lipid metabolism.

3. A variety of time-points were sampled throughout the presented studies. Serum lipid profiles measured at both 3- and 7- days following moderate injury were each easily distinguished from control samples. The study of mTBI showed that changes in lipid abundances were present as early as 24 h post injury. Future work must demonstrate how the differences in lipid abundances vary based on the time-point sampled post-injury.

Additionally, more detailed temporal profiles should be generated to determine the earliest time at which TBI can be objectively diagnosed using either the proposed panel of biomarkers or a similar, independently validated set of biomarkers. Thus, serial sampling at regular intervals such as 1 h, 6 h, 24 h, 72 h, and 168 h post-injury would aid in biochemically determining the optimal time to measure specific biomarkers for the diagnosis and tracking of recovery from injury, such as when the difference between control and injured samples is the greatest and when levels return to baseline. In order to conduct such experiments, blood vessel cannulation can be used to avoid multiple needle entries into a single site to minimize pain and stress in the animals.[10] This method also improves reproducibility of blood collection and accurately limits the volume of blood collected to levels within guidelines set forth by the National Institutes of Health.[11,12,13,14] The metabolism of the detected substances must also be considered to account for molecular degradation, processing, diffusion or excretion, which may mask primary biochemical changes.

4. While major research efforts have focused on determining the pathophysiological response to single impact injury as previously discussed, outcomes stemming from repeated blows to the head can be even more devastating.[15,16] It is well known that boxers suffer from progressive neurological deterioration as a result of repetitive brain trauma.[17,18] Buildup of diffuse amyloid plaques are a hallmark of this disease, now referred to as CTE.[19] CTE has been associated with mood and behavioral changes, memory impairment and Parkinsonism, as well as speech and gait abnormalities.[20] Additionally, CTE develops in at least 17% of individuals who suffer from repeated mTBIs.[21] While advanced imaging techniques may aid in the detection of Aβ plaques,

autopsy is still required to confirm diagnosis of CTE.[22] Approaches such as those described in this thesis may be useful to study the progression of neurological dysfunction by examining lipid alterations as a potential component of underlying mechanisms that may lead to neurodegeneration stemming from repetitive concussive or subconcussive events.

MALDI-MS utilizes the energy of a laser to induce ionization of molecular targets co-crystallized with an energy absorbing matrix with minimal fragmentation. The advent of the RapifleX MALDI Tissue-typer (Bruker Daltonics) instrument has substantially reduced anticipated analysis time, minimizing time needed to for sample acquisition through the introduction of a high frequency 10,000 Hz laser. To this end, we have initiated the use of MALDI-MS to rapidly assess the entire brain of injured rats and reconstruct a 3D image using the lipid distribution acquired during analysis in an effort to understand the pathophysiology of repeated impacts to the head, which commonly occur during practice sessions in the days following sporting events. Time-matched sham animals will be used to examine differences in the brain lipidome resulting from either single impact injury or repeat (5x) injury while controlling for duration of anesthesia exposure. Many of the necessary methods, including matrix deposition and MS acquisition setting optimization are being developed using 2D image generation. Dr. Clint Alfaro, a post-doc in the Fernandez research group, and Eric Gier, a graduate student, have begun experiments to investigate the alterations in lipids directly in brain tissue using the Bruker RapifleX instrument for speed of acquisition and potential for 3D imaging, while a SolariX 12 Tesla FT-ICR (Bruker Daltonics) instrument will be used to provide enhanced resolution of biochemical species being investigated.

5.2.3 Limitations of the Current Work

A few limitations of the experiments conducted should be acknowledged. Best practice protocols for LC-MS based non-targeted lipidomics experiments include a spiked internal standard (IS) to provide a reference for quantification of lipid metabolites.[23] While it would be impractical to include a standard for each of the thousands of individual compounds being analyzed simultaneously, one or more standards per lipid class expected should be spiked into the samples at levels approximating endogenous concentrations during each stage of sample processing. To quantify lipids, it is a common practice to normalize the individual molecular ion-peak intensities using an IS for each lipid class. The calculated ratio of analyte and IS is then multiplied by the concentration of the IS to obtain the concentration of a particular analyte. The IS must be included prior to sample extraction to accurately measure concentrations in blood while correcting for extraction efficiency of the lipids.[24,25] While typical ESI-MS instruments cover 3-4 orders of magnitude, the lipid concentrations can vary in tissue by 10^{12} or more (from millimolar levels of TGs to attomolar concentrations of eicosanoids).[26,27] Additionally, species in non-polar lipid classes and other neural lipids (e.g., CEs, DGs, TGs, etc.) do not have a dominant ionizable head group. Species in these lipid classes do not exhibit identical response factors even in a very low concentration region.[28] For accurate quantification, response factors of individual non-polar species must be pre-determined in relation to their acyl chain length and unsaturation.

The use of a two-phase extraction such as the Bligh and Dyer (BDE) or Folch extraction may be warranted in order to analyze all lipid subtypes for discovery studies, though these experiments may be limited by throughput due to the involvement of

multiple steps in the extraction protocol.[29,30] In 2008, Matyash et al. introduced a novel sample-extraction procedure employing MTBE as an alternative solvent to chloroform.[31] The method involves addition of MeOH and MTBE (1.5:5, *v*/*v*) to the sample and followed by phase separation induced by adding water. The advantage of MTBE extraction over conventional two-phase chloroform-containing solvent systems comes from the low density of the lipid-containing organic phase that forms the upper layer during phase separation, greatly simplifying collection and minimizing sample loss. Furthermore, compared with chloroform, MTBE is non-toxic and non-carcinogenic, which reduces the environmental burden as well as the health risks for exposed personnel.[32]

Additionally, one potential limitation of the studies may stem from a bias towards the detection of the easily ionizable phospholipids such as PCs and PEs, which will suppress the ionization of less abundant lipid classes.[33] These low abundance lipids, including but not limited to eicosanoids, phosphoinositol phosphates, prostaglandins and backbone sphingolipid molecules, are often signaling molecules or metabolites of more abundant lipids.[34,35] Similar issues arise when detecting CLs due to their localization within the mitochondrial membrane.[36] The accurate detection and quantification of these low abundance lipids would lead to a more comprehensive assessment of changes in the global lipidome, specifically for a variety of lipid classes which hold promise for TBI biomarker research. Furthermore, the use of non-polar solvents such as IPA is well suited for the extraction of hydrophobic lipids including FFAs, TGs, and CEs, though more polar lipids such as PIs and sulfatides are better extracted with other solvent systems.[31] Additionally, gangliosides, unlike the majority of all other lipids, are soluble in aqueous

environments, so the use of a biphasic extraction and subsequent analysis of both fractions may be necessary for the determination of all relevant changes in the biological system of interest.[37] These factors must be considered when designing non-targeted lipidomics experiments in order to accurately assess all possible metabolic pathways that may be disrupted in association with disease onset and progression.

Additionally, a number of the proposed lipid biomarker candidates, such as DGs, TGs and CEs, could be influenced by dietary intake. An overall decrease in food intake following blast TBI has been observed previously.[38] Additionally, we conducted a study showing that food intake is decreased in rodents following repetitive injury, though the differences were most pronounced in the first day following injury and results were not significant given the small sample size. Nevertheless, studies involving overnight fasted animals are recommended to definitively demonstrate that changes in circulating lipids are primarily the result of injury status rather than simply associated with changes in food intake. Similarly, the minor effect of mTBI on the serum lipidome could be confounded by a number of variables such as the previously discussed anesthesia duration, location of blood draw and circadian variation in circulating lipids.[39,40] Controlling for these variables will be a critical aspect of future experimental design.

Ultimately, the research into lipid biomarkers of TBI must be translated clinically through the use of human samples. While rats commonly serve as pre-clinical models for TBI, there are a number of fundamental differences between rats and humans. The biggest distinction between rat and human brains is based on size differences. Humans brains are large (1300 g), have increased cortical size due to the development of language skills and thus possess sulci or gyri for increased surface area.[41] However, rat brains are

much smaller (~2 g), are lissencephalic and possess little white matter, which contains more than double the mass content of lipids relative to proteins compared to grey matter.[42] The human brain also expresses a much larger number of genes and encodes more complex DNA.[43] Due to these inherent differences, and difference in the lipid composition of the brains of humans and rodents, it is expected that a novel set of biomarkers will be required for the accurate classification of brain injury in human samples.

The field of lipidomics is rapidly expanding and offers unique insight into pathophysiological changes associated with disease states such as TBI. The use of lipidomics for the discovery of novel biomarkers of TBI fills a gap within the literature, which has to date yet to effectively diagnose mTBI by objective measures and relies heavily on the presence of self-reported symptoms. Comparison of proposed lipid biomarkers with the gold standard protein biomarkers such as GFAP, NSE and UCH-L1, among others, is needed to build off current literature. This would allow for the introduction of combined lipid and protein biomarker panel for the purposes of injury diagnosis, prognosis of outcome, and response to treatment for TBI. The use of NP testing, advanced imaging modalities, and other related measures have also proven effective in adding objectivity to mTBI diagnosis. In the future, it is likely that a diagnostic tool combining multiple biochemical and pathophysiological detection modalities may be the only proper solution to address such a complex problem.

5.3 *Karenia brevis* Allelopathy Compromises the Lipidome, Membrane Integrity, and Photosynthetic Efficiency of Competitors

5.3.1 Summary of Accomplishments

The same analytical methods used to study TBI lipidomics can also be used to understand different biological systems, such as the response of phytoplankton competitors to exposure to the red-tide forming dinoflagellate, *Karenia brevis*. We aimed to study the effects of *K. brevis* allelopathy on the lipidomes of two different phytoplankton competitors: *Asterionellopsis glacialis* and *Thalassiosira pseudonana*, using NMR spectroscopy and MS-based metabolomics. Both species are phytoplankton competitors, though only *A. glacialis* co-exists in nature with *K. brevis* in the Gulf of Mexico. Likely due to a developed resistance to *K. brevis* allelopathy, *A. glacialis* maintained a more robust metabolism following exposure whereas *T. pseudonana* exhibited significant alterations in lipid synthesis, cell membrane integrity, and photosynthetic activity.

MS-based metabolomics analysis of phytoplankton lipidomes led to the identification of 80 distinct lipid metabolites whose concentrations differed significantly in *T. pseudonana* following exposure to *K. brevis* allelopathy. These 80 metabolites represent nine major lipid classes, of which members of five (PCs, SQDGs, MGDGs, DGDGs, and PGs) were generally less abundant when *T. pseudonana* was subjected to *K. brevis* allelopathy, whereas members of four classes (non-SQDG sulfonated lipids, FFAs, PFAAs, and PEs) were generally more abundant. Multivariate models generated using oPLS-DA were capable of differentiating *T. pseudonana* treatment samples from controls with 100% accuracy, with latent variable 1 explaining nearly 80% of the between class

variance, using only these features. In contrast, for the other competitor, *A. glacialis*, concentrations of only six metabolites were significantly affected by allelopathy. Similar multivariate modeling approaches were still capable of differentiating *A. glacialis* treatment samples from controls, albeit with lower accuracy (88%) and LV1 explaining only 21% of the between class variance, reinforcing the hypothesis that *A. glacialis* maintains a more robust metabolism in response to *K. brevis* allelopathy due to an evolved resistance stemming from prior co-habitation.

A majority of lipids formed (PFAA, FFA, and SULF) by allelopathic exposure are either metabolic breakdown products or metabolic precursors of PCs and SQDGs. These findings suggest that A) the stress of allelopathic exposure leads to the degradation of complex lipids into their less complex components; or, B) allelopathic compounds exuded by *K. brevis* inhibit the biosynthetic enzymes within *T. pseudonana* that are responsible for the anabolic synthesis of complex lipids from more simple building blocks, resulting in a build-up of biosynthetic precursors (PFAA, FFA) and a loss of more complex lipids (SQDG, PC).

Globally, concentrations of membrane-associated lipids (MGDG, DGDG, SQDG, PC) were significantly suppressed for *T. pseudonana* exposed to allelopathy, leading membranes of living cells to become more permeable and therefore damaged. Increased membrane permeability as well as decreased photosynthetic capability both likely evolved due to decreases in the concentrations of membrane- and thylakoid-associated lipids. *K. brevis* allelopathy appears to target lipid biosynthesis affecting multiple physiological pathways suggesting that exuded compounds have the ability to significantly alter competitor physiology, giving *K. brevis* an edge over sensitive species.

5.3.2 Moving Forward

The identification of a number of the lipid metabolites observed in this study was aided by the use of the LOBSTAHS databases, which was based on exposure of the *Phaeodactylum tricornutum* diatom to oxidative stress.[44] To fully annotate the lipids of interest, similar software should be developed for the marine diatoms being studied. Additionally, most diatoms have no pattern of co-occurrence with *K. brevis* and the response of each unique species can be compared to that of a number of marine phytoplankton competitors which do co-occur with *K. brevis*, such as *Skeletonema grethae, Odontella aurita, and Stephanopyxis turris*, and may therefore have developed a similar pattern of resistance to allelopathic effects.[45] Such experiments would enable the determination of whether the described patterns of lipid dysregulation are common to phytoplankton or are species specific. This represents just one such application of lipidomics, which can be broadly applied to any biological system utilizing lipids as an energy source to solve a number of other related biological questions, such as determination of health and stability of the marine ecosystem in a variety of other contexts.[46]

5.4 References

1 Hogan, S. R. *et al.* Discovery of Lipidome Alterations Following Traumatic Brain Injury via High-Resolution Metabolomics. *Journal of proteome research* **17**, 2131-2143 (2018).

2 Tang, X., Edwards, E. M., Holmes, B. B., Falck, J. R. & Campbell, W. B. Role of phospholipase C and diacylglyceride lipase pathway in arachidonic acid release and acetylcholine-induced vascular relaxation in rabbit aorta. *Am J Physiol Heart Circ Physiol* **290**, H37-45, doi:10.1152/ajpheart.00491.2005 (2006).

3 Beauchamp, M. H., Landry-Roy, C., Gravel, J., Beaudoin, C. & Bernier, A. Should young children with traumatic brain injury be compared with community or orthopedic control participants? *Journal of neurotrauma* **34**, 2545-2552 (2017).

4 Saw, M. M. *et al.* Differential disruption of blood–brain barrier in severe traumatic brain injury. *Neurocritical care* **20**, 209-216 (2014).

5 Sahyouni, R., Gutierrez, P., Gold, E., Robertson, R. T. & Cummings, B. J. Effects of concussion on the blood–brain barrier in humans and rodents. *Journal of concussion* **1**, 2059700216684518 (2017).

6 Liu, X., Tu, M., Kelly, R. S., Chen, C. & Smith, B. J. Development of a computational approach to predict blood-brain barrier permeability. *Drug metabolism and disposition* **32**, 132-139 (2004).

7 Abbott, N. J., Patabendige, A. A., Dolman, D. E., Yusof, S. R. & Begley, D. J. Structure and function of the blood–brain barrier. *Neurobiology of disease* **37**, 13-25 (2010).

8 Iliff, J. J. *et al.* A paravascular pathway facilitates CSF flow through the brain parenchyma and the clearance of interstitial solutes, including amyloid β. *Science translational medicine* **4**, 147ra111-147ra111 (2012).

9 Plog, B. A. *et al.* Biomarkers of traumatic injury are transported from brain to blood via the glymphatic system. *Journal of Neuroscience* **35**, 518-526 (2015).

10 Upton, R. A. Simple and Reliable Method for Serial Sampling of Blood from Rats. *Journal of Pharmaceutical Sciences* **64**, 112-114, (1975).

11 Lee, G. & Goosens, K. A. Sampling blood from the lateral tail vein of the rat. *JoVE (Journal of Visualized Experiments)*, e52766 (2015).

12 Natali, R., Wand, C., Doyle, K. & Noguez, J. H. Evaluation of a new venous catheter blood draw device and its impact on specimen hemolysis rates. *Practical laboratory medicine* **10**, 38-43 (2018).

13 Diehl, K. H. *et al.* A good practice guide to the administration of substances and removal of blood, including routes and volumes. *Journal of Applied Toxicology: An International Journal* **21**, 15-23 (2001).

14 National Institutes of Health. "Guidelines for survival bleeding of mice and rats." (2012).

15 Prins, M. L., Alexander, D., Giza, C. C. & Hovda, D. A. Repeated mild traumatic brain injury: mechanisms of cerebral vulnerability. *Journal of neurotrauma* **30**, 30-38 (2013).

16 Weil, Z. M., Gaier, K. R. & Karelina, K. Injury timing alters metabolic, inflammatory and functional outcomes following repeated mild traumatic brain injury. *Neurobiology of disease* **70**, 108-116 (2014).

17 Neselius, S. *et al.* CSF-biomarkers in Olympic boxing: diagnosis and effects of repetitive head trauma. *PloS one* **7**, e33606 (2012).

18 Jordan, B.D. "Chronic traumatic brain injury associated with boxing." *Seminars in neurology* **20**, 179-186 (2000).

19 Omalu, B. I. *et al.* Chronic traumatic encephalopathy in a National Football League player. *Neurosurgery* **57**, 128-134 (2005).

20 McKee, A. C. *et al.* Chronic traumatic encephalopathy in athletes: progressive tauopathy after repetitive head injury. *Journal of Neuropathology & Experimental Neurology* **68**, 709-735 (2009).

21 Roberts, G. W., Allsop, D. & Bruton, C. The occult aftermath of boxing. *Journal of Neurology, Neurosurgery & Psychiatry* **53**, 373-378 (1990).

22 Mathis, C., Wang, Y. & Klunk, W. Imaging β-amyloid plaques and neurofibrillary tangles in the aging human brain. *Current pharmaceutical design* **10**, 1469-1492 (2004).

23 Cajka, T., Smilowitz, J. T. & Fiehn, O. Validating quantitative untargeted Lipidomics across nine liquid chromatography–high-resolution mass spectrometry platforms. *Analytical chemistry* **89**, 12360-12368 (2017).

24 Lam, S. M., Tian, H. & Shui, G. Lipidomics, en route to accurate quantitation. *Biochimica et Biophysica Acta (BBA)-Molecular and Cell Biology of Lipids* **1862**, 752-761 (2017).

25 Wang, M., Wang, C. & Han, X. Selection of internal standards for accurate quantification of complex lipid species in biological extracts by electrospray ionization mass spectrometry—What, how and why? *Mass spectrometry reviews* **36**, 693-714 (2017).

26 Cajka, T. & Fiehn, O. Comprehensive analysis of lipids in biological systems by liquid chromatography-mass spectrometry. *TrAC Trends in Analytical Chemistry* **61**, 192-206 (2014).

27 Astarita, G. & Yu, K. New frontiers for mass spectrometry in lipidomics, part II. *LC GC North America* **30** (2012).

28 Yang, K. & Han, X. Accurate quantification of lipid species by electrospray ionization mass spectrometry—meets a key challenge in lipidomics. *Metabolites* **1**, 21-40 (2011).

29 Bligh, E. & Dyer, W. A rapid method of total lipid extraction and purification. *Can. J. Biochem. Physiol* **37**, 911-917 (1959).

30 Folch, J., Lees, M. & Stanley, G. S. A simple method for the isolation and purification of total lipides from animal tissues. *Journal of biological chemistry* **226**, 497-509 (1957).

31 Matyash, V., Liebisch, G., Kurzchalia, T. V., Shevchenko, A. & Schwudke, D. Lipid extraction by methyl-tert-butyl ether for high-throughput lipidomics. *Journal of lipid research* **49**, 1137-1146 (2008).

32 Greim, H. & Reuter, U. Classification of carcinogenic chemicals in the work area by the German MAK Commission: current examples for the new categories. *Toxicology* **166**, 11-23 (2001).

33 Reis, Ana, et al. "A comparison of five lipid extraction solvent systems for lipidomic studies of human LDL." *Journal of lipid research* 54.7 (2013): 1812-1824.

34 Tumanov, Sergey, and Jurre J. Kamphorst. "Recent advances in expanding the coverage of the lipidome." *Current opinion in biotechnology* 43 (2017): 127-133.

35 Merrill Jr, Alfred H., et al. "Sphingolipidomics: high-throughput, structure-specific, and quantitative analysis of sphingolipids by liquid chromatography tandem mass spectrometry." *Methods* 36.2 (2005): 207-224.

36 Cheng, H. *et al.* Shotgun Lipidomics Reveals the Temporally Dependent, Highly Diversified Cardiolipin Profile in the Mammalian Brain: Temporally Coordinated Postnatal Diversification of Cardiolipin Molecular Species with Neuronal Remodeling. *Biochemistry* **47**, 5869-5880 (2008).

37 Kolter T. Ganglioside biochemistry. *ISRN biochemistry*, *2012*, 506160. doi:10.5402/2012/506160.

38 Bauman, R. A., Elsayed, N., Petras, J. M. & Widholm, J. Exposure to sublethal blast overpressure reduces the food intake and exercise performance of rats. *Toxicology* **121**, 65-79, doi: https://doi.org/10.1016/S0300-483X(97)03656-1 (1997).

39 Morgan, L., Hampton, S., Gibbs, M. & Arendt, J. Circadian aspects of postprandial metabolism. *Chronobiology international* **20**, 795-808 (2003).

40 Rivera-Coll, A., Fuentes-Arderiu, X. & Díez-Noguera, A. Circadian rhythmic variations in serum concentrations of clinically important lipids. *Clinical chemistry* **40**, 1549-1553 (1994).

41 Blinkov, S. M. & Glezer, I. i. a. I. *The human brain in figures and tables: a quantitative handbook.* (Basic Books, 1968).

42 Ventura-Antunes, L., Mota, B. & Herculano-Houzel, S. Different scaling of white matter volume, cortical connectivity, and gyrification across rodent and primate brains. *Frontiers in neuroanatomy* **7**, 3 (2013).

43 Consortium, R. G. S. P. Genome sequence of the Brown Norway rat yields insights into mammalian evolution. *Nature* **428**, 493 (2004).

44 Collins, J. R., Edwards, B. R., Fredricks, H. F. & Van Mooy, B. A. LOBSTAHS: an adduct-based lipidomics strategy for discovery and identification of oxidative stress biomarkers. *Analytical chemistry* **88**, 7154-7162 (2016).

45 Poulson-Ellestad, K., Mcmillan, E., Montoya, J. P. & Kubanek, J. Are offshore phytoplankton susceptible to Karenia brevis allelopathy? *Journal of plankton research* **36**, 1344-1356 (2014).

46 Parrish, C. C. Lipids in marine ecosystems. *ISRN Oceanography* (2013).

APPENDIX

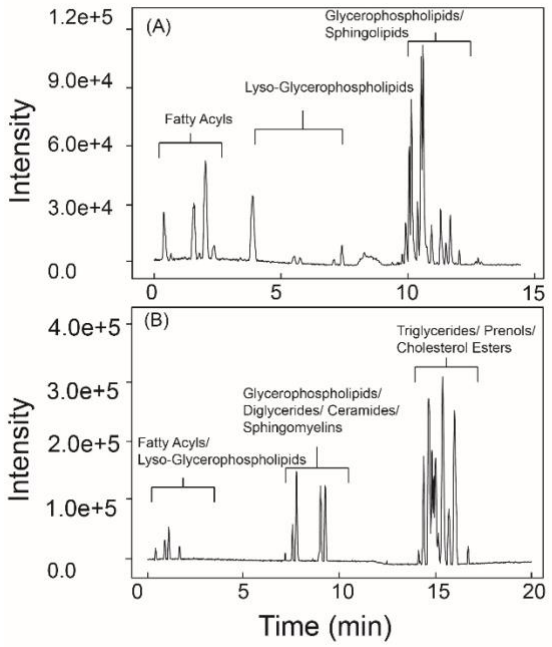

Figure A1: Lipid coverage following protein precipitation with isopropyl alcohol. Representative Base Peak Intensity (BPI) chromatograms for pooled serum samples from moderate TBI experiments analyzed in A) negative ion mode or B) positive ion mode. Common lipid classes observed are labeled by elution region.

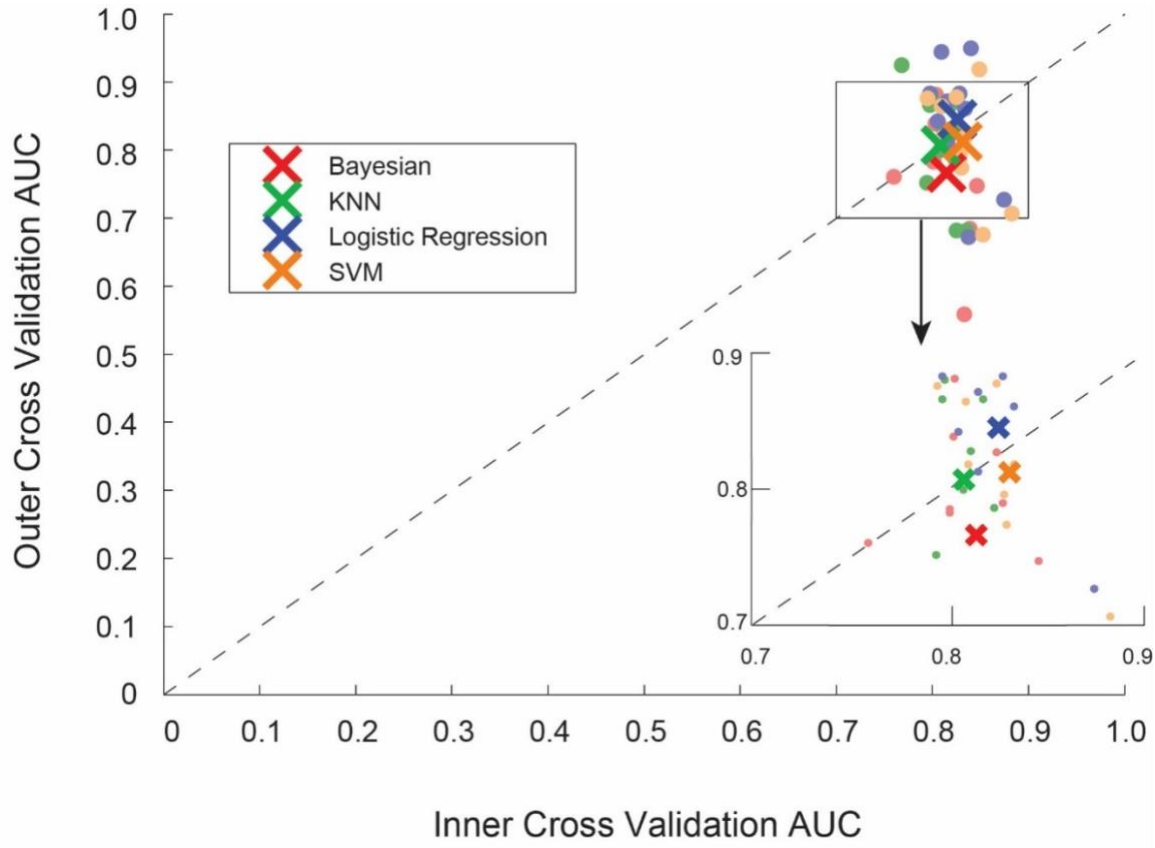

Figure A2: Estimated nested cross validation performance of TBI prediction modeling. Inner cross validation performance is similar to outer cross validation performance, meaning inner cross validation AUC is an unbiased estimate of outer cross validation AUC. Each point represents one iteration of cross validation. The large X's represent the average performance of each of the four classifiers. The region around 0.8 AUC is enlarged for clarity.

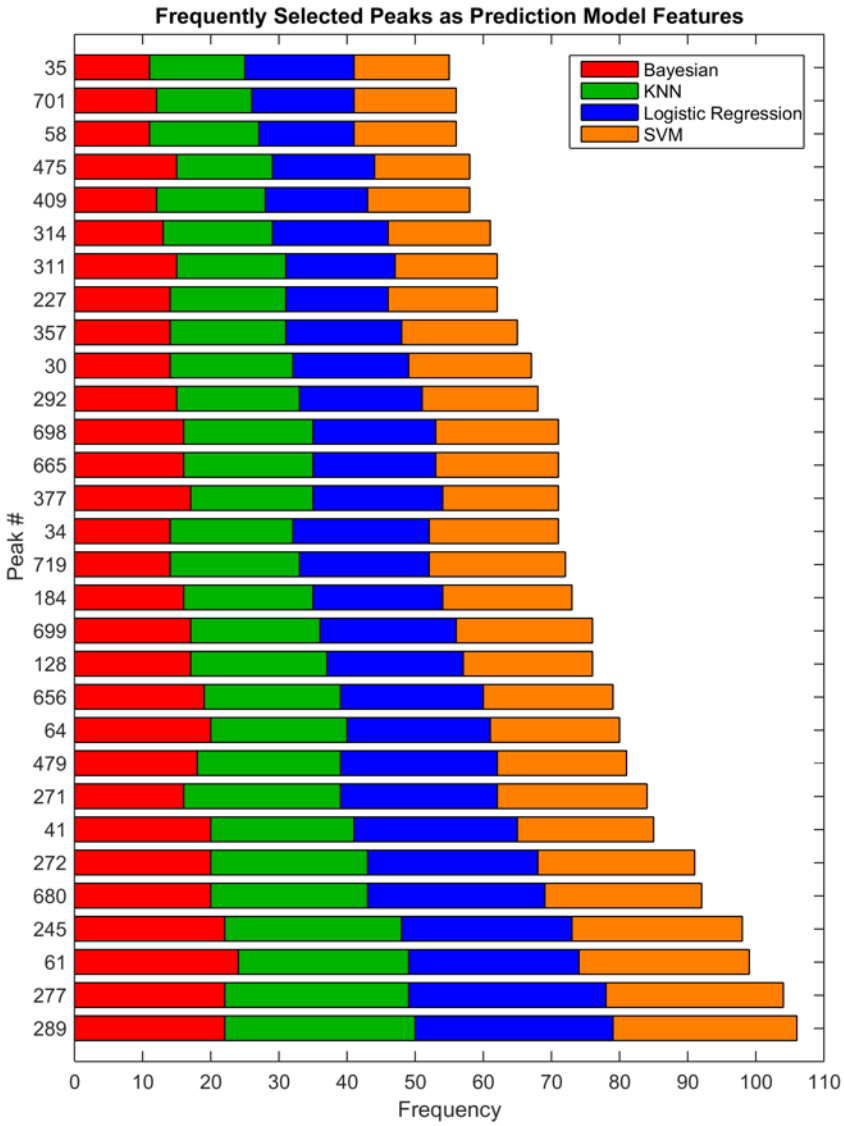

Figure A3: Most commonly selected features to build models for classification of moderate TBI sorted by frequency selected– 120 maximum. Features were selected to maximize variance between control and injury groups.

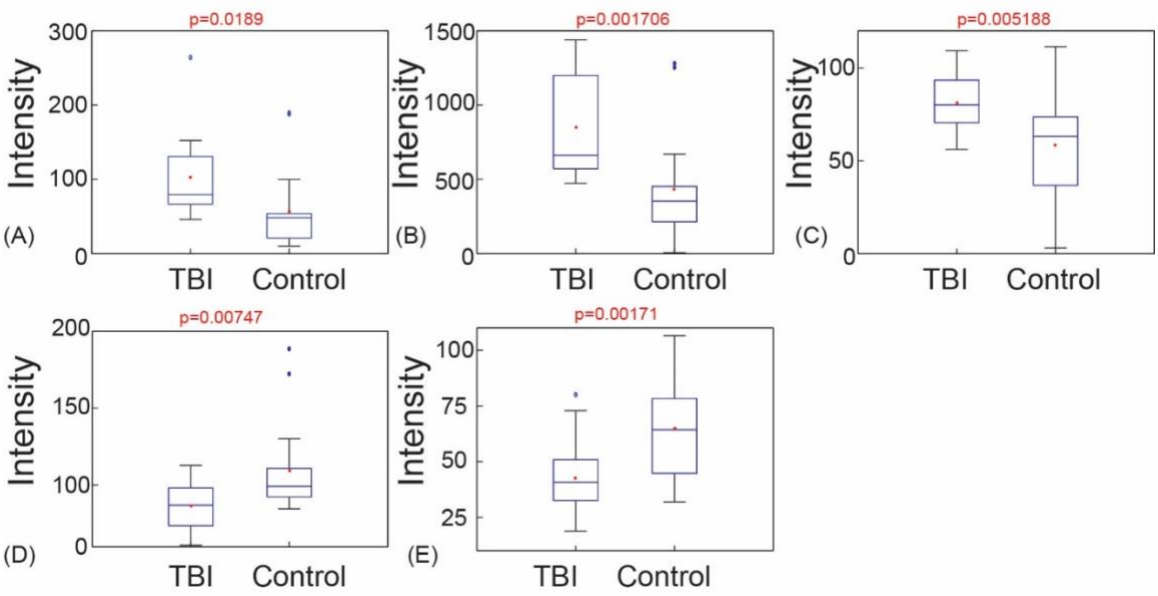

Figure A4: Box plots depicting alterations in features not contained in the 26-feature model for the classification of moderate TBI but that were still selected with high frequency by omniClassifier. A) eicosapentaenoic acid, $[M-H]^-$ = 301.217, #34; B) docosahexaenoic acid, $[M-H]^-$ =327.2322, #35; C) LysoPE(20:4), $[M-H]^-$ = 500.278, #227; D) PE(32:0), $[M-H]^-$ = 750.531, #30; E) PC(40:4), $[M+H]^+$ = 842.661, #475.

Table A1. Methods information. A) Chromatographic gradients for positive and negative mode separations: mobile phase A- water: acetonitrile (40:60) and mobile phase B- 10% acetonitrile in isopropyl alcohol, each with 10 mM ammonium formate and 0.1% formic acid additives; B) Summary of MS acquisition parameters.

A)

Negative Mode			Positive Mode		
Time (min)	**% A**	**% B**	**Time (min)**	**% A**	**% B**
0	95	5	0	70	30
1	95	5	1	70	30
3	90	10	3	60	40
5	80	20	5	54	46
6	58	42	6	52	48
10	26	74	10	45	55
11	10	90	11	30	70
12	0	100	15	26	74
14	0	100	18	0	100
			20	0	100

B)

	Negative mode	**Positive Mode**
Source capillary voltage	-2.0 kV	3.0 kV
Sampling cone voltage	30 V	40 V
Extraction cone voltage	3 V	4 V
Source temperature	90° C	80° C
Desolvation temperature	250° C	150° C
Desolvation gas flow rate	600 L/h	600 L/h
Cone gas flow rate	50	50

Table A2. Detailed chemical (MS/MS) characteristics of the panel of 26 metabolic features that distinguished moderate TBI from control samples**.** The fragment ions are listed in the table were obtained using the corresponding collision energy (CE). The ions selected for fragmentation are underlined. Each metabolite was identified according to the following four rigor levels: 1) identified compounds matched to authentic compound using standards (accurate mass, isotopic abundances, fragmentation spectrum and retention time matched); 2) putatively annotated compounds (accurate mass, isotopic abundances, and fragmentation spectrum matched to databases or consistent with expected fragmentation patterns); 3) putatively characterized compound classes (accurate mass matched to Lipid Maps, HMDB or Metlin database entry, and/or fragmentation showing a few matching characteristic fragment ions, such as lipid head group); and 4) unknown compound.

Feature ID	**CE (eV), instrument, polarity**	**Fragment Ion *m/z***	**Relative Intensity**	**Fragment Annotation**	**Specific Comments [ID level]**
24 PE(20:4_16:0)	40 V Xevo (−)	<u>738.5081</u> 482.2678 452.2884 434.2673 303.2396 255.2424 196.0369 140.0145 78.9637	0.10 0.01 0.10 0.02 1.00 0.58 0.04 0.07 0.04	[M – H]- NL FA 16:0 Loss of FA 20:4 as ketene NL FA 20:4 [FA 20:4 – H]- [FA 16:0 – H]- PE headgroup Ethanolamine phosphate [PO3]-	Consistent with predicted spectrum1 (Lipid Maps) - [2]
41 Arachidonic acid (AA)	20 V Xevo (−)	<u>303.2325</u> 285.2262 259.2401 231.2073 205.1944 177.1663 59.0131	1.00 0.02 0.14 0.01 0.05 0.01 0.13	[M – H]- [M – H – H_2O]- [M – H – CO_2]- - [$C_{15}H_{25}$]- - -	Consistent with Lipid Maps database entry [2]

Table A2 (continued).

58 Cer(d18:1_22:0)	HCD 30 QE HF (−)	666.6058 620.5979 590.5876 572.5766 380.352 364.3581 339.3264 321.3159 263.2377 237.2223	0.01 1.00 0.10 0.08 0.08 0.50 0.10 0.10 0.10 0.15	[M + HCO_2]- [M – H]- [M – HCHO]- [M – HCHO – H_2O]- NL 240.2 (sphingosine base) NL 256.2 (sphingosine base) [FA 22:0 – H]- [FA 22:0 – H_2O]- C_{18} sphingosine fragment C_{18} sphingosine fragment	Consistent with predicted spectrum (Lipid Maps) - [2]
61 Cholesterol sulfate (CS)	HCD 30 QE HF (-)	465.3042 407.2792 210.8419 96.9601	1.00 0.15 0.03 0.53	[M – H]- - - [HSO_4]-	Consistent with spectrum HMDB entry [2]
64 PC(20:2_18:0)	HCD 30 QE HF (−)	858.6259 798.6026 727.5843 554.2817 508.3405 391.2258 307.2643 283.2643 224.0694 168.0431 152.9959 78.9588	0.09 1.00 0.01 0.01 0.01 0.02 0.17 0.10 0.02 0.44 0.03 0.53	[M + HCO_2]- [M – CH_3]- Loss of Choline & HCO_2 - Loss of FA 20:2 as ketene - [FA 20:2 – H]- [FA 18:0 – H]- [GPC – CH_3 – H_2O]- Phosphocholine – CH_3 Glycerol-3-phosphate – H_2O [PO_3]-	Consistent with predicted spectrum (Lipid Maps) - [2]

Table A2 (continued).

103 PC(16:0_16:0)	HCD 30 QE HF (−)	778.5594 718.5397 480.3098 331.2643 255.2329 224.0693 168.0430 78.9588	0.03 0.18 0.04 0.10 1.00 0.01 0.03 0.03	[M + HCO_2]- [M – CH_3]- Loss of FA 16:0 as ketene - [FA 16:0 – H]- [GPC – CH_3 – H_2O]- Phosphocholine – CH_3 [PO_3]-	Consistent with predicted spectrum (Lipid Maps) [2]2
118 PE(18:2_18:0) PC(18:2_16:0)	HCD 30 QE HF (−)	742.5406 480.3097 283.2644 279.2332 196.0382 140.0121 78.9589 742.5397 480.3095 462.2993 279.2329 255.2330 224.0694 168.0430 152.958 78.9588	0.10 0.05 0.36 1.00 0.03 0.04 0.03 0.06 0.05 0.01 1.00 0.26 0.02 0.02 0.01 0.03	[M–H]- Loss of FA 18:2 as ketene [FA 18:0 – H]- [FA 18:2 – H]- PE headgroup Ethanolamine Phosphate [PO_3]- [M – CH_3]- Loss of FA 18:2 as ketene NL FA 18:2 – CH_3 [FA 18:2 – H]- [FA 16:0 – H]- [GPC – CH_3 – H_2O]- Phosphocholine – CH_3 Glycerol-3-phosphate – H_2O [PO_3]-	Consistent with predicted structure(s) (Lipid Maps) - [2]3

Table A2 (continued).

128 DG(22:6_18:1)	30 V Xevo (-)	711.5165 665.6251 268.8004 210.8417 152.8832 92.9277	0.01 0.01 0.25 0.15 0.14 1.00	$[M + HCO_2]^-$ $[M - H]^-$ - - - -	Accurate mass match (Lipid Maps) [2][4],*
129 $C_{43}H_{84}NO_8P$	HCD 30 QE HF (−)	818.5886 758.5708 494.3300 464.3144 446.3045 331.2643 303.2321 281.2485 279.2323 269.2487 255.2330 224.0692 168.0430 78.9588	0.01 0.36 0.03 0.05 0.02 0.05 0.36 1.00 0.40 0.38 0.12 0.03 0.04 0.05	$[M + HCO_2]^-$ $[M - CH_3]^-$ Loss of FA 18:1 as ketene Loss of FA 20:0 as ketene NL FA 20:0 – CH_3 [FA 22:4 – H]- [FA 20:4 – H]- [FA 18:1 – H]- [FA 18:0 – H]- [FA 17:0 – H]- [FA 16:0 – H]- $[GPC - CH_3 - H_2O]^-$ Phosphocholine – CH_3 $[PO_3]^-$	Consistent with multiple possible PC structures [3]
245 Not identified	HCD 30 QE HF (−)	262.9005 242.9865 222.9825 219.1391 183.1025	0.01 0.34 0.10 0.48 0.70	- - - - -	---- [4]

Table A2 (continued).

271 DG(22:6_18:2)	10 V Xevo (−)	709.5049 663.6487 549.5652 421.0892 263.0663 229.0138	1.00 0.05 0.10 0.07 0.04 0.02	$[M + HCO_2]^-$ $[M - H]^-$ - - - -	Accurate mass match (Lipid Maps) [2][5,*]
272 Docosapentaenoic acid (DPA)	20 V Xevo (−)	329.2468 311.2415 285.2573 259.1709 231.2135	1.00 0.15 0.30 0.05 0.10	$[M - H]^-$ $[M - H - H_2O]^-$ $[M - H - CO_2]^-$ - $[C_{17}H_{27}]^-$	Consistent with Lipid Maps database entry [2]
277 DG(20:4_18:1)	10 V Xevo (+)	660.5562 643.5270 625.5195 447.3466 361.2734 339.2891 287.2368 247.2419	0.05 1.00 0.38 0.10 0.20 0.40 0.05 0.12	$[M + NH_4]^+$ $[M + H]^+$ $[M + H - H_2O]^+$ - NL FA 18:1 + NH_3 NL FA 20:4 + NH_3 FA 20:4 $[RC=O]^+$ FA 18:1 $[RC=O]^+$ - H_2O	Consistent with predicted spectrum (Lipid Maps) - [2]*
289 FFA(18:0)	HCD 30 QE HF (−)	283.2642 265.1809 254.9863 242.9885 216.9892	1.00 0.03 0.04 0.02 0.05	$[M - H]^-$ $[M - H - H_2O]^-$ - - -	Consistent with spectrum HMDB entry [2]

Table A2 (continued).

292 Not identified	HCD 30 QE HF (−)	297.0981 255.1352 175.0247 121.0658 113.0244 102.9568 85.0293 75.0084 71.0135 59.0133	0.18 0.05 0.12 0.71 1.00 0.30 0.67 0.28 0.16 0.25	- - - - - - - - - -	--- [4]
314 FFA(18:2 + 1 O)	HCD 30 QE HF (−)	295.2269 277.2165 253.1188 223.1082 195.1384 171.1022 124.0400 94.0296	1.00 0.21 0.34 0.02 0.08 0.06 0.19 0.26	[M – H]- [M – H – H_2O]- [M – H – CO_2]- - - - - -	Accurate mass match (Lipid Maps) --- [3]
357 PE(18:0_22:4)	HCD 30 QE HF (−)	794.5697 528.3086 510.3400 331.2639 303.2324 283.2639 259.2428 224.0691 196.0369 168.0429 152.9957 78.9597	0.06 0.01 0.08 0.04 1.00 0.70 0.09 0.06 0.02 0.06 0.01 0.06	[M – H]- Loss of FA 18:0 as ketene NL FA 18:0 [FA 22:4 – H]- [FA 20:4 – H]- [FA 18:0 – H]- - [GPC – CH_3 – H_2O]- PE headgroup Phosphocholine – CH_3 Glycerol-3-phosphate – H_2O [PO_3]-	PE species matched to predicted spectrum [2], # PC species likely co-selected.

Table A2 (continued).

377 SM(d18:1/22:1)	HCD 30 QE HF (-)	829.6448 769.6223 449.3156 168.0430 78.9589	0.01 1.00 0.02 0.49 0.59	[M + HCO_2]- [M – CH_3]- Loss of FA 22:1 as ketene Phosphocholine – CH_3 [PO_3]-	Consistent with predicted spectrum (Lipid Maps) - [2], #
409 LysoPC(20:2)	HCD 30 QE HF (-)	592.3619 532.3398 307.2637 242.0794 224.0690 168.0426 152.9954 96.9599 78.9586	0.01 0.30 1.00 0.02 0.08 0.01 0.01 0.20 0.05	[M + HCO_2]- [M – CH_3]- [FA 20:2 – H]- Loss of FA 20:2 as ketene [GPC – CH_3 – H_2O]- Phosphocholine – CH_3 Glycerol-3-phosphate – H_2O [H_2PO_4]- [PO_3]-	Consistent with predicted spectrum (Lipid Maps) - [2], #
479 PS(16:0_20:4)	HCD 30 QE HF (−)	782.4981 695.4656 409.2355 391.2251 303.2324 279.2324 255.2328 196.0379 152.9957 140.0115 96.9697 78.9588	0.02 0.15 0.10 0.22 0.14 0.71 1.00 0.02 0.34 0.03 0.04 0.17	[M-H]- Loss of serine Loss of FA 20:4 as ketene NL FA 20:4 [FA 20:4 – H]- [FA 18:2 – H]- [FA 16:0 – H]- - Glycerol-3-phosphate – H_2O - [H_2PO_4]- [PO_3]-	Consistent with predicted spectrum (Lipid Maps) - [2], #

Table A2 (continued).

656 DG(22:6_18:1)	20 V Xevo (+)	684.5526 667.5300 385.2997 339.3150 311.2371 293.2271	0.01 0.05 0.17 1.00 0.08 0.05	$[M + NH_4]^+$ $[M + H]^+$ NL FA 18:1 + NH_3 NL FA 22:6 + NH_3 FA 22:6 $[RC=O]^+$ FA 22:6 $[RC=O]^+ - H_2O$	Consistent with predicted spectrum (Lipid Maps) - [2]
665 PC(18:1_15:0) PC(17:1_16:0)	HCD 30 QE HF (−)	790.5604 730.5388 506.3244 492.3086 480.3083 466.2934 281.2482 267.2326 255.2327 241.2170 224.0691 168.0427 78.9587	0.01 0.25 0.01 0.01 0.01 0.04 1.00 0.33 0.18 0.46 0.05 0.05 0.05	$[M + HCO_2]^-$ $[M - CH_3]^-$ Loss of FA 15:0 as ketene NL FA 18:1 NL FA 17:1 Loss of FA 18:1 as ketene $[FA\ 18:1 - H]^-$ $[FA\ 17:1 - H]^-$ $[FA\ 16:0 - H]^-$ $[FA\ 15:0 - H]^-$ $[GPC - CH_3 - H_2O]^-$ Phosphocholine – CH_3 $[PO_3]^-$	Consistent with multiple possible PC structures [2], #
680 DG(22:6_18:2)	20 V Xevo (+)	682.5402 665.4964 647.4899 385.2837 337.2716 311.2371 293.2271 263.2401 245.2193	0.02 0.10 0.05 0.18 1.00 0.10 0.10 0.10 0.05	$[M + NH_4]^+$ $[M + H]^+$ $[M + H - H_2O]^+$ NL FA 18:2 + NH_3 NL FA 22:6 + NH3 FA 22:6 $[RC=O]^+$ FA 22:6 $[RC=O]^+ - H_2O$ FA 18:2 $[RC=O]^+$ FA 18:2 $[RC=O]^+ - H_2O$	Consistent with predicted spectrum (Lipid Maps) - [2]

Table A2 (continued).

698 $C_{47}H_{84}NO_8P$	HCD 30 QE HF (-)	866.5910 806.5698 568.3400 520.3397 494.3244 329.2482 303.2324 295.2637 269.2483 259.2428 224.0691 168.0428 78.9587	0.05 0.40 0.01 0.10 0.05 0.30 1.00 0.70 0.22 0.10 0.08 0.10 0.07	$[M + HCO_2]^-$ $[M - CH_3]^-$ - Loss of FA 20:4 as ketene - $[FA\ 22:5 - H]^-$ $[FA\ 20:4 - H]^-$ $[FA\ 19:0 - H]^-$ $[FA\ 17:0 - H]^-$ $[C_{19}H_{32}]^-$ $[GPC - CH_3 - H_2O]^-$ Phosphocholine – CH_3 $[PO_3]^-$	Consistent with multiple possible PC structures [3], #
699 LysoPC(18:2 + 1 O)	HCD 30 QE HF (−)	582.3412 522.3202 420.5263 369.4939 304.6898 297.2235 224.0692 168.0430	0.01 0.90 0.05 0.05 0.41 1.00 0.12 0.05	$[M + HCO_2]^-$ $[M - CH_3]^-$ - - - $[FA\ 18:2 + 1\ O - H]^-$ $[GPC - CH_3 - H_2O]^-$ Phosphocholine – CH_3	Consistent with predicted spectrum. Fragment matched to feature #314 [2], #
719 PC(18:2_22:1)	HCD 30 QE HF (−)	884.6381 824.6166 562.3865 544.3866 337.3108 279.2325 224.0690 168.0428 96.9600	0.01 0.20 0.05 0.02 0.42 1.00 0.03 0.03 0.06	$[M + HCO_2]^-$ $[M - CH_3]^-$ Loss of FA 18:2 as ketene NL FA 18:2 $[FA\ 22:1 - H]^-$ $[FA\ 18:2]^-$ $[GPC - CH_3 - H_2O]^-$ Phosphocholine – CH_3 $[H_2PO_4]^-$	Consistent with predicted spectrum (Lipid Maps) - [2], #

Table A2 (continued).

[1]http://www.lipidmaps.org/tools/structuredrawing/GP_p_form.php
[2]Fragment ions observed were consistent with PC(16:0_16:0), however, fragment ions corresponding to arachidonic acid (20:4) were also observed in the spectrum, suggesting possible co-selection of precursor ions.
[3]The high resolution of the QE HF instrument reveled two precursors under feature # 118 detected with the lower resolution Xevo instrument. Each was examined individually and matched a specific lipid species.
[4]Although this feature could only be assigned a level 3 confidence based on negative ion mode measurements, it is "paired" to another feature in the panel detected in positive ion mode with a higher level of confidence (feature #656).
[5]Although this feature could only be assigned a level 3 confidence based on negative ion mode measurements, it is "paired" to another feature in the panel detected in positive ion mode with a higher level of confidence (feature #680).
[*]Accurate mass matched in negative mode, fragmented in positive mode for FA chain and headgroup info
[#] Accurate mass matched in positive mode, fragmented in negative mode for FA chain and headgroup info